INCOMPRESSIBLE VISCOUS FLOW ACROSS BANKS OF TUBES AT LOW REYNOLDS NUMBERS

By

KOHEI ISHIHARA

Bachelor of Science
Kyoto University
Kyoto, Japan
1965

Master of Science
Oklahoma State University
Stillwater, Oklahoma
1967

Submitted to the faculty of the Graduate College
of the Oklahoma State University
in partial fulfillment of the requirements
for the degree of
DOCTOR OF PHILOSOPHY
May, 1971

INCOMPRESSIBLE VISCOUS FLOW

ACROSS BANKS OF TUBES AT

LOW REYNOLDS NUMBERS

Thesis Approved:

Kenneth J. Bell

Thesis Adviser

John B. West

Robert L. Robinson, Jr.

Gerald D. Parker

D. D. Durham

Dean of the Graduate College

PREFACE

A theoretical investigation was made to predict the flow patterns and friction factors for incompressible viscous flow across tube banks. Numerical solutions of the Navier-Stokes equations in terms of stream function and vorticity were obtained by means of a finite difference approximation for flow across inline square tube banks. The results for two pitch ratios were presented and discussed. The computed friction factors were compared with experimental data.

I am indebted to Dr. Kenneth J. Bell, my adviser, for his advice and guidance not only on this doctoral work but also on my entire study in this institution throughout my graduate years. I wish to express my thanks to Dr. R. L. Panton of the School of Mechanical Engineering for his helpful discussions in relation to this study. Thanks are also extended to each member of my advisory committee, Drs. J. B. West and R. L. Robinson of the School of Chemical Engineering and Drs. J. D. Parker and W. G. Tiederman of the School of Mechanical Engineering. I would like to thank my wife, Atsuko, and my parents for their giving me much encouragement throughout my graduate study at the Oklahoma State University.

I am also indebted to the Oklahoma State University for providing financial support and for the use of computing facilities during the course of the project. I also wish to thank the Phillips Petroleum Company which provided me with a fellowship during my last three consecutive academic years.

TABLE OF CONTENTS

Chapter Page

LIST OF TABLES

LIST OF FIGURES

Figure | Page

Figure Page

Figure | Page

CHAPTER I

INTRODUCTION

Most recent and reliable design methods for baffled shell and tube heat exchangers are based upon the heat transfer and fluid friction factors of the ideal tube bank which approximates the array of tubes between each pair of baffles. Successful empirical correlations of the shell side friction factors and heat transfer factors for ideal tube banks have been obtained for most tube layouts of interest over a wide range of Reynolds number.

However, there has been no significant progress in the theoretical investigation into the tube bank flow and heat transfer mechanisms which are important for evaluating design parameters and for providing the insight and accurate understanding of experimental data.

The purpose of this study was to survey the fluid dynamics and heat transfer mechanisms during flow across banks of tubes by exploring possible semi-empirical models and analytical and/or numerical methods to predict heat transfer and friction factors for ideal tube banks, and finally to compare these predictions with the available experimental data.

Fluid flow models and methods originally intended for investigation were:

I. Mechanistic models, where arrays of tubes are assumed to behave as:

1. A series of nozzles

2. A porous medium

3. A mesh of woven wires

II. Analytical-empirical models in which fluid flow is assumed to be equivalent to:

1. Flow across a single cylinder, corrected for the influence of neighboring tubes

2. Flow across an infinite transverse row of tubes, corrected for the influence of preceding and succeeding tube rows

III. Analytical solutions of related geometries such as:

1. Flow in converging and diverging ducts

2. Flow over wedges

IV. Boundary layer analysis for a single cylinder with a wake correction

V. Variational method for solution of the Navier-Stokes equations for laminar flow

VI. Numerical integration of the Navier-Stokes equations for a unit cell of tube bank

Only some of the simplified flow models were investigated, but numerical methods were explored in detail. Heat transfer calculations were not attempted as part of this thesis, but are mentioned in the recommendations of Chapter VI.

CHAPTER II

BACKGROUND

Tube Bank Arrangements

Three tube arrangements in shell and tube heat exchangers are most commonly used for satisfing the ordinary requirements for industrial practice on heat exchange and pumping power. Figure 1 shows the schematic of these three tube layouts and the unit cells of tube banks defined.

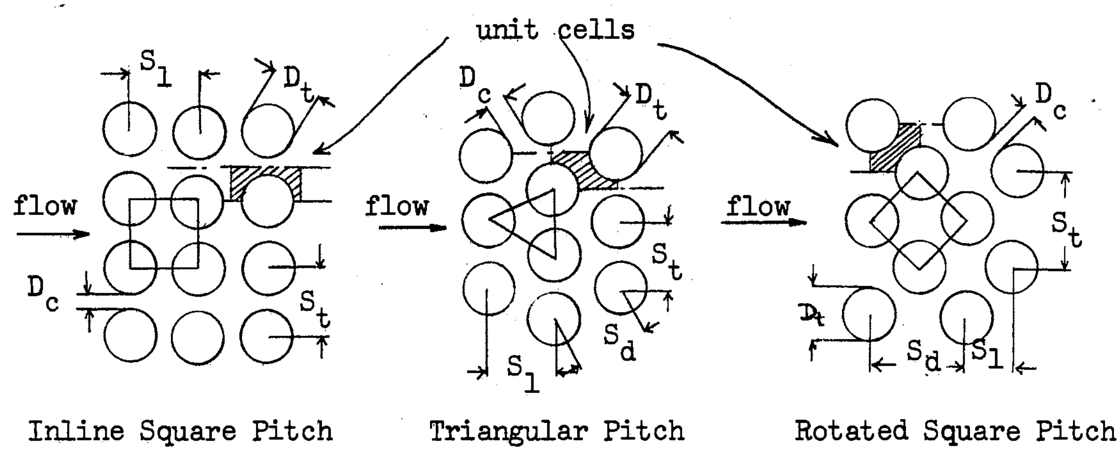

Figure 1. Tube Layout Schematic

The unit cell of a tube bank may be defined as an element of flow channel and part of tube(s) in which all the characteristics of flow across tube bank can be represented. The tube clearance, D_c, is the shortest distance between adjacent tubes. The tube pitch is defined as the shortest center-to-center distance between adjacent tubes (S_l, S_t, and S_d). The most common term used in this study is the pitch ratio, defined as the ratio of the pitch to the outside diameter of the tube (e.g., S_t/D_t and S_l/D_t).

Fluid Dynamics in Ideal Tube Banks

There is no clear-cut Reynolds number criterion for the laminar-turbulent transition for flow in tube banks, unlike for flow in cylindrical conduits. The University of Delaware Experiment Station Bulletin No. 5 (10) states:

> Because the cross sectional area of the flow channel is not constant, the inertia terms (those involving velocities to the second degree) in the Navier-Stokes equations are not zero (though they become vanishingly small compared to the viscous terms at very low Reynolds numbers) and the onset of true turbulence is masked by kinetic or inertial effects on the pressure drop. On the other hand, inertial phenomena minimize the effect of disturbances in the entering flow and other entrance length phenomena and eliminate (so far as has been observed) the possibility of quasi-stable laminar flow at high Reynolds numbers in tube banks.

However, for the sake of convenience and uniformity, the following divisions of the flow regions have been usually adopted:

$0 < Re < 100$	laminar
$100 < Re < 4000$	transition
$4000 < Re$	turbulent

The laminar flow regime of tube bank flow which may be taken as the Stokes flow or creeping flow regime is the Reynolds number range over which the friction factor is very nearly inversely proportional to the Reynolds number, and the initial deviation from this linearity is due to inertial phenomena rather than to the random velocity fluctuations that are characteristic of turbulent flow.

Transition flow regime is characterized by the appearance of occasional eddies in the main flow stream in the tube banks: the friction factor becomes greater than the value expected from laminar flow, which indicates the irreversible momentum loss due to random eddies. For inline tube banks, the friction factor curve goes through a minimum and then increases smoothly to the value for fully developed turbulence.

In the turbulent flow regime, where random velocity fluctuations and continuous well-developed eddies exist, the friction factor becomes proportional to about -0.2 to -0.4 power of the Reynolds number.

Literature Survey

The discussion of publications in this section will primarily concern fluid flow and pressure drop for incompressible viscous flow across tube banks.

Experimental Work

Extensive experimental data of pressure drop and heat transfer for flow across banks of tubes were presented by Huge (2) and Pierson (3) in 1937. The most recent and most comprehensive experimental investigations to develop design methods for shell and tube heat exchangers were initiated at the University of Delaware in 1946 and completed in 1963 (1, 4, 5). The chief result of the Delaware project was the accumulation of a large amount of carefully-obtained data whose interpretation has been published as correlations of pressure drop and heat transfer coefficients and as proposed methods of shell and tube heat exchanger design (6).

Empirical Correlation

In 1933, Chilton and Genereaux (7) proposed a friction factor correlation with the scattered, meager pressure drop data available at that time. They presented the following correlations,

$$f = \frac{13.2}{Re_c} \qquad \text{(laminar flow; rotated square pitch)} \tag{2-1}$$

$$f = \frac{0.57}{Re_c^{0.2}} \qquad \text{(turbulent flow; rotated square pitch)} \tag{2-2}$$

$$f = \frac{0.264}{Re_c^{0.2}} \qquad \text{(turbulent flow; inline square pitch)} \tag{2-3}$$

where

$$f = \frac{2 \Delta P \ g_c \rho}{4 \ G_m^2 \ N_t} \tag{2-4}$$

and

$$Re_c = \frac{D_c \ G_m}{\mu} \tag{2-5}$$

No correlation was presented for laminar flow in inline tube layouts due to the absence of data.

In 1937 Grimison (8), using the data reported by Huge and Pierson (all of it in the turbulent flow regime), presented graphical correlations of friction factor as a function of Reynolds number based on tube diameter, D_t,

$$Re = \frac{D_t G_m}{\mu} \qquad (2\text{-}6)$$

with the parameters of the transverse tube spacing to the tube diameter, S_t/D_t, and the ratio of the longitudinal tube spacing to the tube diameter, S_l/D_t.

Gunter and Shaw (9) in 1945, also based on the data by Huge and Pierson, attempted to develop a single friction factor correlation applicable to all the tube layouts and spacings, by using the volumetric hydraulic diameter D_v, instead of tube diameter, D_t.

However, as was pointed out by Boucher and Lapple (10) in 1948 in their critical comparison of the reported data and proposed correlations for pressure drop of Newtonian fluids across tube banks, no equivalent diameter should be expected to correlate the data from geometrically different tube banks into a single curve, because hydrodynamic similarity requires geometric similarity.

Recommended empirical correlations from the Delaware project (1) are hence presented in the form of graphical correlations of the friction factors defined by Equation 2-4 for different tube layouts as a function of Reynolds number based on tube diameter, or Equation 2-6.

Theoretical Study

There has been little progress in theoretical investigation on tube bank flow phenomena. The difficult geometry involved and the complex mathematical solutions anticipated have so far discouraged seeking a rigorous solution.

The Navier-Stokes equations have been recognized as the appropriate system of partial differential equations for describing flow of viscous fluids. The difficulty of solving the Navier-Stokes equations is due to the non-linearity of the equations introduced by the convective terms. In analytical approaches to solving the equations for the limiting case of very low Reynolds number, the non-linear terms are either neglected or linearized: in the Stokes solution, the convective terms are neglected; in the Oseen's solution, those terms are approximated by utilizing a constant free stream velocity.

Three attempts have been made to predict the tube bank friction factor without resort to flow experiment.

In 1957 Tamada and Fujikawa (11) solved Oseen's linearized equation for steady state laminar flow past an infinite row of regularly spaced cylinders in a plane perpendicular to the uniform stream (Figure 2).

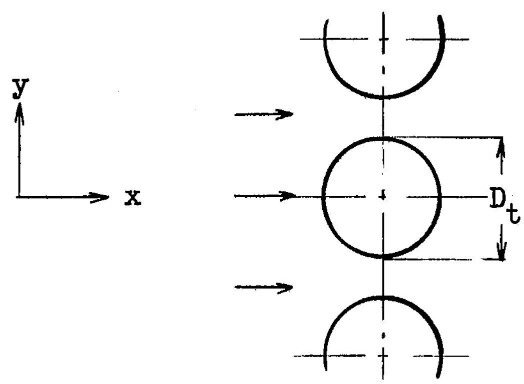

Figure 2. Flow Normal to a Single Row of Cylinders

Oseen's linearized equation is expressed in terms of vorticity ζ,

$$\left(\nabla^2 - \frac{Re}{D_t}\frac{\partial}{\partial x}\right)\zeta = 0 \tag{2-7}$$

where ζ is defined by

$$\zeta = \frac{\partial v}{\partial x} - \frac{\partial u}{\partial y} \tag{2-8}$$

The solution is obtained as an infinite series in Reynolds number with a parameter of the pitch ratio, S_t/D_t. Their solution verifies some of the observed features of tube bank flow at low Reynolds numbers:

1. At a fixed fluid velocity, the drag on a cylinder in the infinite row is greater than the drag on the same cylinder when alone in a uniform flow.
2. As the Reynolds number increases, the drag on the cylinder deviates more from the drag for a cylinder in the uniform flow.
3. The drag is proportional to the velocity at low Reynolds numbers.

However, the solution does not account for the interaction effect of the neighboring rows that is characteristic of tube bank flow.

In 1959, Happel (12) proposed an "equivalent free surface" model for flow normal to arrays of cylinders, thereby conveniently describing the boundary conditions in the polar coordinate system (Figure 3).

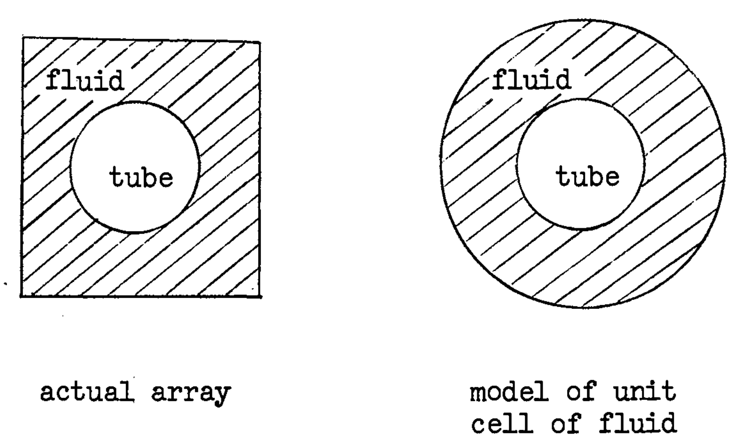

Figure 3. "Equivalent Free Surface" Model

Happel solved the Stokes equation expressed in terms of the stream function ψ, or the biharmonic equation for ψ,

$$\nabla^4 \psi = 0 \tag{2-9}$$

where ψ is defined as

$$v_r = \frac{\partial \psi}{r \partial \theta} \tag{2-10}$$

$$v_\theta = - \frac{\partial \psi}{\partial r} \tag{2-11}$$

His result for rotated square array is in good agreement with the pressure drop reported by Bergelin et al (4) in the Delaware project for Re $<$ 100, but about 30 to 55 percent low for the other tube layouts.

Friedl and Bell (13) in 1960 applied an electro-conductive analogy to the creeping flow regime, assuming that the streamlines and isopotential lines of the steady potential flow of an inviscid fluid are identical with the stream lines and constant pressure lines of creeping flow. The isopotential lines were found by laying out the tube bank array on conducting paper and applying a voltage difference between edges of the paper (Figure 4).

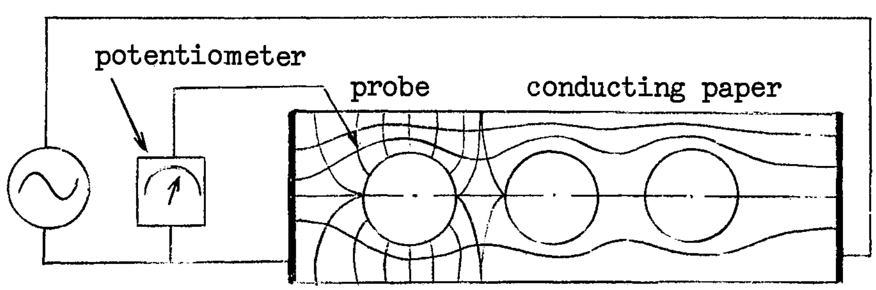

Figure 4. Electro-conductive Analogy

The isopotential field was divided into an arbitrary number of flow elements bounded by solid surfaces and two arbitrarily spaced isopotential lines. The pressure drop for each flow element was computed utizing the solutions derived by Graetz (14) for laminar flow through rectangular conduits. The total pressure drop was then found by integrating the pressure gradients for the flow elements along a stream line through the entire tube bank. Friction factors calculated for three tube arrays (inline square, rotated square and equilateral triangular) were within -2 to -14 percent of the Delaware experimental friction factors over the Reynolds number range of 2 to 50.

All of these attempts have been limited to the friction factors at low Reynolds number, or creeping flow, and they failed to give much physical insight into flow phenomena in tube banks. No treatment has yet been proposed either for the friction factor at higher Reynolds numbers or for heat transfer over any range of Reynolds number.

CHAPTER III

SIMPLIFIED FLOW MODELS

Tamada and Fujikawa's attempt (11) is mathematically too complex and tedious. Happel's "equivalent free surface" model (12) is physically unrealistic. Friedl and Bell's electro-conductive analogy (13) is based upon an unproven assumption concerning the basic fluid dynamics.

In the early stage of the project, simplified flow models which would give more realistic and useful pictures of tube bank flow were investigated in an attempt to obtain tube bank friction factors as a function of Reynolds number.

The flow models attempted are presented in the following sections. The variational method reported in the last section is discussed in somewhat more detail.

Model I: Converging and Diverging Channel Flow

In this case, the flow between two tubes in a tube bank was assumed to be the flow through a family of converging and diverging channels (Figure 5). The equation of continuity and the equations of motion applied at an angular position of ϕ were reduced to the dimensionless equation of velocity distribution. The derivation of the equation is given in Appendix A. The resulting expression was written

$$F''' + 2Re_r F\, F' + 4F' = 0 \qquad (3\text{-}1)$$

where the dimensionless velocity profile is defined by

$$F(\phi) = \frac{v_r}{v_{\phi_{\mathfrak{L}}}} \tag{3-2}$$

and Re_r is the Reynolds number on the centerline x = 0 defined by $v_{\phi_{\mathfrak{L}}} r/\mu$. The boundary conditions for Equation 3-1 are

$$\begin{aligned} F(\phi) &= 0 \quad \text{at the wall} \\ \left.\begin{aligned} F(0) &= 1 \\ F'(0) &= 0 \end{aligned}\right\} & \text{on the centerline } x = 0 \end{aligned} \tag{3-3}$$

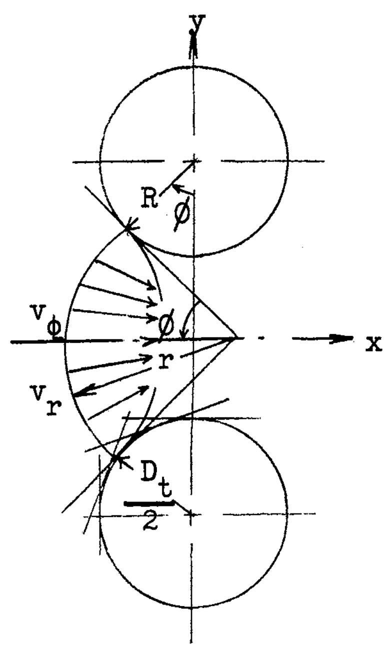

Figure 5. Converging and Diverging Channel Flow Model

The attempt to obtain the solution of Equation 3-1 was not successful. When the converging section of the flow channel is assumed to consist of a boundary layer flow near the tube surface and of potential flow in the core region, which approximates the flow at high Reynolds number, the analytical solution has been reported (15):

$$F(\theta) = 3 \tanh^2 \left[\sqrt{\frac{Re_r}{2}}(\theta - \phi) + 1.1462 \right] - 2 \qquad (3\text{-}4)$$

The friction factor for the converging section of the channel is calculated from Equation 3-4 in terms of tube bank Reynolds number defined by Equation 2-6,

$$f = \frac{14.7}{\sqrt{Re(P_t - 1)}} \qquad (3\text{-}5)$$

where P_t is the transverse pitch ratio equal to S_t/D_t. The derivation of the equation is presented in Appendix A. The experimental evidence of f being proportional to -0.2 to -0.4 power of Re at turbulent region does not support this expression, although Equation 3-5 is at most valid only for the forward halves of the tubes.

Model II: Non-uniform Duct Flow

Assuming a creeping flow between two tubes with no pressure gradient in y-direction (Figure 6), the Hagen-Poiseuille equation may be written in differential form as,

$$-\frac{dP}{dx} = \frac{3}{2} \frac{\mu W}{\rho g_c C_1^3} \qquad (3\text{-}6)$$

where W = mass flow rate between tubes per unit depth of tube

$$= \bar{u}\,(P_t - 1)\,D_t \tag{3-7}$$

C_1 = one half the clearance between tubes

$$= P_t - \sqrt{2X - X^2} \tag{3-8}$$

and $X = x/R$

Equation 3-6 is rearranged with Equations 3-7, 3-8 and the tube bank friction factor definition, Equation 2-4, and then integrated from x = 0 to x = 2R to result in

$$f = \frac{6}{Re}\,\frac{P_t - 1}{P_t^3}\,f(P_t) \tag{3-9}$$

where

$$f(P_t) = \int_0^1 \frac{dX}{[P_t - \sqrt{2X - X^2}\,]^3} \tag{3-10}$$

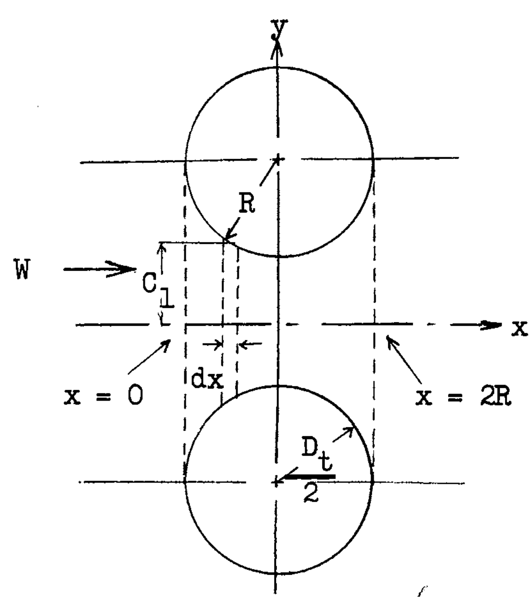

Figure 6. Non-uniform Duct Flow Model

The function $f(P_t)$ has been calculated as a function of P_t (18) and is given graphically in Figure 7.

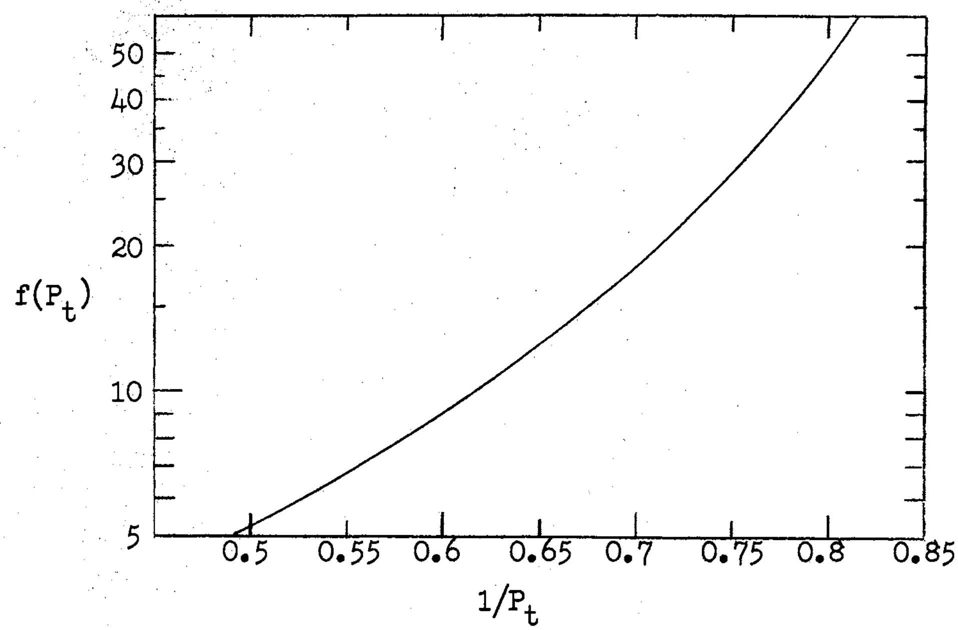

Figure 7. Function $f(P_t)$

For $P_t = 1.50$ and $P_t = 1.25$, $f(P_t)$ is 13.9 and 48.7, respectively, and the tube bank friction factors become

$$f = \frac{15.5}{Re} \qquad \text{for } P_t = 1.50 \qquad (3\text{-}11)$$

and

$$f = \frac{37.5}{Re} \qquad \text{for } P_t = 1.25 \qquad (3\text{-}12)$$

The Delaware isothermal friction factor data for inline square tube banks show that in the creeping flow range

$$f = \frac{18.0}{Re} \qquad \text{for } P_t = 1.50 \qquad (3\text{-}13)$$

and

$$f = \frac{48.0}{Re} \qquad \text{for } P_t = 1.25 \tag{3-14}$$

Thus Equations 3-11 and 3-12 are in fairly good agreement with the experimental data, indicating some validity of the model in the creeping flow range.

Model III: Channel-Wake Flow

In this model, at high flow rates, tube bank flow is assumed to be a combination of flow in a duct and wakes between succeeding tube rows (Figure 8).

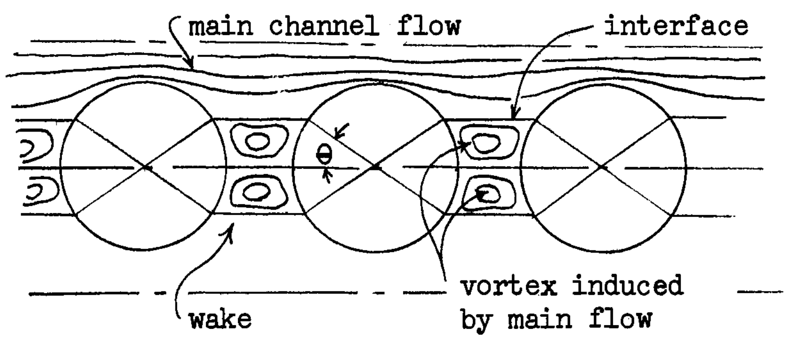

Figure 8. Channel-Wake Flow Model

For the duct flow, the method of Model II was applied using the turbulent friction factor equation for uniform duct, or the Blasius equation (19),

$$f = \frac{0.079}{Re^{\frac{1}{4}}} \tag{3-15}$$

For wakes, the pressure loss was assumed to be the energy dissipated through the vortex motion of the fluid. The Rayleigh flow (15) induced by sudden motion of a plate was assumed in order to calculate the energy transfered to the vortex from the main channel flow; that is, a sheet of fluid is continuously accelerated by the main flow at the interface of the flow regions. The derivation of the equations is given in Appendix B. The final expression obtained is

$$f = \frac{0.079}{Re^{\frac{1}{4}}} \frac{(P_t - 1)^2}{P_t^3} f_\theta(P_t) + \frac{1.13\ (P_t - 1)^{3/2}}{\sqrt{Re}\ (P_t - \cos\theta)(P_t - \sin\theta)} \tag{3-16}$$

where

$$f_\theta(P_t) = \int_{1 - \cos\theta}^{1} \frac{dX}{[P_t - \sqrt{2X - X^2}\ ]^3} \tag{3-17}$$

The contribution of the second term of the right hand side of Equation 3-16 is found to be too small to be reasonable as the energy dissipated by the wakes.

Indirect Solution of the Navier-Stokes Equations by the Variational Method

The variational method makes use of the principle that the stable configuration is the one which minimizes the rate of entropy production. The method has been found to be particularly useful to obtain approximate solutions for a wide variety of problems, especially in structural engineering and elasticity. The variational techniques applicable to transport phenomena have been well summarized in the textbook by Schechter (20). Schechter (21) has solved the steady flow of a non-Newtonian power-law fluid in a cylindrical conduit by the variational method. Delleur and Sooky (22) have obtained approximate velocity distributions for Newtonian flow in rectangular duct.

The variational principle states that the motion of an incompressible fluid which satisfies the equation of continuity, the equation of motion, and the specified boundary conditions along the whole boundary is such that the dissipation integral,

$$I = \iiint F \, dx \, dy \, dz \tag{3-18}$$

attains a minimum for steady uniform flow, where F is the variational function specific to the particular problem and represents the rate of total energy change in an unit volume of the system. It has been proved (23) that minimizing the integral of Equation 3-18 is equivalent to solving the Navier-Stokes equations with the inertia terms neglected.

The variational function for the two-dimensional power-law fluid flow across an unit cell of tube bank shown in Figure 9 may be written,

$$F = \left[2 \left\{ \left(\frac{\partial U}{\partial X}\right)^2 + \left(\frac{\partial V}{\partial Y}\right)^2 \right\} + \left(\frac{\partial V}{\partial X} + \frac{\partial U}{\partial Y}\right)^2 \right]^{\frac{n+1}{2}} - Re_n f_n \left(U + V\frac{\partial X}{\partial Y}\right) \tag{3-19}$$

The derivation of Equation 3-19 is presented in Appendix C. Here, n is the power-law index in shear stress-strain expression; thus Equation 3-19 reduces to the Newtonian case when $n = 1$; X and Y are normalized by R; U and V by $\bar{u}$; and Re and f are defined by Equation 2-6 and Equation 2-4, respectively.

In applying the variational principle for steady, incompressible flow, use is usually made of the Ritz-Galerkin method (20), in which a trial velocity profile is to be so chosen that the boundary conditions are satisfied and the dissipation integral becomes a minimum.

In this particular tube bank flow problem, first, velocity distributions for U and V are assumed which satisfy all the boundary conditions on a unit cell of tube bank (Figure 9), that is,

$$\left.\begin{array}{l} U = 0 \\ V = 0 \end{array}\right\} \text{ on the tube surface} \tag{3-20}$$

$$\frac{\partial U}{\partial Y} = 0 \qquad \text{at } Y = \pm P_t \tag{3-21}$$

$$\left.\begin{array}{l} U = U_{max} \\ V = 0 \end{array}\right\} \text{ at } Y = \pm P_t \tag{3-22}$$

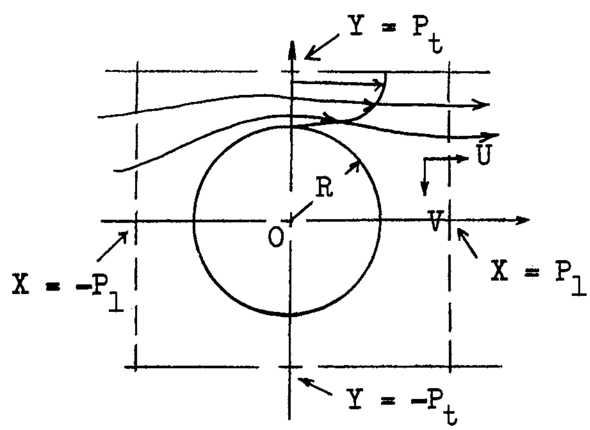

Figure 9. Unit Cell and Flow Model for Variational Method

The assumed velocity profiles that are functions of X and Y with parameters, C_i, to be specified, are then substituted into the dissipation integral I of Equation 3-18, or

$$I = \int_{-P_t}^{P_t}\int_{-P_l}^{P_l} \left\{ \left[2\left(\frac{\partial U}{\partial X}\right)^2 + 2\left(\frac{\partial V}{\partial Y}\right)^2 + \left(\frac{\partial U}{\partial Y} + \frac{\partial V}{\partial X}\right)^2 \right]^{\frac{n+1}{2}} - \Phi \left(U + V\frac{\partial X}{\partial Y}\right) \right\} dXdY \tag{3-23}$$

where $\Phi = Re_n f_n$

and P_l = longitudinal pitch ratio, S_l/D_t.

The integral I is then minimized with respect to each of the parameters in the assumed velocity profiles by the following set of conditions:

$$\frac{\partial I}{\partial C_i} = \iint \frac{\partial F}{\partial C_i} \, dX \, dY = 0 \qquad (i = 1,2, \ldots\ldots n_p) \qquad (3\text{-}24)$$

where n_p is the number of parameters in the U- and V-profiles.

One of the velocity profile parameters can be determined a priori from the continuity condition that

$$1 = \frac{1}{P_t - 1} \int_1^{P_t - 1} U_{X=0} \, dY \qquad (3\text{-}25)$$

Equations 3-24 and 3-25 can be solved to find the optimum values for the parameters C_i and Φ which in turn minimize the dissipation integral.

Since Equation 3-23 can be integrated analytically for n = 1, it was first solved with the Newtonian case. The first trial velocity distributions attempted were

$$U = (C_1 + C_2X^2)(X^2 + Y^2 - 1) \qquad (3\text{-}26)$$

$$V = C_3X\,Y\,(P_t^2 - Y^2)(X^2 + Y^2 - 1) \qquad (3\text{-}27)$$

These satisfy the non-slip condition on the tube surface and the maximum velocity condition along the boundary line of a unit cell, $Y = \pm P_t$. It must be noted however that the U-profile does not satisfy the condition of zero velocity gradient along the same boundary line of $Y = \pm P_t$, i.e., Equation 3-21, since

$$\frac{\partial U}{\partial Y} = 2\,Y\,(C_1 + C_2\,X^2) \tag{3-28}$$

does not become zero at $Y = \pm P_t$.

The details of integration and minimization of the dissipation integral with these first trial velocities are given in Appendix D.

The following friction factor vs. Reynolds number relations result when the last term in the right hand side of Equation 3-23, i.e., $V\frac{\partial X}{\partial Y}$, is neglected:

$$f = \frac{18.4}{Re} \qquad \text{for } P_t = 1.50 \tag{3-29}$$

$$f = \frac{45.5}{Re} \qquad \text{for } P_t = 1.25 \tag{3-30}$$

These results give unexpectedly good comparison with the experimental data (Equations 3-13 and 3-14) despite the fact that the trial velocity profiles Equations 3-26 and 3-27, do not satisfy the condition of zero velocity gradient at $Y = \pm P_t$ or Equation 3-21.

It is interesting to note that when $\frac{\partial X}{\partial Y}$ term was not neglected but assumed to be

$$\frac{\partial X}{\partial Y} = \frac{X}{Y} \tag{3-31}$$

the final results become,

$$f = \frac{21.7}{Re} \qquad \text{for } P_t = 1.50 \tag{3-32}$$

and

$$f = \frac{52.8}{Re} \qquad \text{for } P_t = 1.25 \tag{3-33}$$

In the next step, a more sophisticated and presumably better velocity profile for U was tried: the second trial velocity profiles were

$$U = (C_1 + C_2 X^2)(X^2 + Y^2 - 1)(2 P_t^2 - 1 - Y^2 + X^2) \tag{3-34}$$

$$V = C_3 X Y (P_t - Y^2)(X^2 + Y^2 - 1) \tag{3-27}$$

which satisfy all the boundary requirements including Equation 3-21 as can be shown by

$$\frac{\partial U}{\partial Y} = 4 Y (C_1 + C_2 X^2)(P_t^2 - Y^2) \Big|_{Y = \pm P_t} = 0 \tag{3-35}$$

Equations 3-34 and 3-27 are substituted into Equation 3-23. Upon integration, the dissipation integral is then minimized with respect to velocity parameters, C_i. The details of the manipulation of this process are given in Appendix D.

The following final results are obtained for the case of $\frac{\partial X}{\partial Y} = 0$;

$$f = \frac{98.3}{Re} \qquad \text{for } P_t = 1.50 \tag{3-36}$$

and

$$f = \frac{478}{Re} \qquad \text{for } P_t = 1.25 \tag{3-37}$$

and for the case of $\frac{\partial X}{\partial Y} = \frac{X}{Y}$;

$$f = \frac{111}{Re} \qquad \text{for } P_t = 1.50 \qquad (3\text{-}38)$$

and

$$f = \frac{555}{Re} \qquad \text{for } P_t = 1.25 \qquad (3\text{-}39)$$

Contrary to the fact that the second trial velocity is presumably better than the first one, the results obtained are worse.

In order to check the analytical solution of the variational method for n = 1 as well as to explore the case of $n \neq 1$ once the Newtonian case was successful, a computer program was written to perform the numerical double integration of I of Equation 3-23 and its derivatives $\frac{\partial I}{\partial C_i}$ and to execute the minimization process by the steepest-descent method. The double integration was carried out using the simple trapezoidal rule by discretizing the flow channel area of a unit cell of tube bank with square meshes. The steepest-descent method of Booth (24) was applied for optimizing the assumed velocity profile that would minimize the dissipation integral. Derivation of the equations for the Booth method is presented in Appendix E, which is adapted from the paper by Simon and Briggs (25). A block diagram of the computer program is shown in Figure 10.

The calculations were tried for the Newtonian fluid case of n = 1 for pitch ratios of 1.50 and 1.25. But the solutions using the first velocity profiles Equations 3-26 and 3-27 with $\frac{\partial X}{\partial Y} = 0$,

$$f = \frac{30.4}{Re} \qquad \text{for } P_t = 1.50 \qquad (3\text{-}40)$$

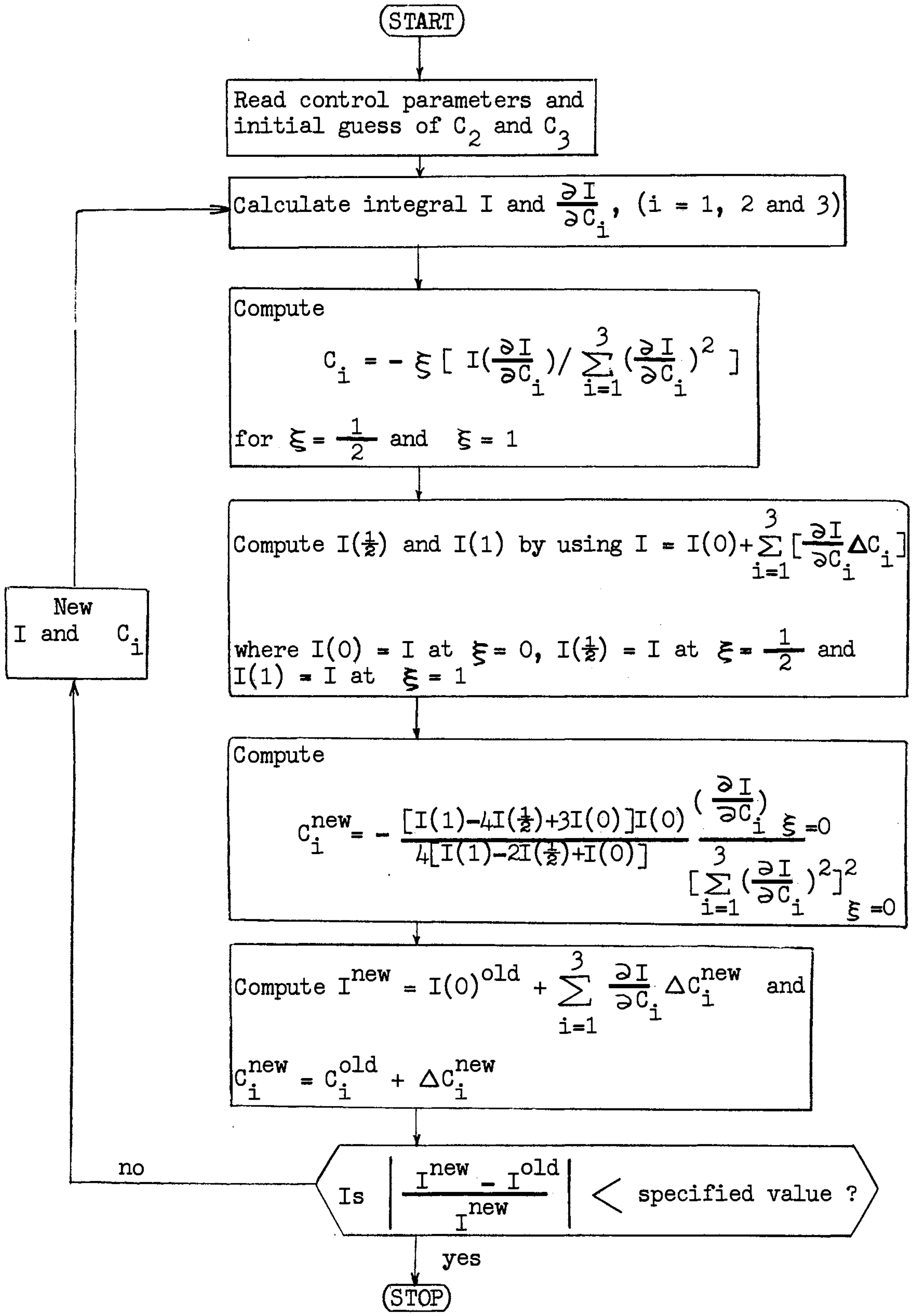

Figure 10. Computer Block Diagram for Variational Method

and

$$f = \frac{1708}{Re} \qquad \text{for } P_t = 1.25 \qquad (3\text{-}41)$$

did not reproduce the analytical solutions of Equation 3-29 for P_t = 1.50 and Equation 3-30 for P_t = 1.25.

After considerable time spent on checking the computer program and the minimization procedure used and yet obtaining no reasonable results, the variational method was abandoned.

CHAPTER IV

NUMERICAL SOLUTIONS OF THE NAVIER-STOKES EQUATIONS

The difficulty of obtaining an analytical solution for the flow over any submerged object beyond the creeping flow regime is that the non-linear convective effects are no longer negligible and the eddy behind the body leads to a region of separated flow which is not easily amenable to analytical treatment.

Numerical solution of the Navier-Stokes equations is, therefore, coming to play an important role in theoretical research in fluid dynamics, especially because of the advent of high speed electronic computers. The main roles of numerical solutions are that they can (i) give the minute details of phenomena of interest thus providing insight into the characteristics of the flow field, and therefore (ii) reduce the amount of experimental effort needed for the evaluation of design parameters, and also (iii) be suggestive of new approaches to analytical solution.

The foundations of numerical methods for solving fluid flow problems were laid about forty years ago by Thom (26). Among the flow problems which have been solved by numerical methods are (i) uniform flow past a single cylinder (26, 27, 28, 29, 30), (ii) flow in a conduit expansion (31), (iii) flow through pipe orifices (32), and (iv) flow in rectangular cavities (33). All these flow problems are relatively easily attacked because of possible variable transformations, in the case of (i) due to only one cylinder in the field, and because of rectangular boundaries in the cases of (ii) - (iv), where no irregular "star" exists at the boundaries.

The difficult geometry involved has however so far apparently discouraged seeking numerical solutions of the Navier-Stokes equations for the flow in tube banks.

The basic method of solution employed here is the classical "two-field" method used by Thom (26): replacement of the fourth-order non-linear partial differential equations of Navier-Stokes for the stream function ψ, by two second order simultaneous equations for the stream function and the vorticity ζ. These equations are then replaced by their simplest finite difference approximations. In the case of two-dimensional flow, this coupled pair of finite difference equations has been known to exhibit superior convergence properties compared with finite difference expressions of the fourth-order partial differential equations involving the stream function when iterative methods are used for the solution.

The difficulty of handling irregular "stars" on the boundary and lack of a single pertinent coordinate system for the tube bank geometry were overcome by smooth matching of the two coordinate systems - polar and rectangular - at the boundaries of the unit cells in the tube bank and by marching down the computation from inlet to outlet through the series of unit cells in the tube bank.

The computer program has been developed for solving stream function and vorticity fields of an inline square tube layout with any number of tube rows in tube arrays having effectively infinite extent in the direction normal to the flow. Only three tube rows are, however, considered in the actual computation due to practical limitations of computer capacity available; this is sufficient to give interaction effects of neighboring rows as well as entrance and exit effects which are characteristic of flow across tube banks.

Fundamental Governing Equations

For two-dimensional, steady, incompressible, viscous Newtonian fluid flow, the governing equations in rectangular coordinates are: (primed quantities are dimensional)

Equation of continuity

$$\frac{\partial u'}{\partial x'} + \frac{\partial v'}{\partial y'} = 0 \tag{4-1}$$

Equation of motion

$$u' \frac{\partial u'}{\partial x'} + v' \frac{\partial u'}{\partial y'} = - \frac{1}{\rho} \frac{\partial P'}{\partial x'} + \nu \left(\frac{\partial^2 u'}{\partial x'^2} + \frac{\partial^2 u'}{\partial y'^2}\right) + g'_x \tag{4-2}$$

$$u' \frac{\partial v'}{\partial x'} + v' \frac{\partial v'}{\partial y'} = - \frac{1}{\rho} \frac{\partial P'}{\partial y'} + \nu \left(\frac{\partial^2 v'}{\partial x'^2} + \frac{\partial^2 v'}{\partial y'^2}\right) + g'_y \tag{4-3}$$

Introducing the stream function ψ' defined by

$$u' = \frac{\partial \psi'}{\partial y'} \tag{4-4}$$

$$v' = - \frac{\partial \psi'}{\partial x'} \tag{4-5}$$

then, the equation of continuity 4-1 is satisfied as

$$\frac{\partial u'}{\partial x'} + \frac{\partial v'}{\partial y'} = \frac{\partial^2 \psi'}{\partial x' \partial y'} - \frac{\partial^2 \psi'}{\partial y' \partial x'} = 0 \tag{4-6}$$

Cross-differentiating the equations of motion, 4-2 and 4-3, with resepct to y' and x', respectively, and utilizing the continuity condition 4-1, one gets after rearrangement

$$u' \frac{\partial^2 u'}{\partial x' \partial y'} + v' \frac{\partial^2 u'}{\partial y'^2} = -\frac{1}{\rho} \frac{\partial^2 p'}{\partial y' \partial x'} + \nu \left(\frac{\partial^3 u'}{\partial y' \partial x'^2} + \frac{\partial^3 u'}{\partial y'^3} \right) + \frac{\partial g'_x}{\partial y'} \tag{4-7}$$

$$v' \frac{\partial^2 v'}{\partial x' \partial y'} + u' \frac{\partial^2 v'}{\partial x'^2} = -\frac{1}{\rho} \frac{\partial^2 p'}{\partial x' \partial y'} + \nu \left(\frac{\partial^3 v'}{\partial x'^3} + \frac{\partial^3 v'}{\partial x' \partial y'^2} \right) + \frac{\partial g'_y}{\partial x'} \tag{4-8}$$

Subtracting one from the other and thereby eliminating the pressure terms, one finds

$$u' \frac{\partial}{\partial x'} \left(\frac{\partial u'}{\partial y'} - \frac{\partial v'}{\partial x'} \right) + v' \frac{\partial}{\partial y'} \left(\frac{\partial u'}{\partial y'} - \frac{\partial v'}{\partial x'} \right) =$$

$$\nu \left[\frac{\partial^2}{\partial x'^2} \left(\frac{\partial u'}{\partial y'} - \frac{\partial v'}{\partial x'} \right) + \frac{\partial^2}{\partial y'^2} \left(\frac{\partial u'}{\partial y'} - \frac{\partial v'}{\partial x'} \right) \right] \tag{4-9}$$

where it is assumed that the conservative body force $\vec{g}$ provides

$$\frac{\partial g'_x}{\partial y'} - \frac{\partial g'_y}{\partial x'} = 0 \tag{4-10}$$

Defining the vorticity ζ',

$$\zeta' = \frac{\partial u'}{\partial y'} - \frac{\partial v'}{\partial x'} \tag{4-11}$$

Equation 4-9 then reduces to

$$\frac{\partial \psi'}{\partial y'}\frac{\partial \zeta'}{\partial x'} - \frac{\partial \psi'}{\partial x'}\frac{\partial \zeta'}{\partial y'} = \nu \left[\frac{\partial^2 \zeta'}{\partial x'^2} + \frac{\partial^2 \zeta'}{\partial y'^2} \right] \tag{4-12}$$

It should be noted that the vorticity ζ' is defined by Equation 4-11 to be positive instead of the usual definition of

$$\zeta' = \frac{\partial v'}{\partial x'} - \frac{\partial u'}{\partial y'} \tag{4-13}$$

The reason for our definition is simply for computational convenience of handling vast numbers of computed values. This does not make any difference in the results obtained as far as the definition is consistently used throughout the derivation of equations and the computation with them. Equation 4-12, together with Equation 4-11 which is expressed in terms of ψ' on the right hand side, i.e.,

$$\zeta' = \frac{\partial^2 \psi'}{\partial x'^2} + \frac{\partial^2 \psi'}{\partial y'^2} \tag{4-14}$$

makes up the "two-field" expressions - stream function and vorticity formulation - of the Navier-Stokes equations.

It is convenient to work with these expressions being non-dimensionalized. The following non-dimensional variables are introduced:

$$x = x'/R', \quad y = y'/R' \tag{4-15}$$

$$u = u'/\bar{u}', \; v = v'/\bar{u}' \tag{4-16}$$

$$\psi = \psi'/R'\,\bar{u}' \tag{4-17}$$

$$\zeta = \zeta' R'/\bar{u}' \tag{4-18}$$

Thus, the dimensionless Navier-Stokes equations in terms of stream function and vorticity for two-dimensional, steady, incompressible, viscous, Newtonian fluid flow are expressed in rectangular coordinates by

$$\frac{\partial\psi}{\partial y}\frac{\partial\zeta}{\partial x} - \frac{\partial\psi}{\partial x}\frac{\partial\zeta}{\partial y} = \frac{2}{Re}\left[\frac{\partial^2\zeta}{\partial x^2} + \frac{\partial^2\zeta}{\partial y^2}\right] \tag{4-19}$$

$$\zeta = \frac{\partial^2\psi}{\partial x^2} + \frac{\partial^2\psi}{\partial y^2} \tag{4-20}$$

where vorticity and stream function are redefined by

$$\zeta = \frac{\partial u}{\partial y} - \frac{\partial v}{\partial x} \tag{4-21}$$

$$u = \frac{\partial\psi}{\partial y} \tag{4-22}$$

$$v = -\frac{\partial\psi}{\partial x} \tag{4-23}$$

and the Reynolds number is defined by

$$Re = \frac{2R' \, \overline{u}'}{\nu} \tag{4-24}$$

Similarly in the polar coordinate systems, the dimensionless governing equations become

$$\frac{\partial \psi}{\partial r} \frac{\partial \zeta}{r \partial \theta} - \frac{\partial \psi}{r \partial \theta} \frac{\partial \zeta}{\partial r} = \frac{2}{Re} \left[\frac{\partial^2 \zeta}{\partial r^2} + \frac{\partial \zeta}{r \partial r} + \frac{\partial^2 \zeta}{r^2 \partial \theta^2} \right] \tag{4-25}$$

$$\zeta = \frac{\partial^2 \psi}{\partial r^2} + \frac{\partial \psi}{r \partial r} + \frac{\partial^2 \psi}{r^2 \partial \theta^2} \tag{4-26}$$

where

$$r = r'/R' \tag{4-27}$$

$$v_\theta = v'_\theta \,/\, \overline{u}' = \frac{\partial \psi}{\partial r} \tag{4-28}$$

$$v_r = v'_r \,/\, \overline{u}' = - \frac{\partial \psi}{r \partial \theta} \tag{4-29}$$

and

$$\zeta = \frac{1}{r} \left[\frac{\partial}{\partial r}(r \, v_\theta) - \frac{\partial v_r}{\partial \theta} \right] \tag{4-30}$$

Geometry and Boundary Conditions

The geometry employed and the boundary conditions involved in computation are illustrated in the schematic diagram of Figure 11. The reference length taken is the radius of a tube R equal to 1. The distance between upper and lower symmetry lines becomes therefore the transverse pitch ratio P_t.

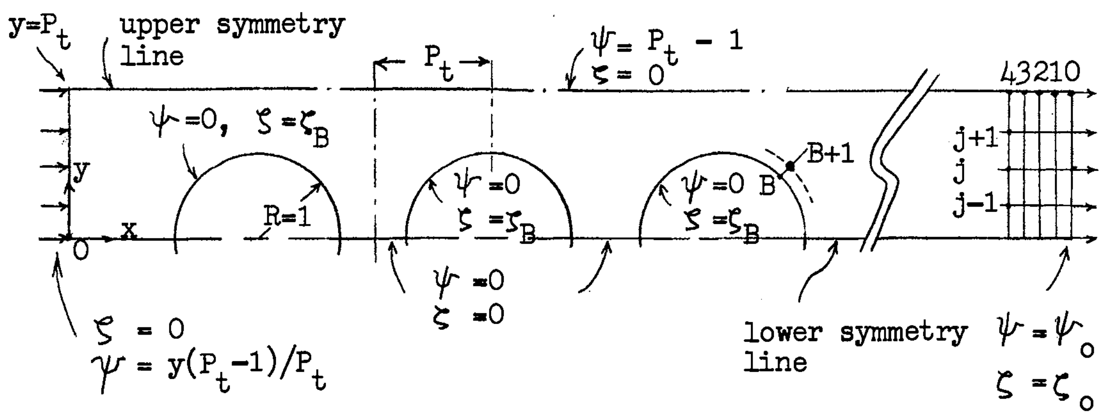

Figure 11. Geometry and Boundary Conditions

Incoming Flow: For uniform inflow, the vorticity is prescribed as zero at an inlet section some distance upstream of the first tube. The stream function is a linear function of the distance from lower symmetry line, i.e., $\psi = y(P_t - 1)/P_t$, such that the incoming flow velocity profile is uniform. The stream function at upper symmetry line $y = P_t$ is set equal to $(P_t - 1)$ so that the volumetric flow rate between lower and upper symmetry lines becomes $(\psi'_{y'=R'P_t} - \psi'_{y'=0})$.

Hence,

$$\psi'_{y'=P_tR'} - \psi'_{y'=0} = \int_0^{P_tR'} \left(\frac{\partial \psi'}{\partial y'}\right) dy' = P_t\, R'\, u'_\infty \qquad (4\text{-}31)$$

but

$$u'_\infty = \bar{u}'(P_t - 1)/P_t \qquad (4\text{-}32)$$

where u'_∞ is the incoming uniform velocity.

From Equations 4-31, 4-32 and 4-17, one gets

$$\psi_{Y = P_t} = \frac{\psi'_{y'=P_t R'}}{\bar{u}' \; R'} = P_t - 1 \qquad (4\text{-}33)$$

Length of the inlet section was about 6.5 R at Re = 1, which furnished an adequate inlet section in which the stream function was uniform to the order of 10^{-4}. It was found that as the Reynolds number increased the diffusion of vorticity upstream became increasingly smaller and consequently the inlet length could be shortened to as little as 2.5 R at Re = 100.

Upper Symmetry Line: Since no mass and momentum transport occurs across the axis of symmetry throughout the tube bank, the following set of conditions is pertinent:

$$\begin{aligned} \psi &= P_t - 1 \\ \zeta &= 0 \end{aligned} \qquad (4\text{-}34)$$

Lower Symmetry Line: Similarly, the following pair of values is set on this boundary;

$$\psi = 0 \quad \text{and} \quad \zeta = 0 \qquad (4\text{-}35)$$

Tube Surface: To satisfy the non-slip condition at the tube surfaces, the normal and tangential gradients of the stream function must be zero at these boundaries. The tangential conditions are satisfied by setting ψ = constant, or more specifically ψ = 0, along the tube surfaces. A special boundary formula which satisfies the normal conditions has to be developed for estimating the vorticity on the tube surfaces.

The technique employed here is similar to that used by Hung and Macagno (31) for specifying boundary conditions at the straight walls of a conduit: essentially, expanding both ψ and ζ in Maclaurin series about the boundary values at the wall and utilizing the governing equations and boundary conditions to provide expressions for the higher order derivatives. The full derivation of the equation is given in Appendix F. The final expression for estimating tube surface vorticity ζ_B is

$$\zeta_B = \left(\frac{1}{1 - \frac{h}{2R} + \frac{3h^2}{8R^2}} \right) \left[\frac{3}{h^2}\psi_{B+1} - \frac{1}{2}\zeta_{B+1} \right] \quad (4\text{-}36)$$

where h is mesh size in r-direction, ψ_{B+1} and ζ_{B+1} are the stream function and the vorticity at the mesh point next to the surface node B, as shown in Figure 11. This expression should be accurate to the order of h^{-3}. Estimation of the tube surface vorticity by Equation 4-36 is done at every computational sweep from upstream inlet section to downstream outlet section.

<u>Outgoing Flow</u>: Outgoing flow at the downstream end must be given careful consideration because the conditions on this outlet section are expected to have a strong influence on the size and configuration of the eddy behind the last tube in tube rows. The condition of uniform velocity distribution must be imposed sufficiently far downstream so that the wake structure behind the last tube is not influenced by computational feedback.

But for computational solution, the length of outlet section should be as short as compatible with the desired accuracy and computational effort required. Instead of imposing a particular profile at the outlet section, e.g., $\psi = y(P_t - 1)/P_t$ and $\zeta = 0$, a rather more flexible and plausible condition is prescribed based on Milne's predictor formula at every iteration (34):

$$\zeta_{o,j} = \zeta_{4,j} - 2\,\zeta_{3,j} + 2\,\zeta_{1,j} \qquad (4\text{-}37)$$

$$\psi_{o,j} = \psi_{4,j} - 2\,\psi_{3,j} + 2\,\psi_{1,j} \qquad (4\text{-}38)$$

where j is the index for y-coordinate at the outlet region (Figure 11). These formulae have been successfully used by Hung and Macagno (31) to project the trend resulting from upstream flow patterns, and the result is adopted as valid for the next iteration. This method was checked against the results obtained with fixed outlet profile, i.e., $\zeta = 0$ and $\psi = y(P_t - 1)/P_t$, at Re = 1, 5, and 10 for P_t = 1.50, and was found completely satisfactory.

The distance of the downstream end from the last tube of three tube rows was about 6.5 times the tube radius or 6.5 R for Re = 1 to 18.5 R for Re =100 for both pitch ratios.

Finite Difference Approximation

The simplest central difference scheme with second order accuracy has been widely accepted for the finite difference expressions as an approximation of the Navier-Stokes equations without extreme complications of the higher order formulations. Thus the central differencing formula adopted here (35) is, for the first derivative;

$$\frac{\partial[\ ]_{i,j}}{\partial x} = \frac{[\ ]_{i+1,j} - [\ ]_{i-1,j}}{2h} + O(h^2) \tag{4-39}$$

and for the second derivative (35);

$$\frac{\partial^2[\ ]_{i,j}}{\partial x^2} = \frac{[\ ]_{i+1,j} - 2[\ ]_{i,j} + [\ ]_{i-1,j}}{h^2} + O(h^2) \tag{4-40}$$

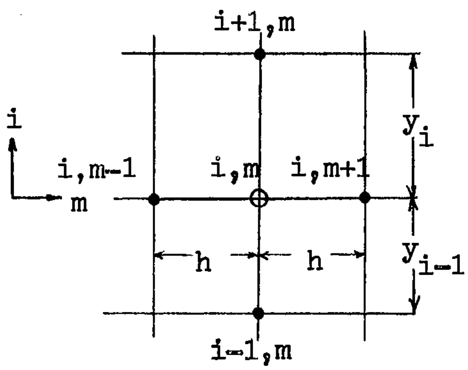

Figure 12.

Rectangular Field Nodes

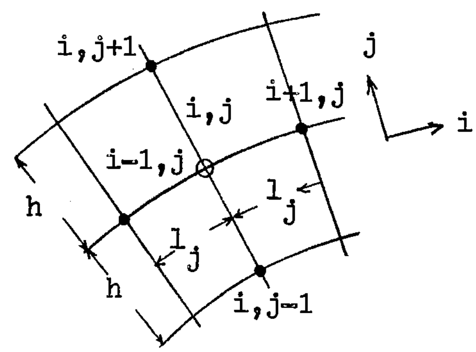

Figure 13.

Polar Field Nodes

Finite difference expressions of the governing equations 4-19 and 4-20 with variable rectangular mesh sizes in y- or j-direction may be written in rectangular coordinate system (Figure 12), respectively;

$$\frac{\psi^k_{i+1,m}-\psi^{k+1}_{i-1,m}}{y_i+y_{i-1}}\,\frac{\zeta^k_{i,m+1}-\zeta^{k+1}_{i,m-1}}{2h} - \frac{\psi^k_{i,m+1}-\psi^{k+1}_{i,m-1}}{2h}\,\frac{\zeta^k_{i+1,m}-\zeta^{k+1}_{i-1,m}}{y_i+y_{i-1}} =$$
$$\frac{2}{Re}\left[\frac{\zeta^k_{i,m+1}-2\zeta^{k+1}_{i,m}+\zeta^{k+1}_{i,m-1}}{h^2} + \frac{2}{y_i y_{i-1}(y_i+y_{i-1})}(y_{i-1}\zeta^k_{i+1,m}+y_i\zeta^{k+1}_{i-1,m})\right.$$
$$\left. - \frac{2}{y_i y_{i-1}}\zeta^{k+1}_{i,m}\right] \tag{4-41}$$

and

$$\zeta^{k+1}_{i,m} = \frac{\psi^{k}_{i,m+1} - 2\psi^{k+1}_{i,m} + \psi^{k+1}_{i,m-1}}{h^2} + \frac{2}{y_i y_{i-1}(y_i + y_{i-1})}[y_{i-1}\psi^{k}_{i+1,m}$$

$$+ y_i \psi^{k+1}_{i-1,m}] - \frac{2}{y_i y_{i-1}} \psi^{k+1}_{i,m} \tag{4-42}$$

where superscript k denotes the iteration number.

After rearrangement of the equations, one gets the following working formulae,

$$\zeta^{k+1}_{i,m} = \left(\frac{1}{h^2 + y_i y_{i-1}}\right)\Big[\frac{y_i y_{i-1}}{2}(\zeta^{k}_{i,m+1} + \zeta^{k+1}_{i,m-1}) + \frac{h^2}{y_i + y_{i-1}}(y_{i-1}\zeta^{k}_{i+1,m}$$

$$+ y_i \zeta^{k+1}_{i-1,m}) + \frac{Rehy_i y_{i-1}}{8(y_i + y_{i-1})}\Big\{(\psi^{k}_{i,m+1} - \psi^{k+1}_{i,m-1})(\zeta^{k}_{i+1,m}$$

$$- \zeta^{k+1}_{i-1,m}) - (\psi^{k}_{i+1,m} - \psi^{k+1}_{i-1,m})(\zeta^{k}_{i,m+1} - \zeta^{k+1}_{i,m-1})\Big\}\Big] \tag{4-43}$$

and

$$\psi^{k+1}_{i,m} = \left(\frac{1}{h^2 + y_i y_{i-1}}\right)\Big[\frac{y_i y_{i-1}}{2}(\psi^{k}_{i,m+1} + \psi^{k+1}_{i,m-1}) + \frac{h^2}{y_i + y_{i-1}}(y_{i-1}\psi^{k}_{i+1,m}$$

$$+ y_i \psi^{k+1}_{i-1,m}) - \frac{h^2 y_i y_{i-1}}{2}\zeta^{k+1}_{i,m}\Big] \tag{4-44}$$

Similarly in the polar coordinate systems of Figure 13, Equations 4-25 and 4-26 are approximated by the following finite difference expressions, respectively;

$$\frac{\psi^{k}_{i,j+1}-\psi^{k+1}_{i,j-1}}{2l_j}\,\frac{\zeta^{k}_{i+1,j}-\zeta^{k+1}_{i-1,j}}{2h}-\frac{\psi^{k}_{i+1,j}-\psi^{k+1}_{i-1,j}}{2h}\,\frac{\zeta^{k}_{i,j+1}-\zeta^{k+1}_{i,j-1}}{2l_j}$$

$$=\frac{2}{Re}\left[\frac{\zeta^{k}_{i,j+1}-2\zeta^{k+1}_{i,j}+\zeta^{k+1}_{i,j-1}}{h^2}+\frac{\zeta^{k}_{i,j+1}-\zeta^{k+1}_{i,j-1}}{2rh}+\frac{\zeta^{k}_{i+1,j}-2\zeta^{k+1}_{i,j}+\zeta^{k+1}_{i-1,j}}{l_j^2}\right] \tag{4-45}$$

and

$$\zeta^{k+1}_{i,j}=\frac{\psi^{k}_{i,j+1}-2\psi^{k+1}_{i,j}+\psi^{k+1}_{i,j-1}}{h^2}+\frac{\psi^{k}_{i,j+1}-\psi^{k+1}_{i,j-1}}{2rh}+\frac{\psi^{k}_{i+1,j}-2\psi^{k+1}_{i,j}+\psi^{k+1}_{i-1,j}}{l_j^2} \tag{4-46}$$

After rearrangement, one obtains

$$\zeta^{k+1}_{i,j}=\frac{h^2l_j^2}{2(h^2+l_j^2)}\left[\frac{\zeta^{k}_{i,j+1}+\zeta^{k+1}_{i,j-1}}{h^2}+\frac{\zeta^{k}_{i,j+1}-\zeta^{k+1}_{i,j-1}}{2rh}+\frac{\zeta^{k}_{i+1,j}+\zeta^{k+1}_{i-1,j}}{l_j^2}\right]+\frac{Re\,h\,l_j}{16(h^2+l_j^2)}\left[(\psi^{k}_{i+1,j}-\psi^{k+1}_{i-1,j})(\zeta^{k}_{i,j+1}-\zeta^{k+1}_{i,j-1})-(\psi^{k}_{i,j+1}-\psi^{k+1}_{i,j-1})(\zeta^{k}_{i+1,j}-\zeta^{k+1}_{i-1,j})\right] \tag{4-47}$$

and

$$\psi^{k+1}_{i,j}=\frac{h^2l_j^2}{2(h^2+l_j^2)}\left[\frac{\psi^{k}_{i,j+1}+\psi^{k+1}_{i,j-1}}{h^2}+\frac{\psi^{k}_{i,j+1}-\psi^{k+1}_{i,j-1}}{2rh}+\frac{\psi^{k}_{i+1,j}+\psi^{k+1}_{i-1,j}}{l_j^2}-\zeta^{k+1}_{i,j}\right] \tag{4-48}$$

Equations 4-43 and 4-44 for rectangular sections, and Equations 4-47 and 4-48 for polar sections may be used for iterative computation of the inner fields (i.e., field not including boundary and matching planes) of the respective coordinate sections. But expecting quicker convergence, the method of successive over-relaxation was incorporated into the stream function computation. The over-relaxation parameter proposed by Russel (36)

$$\omega = \frac{2}{1 + \pi\sqrt{\frac{I^2 + J^2}{2I^2J^2}}} \qquad (4\text{-}49)$$

was adopted for iterative computation at inner mesh points, where I and J are number of increments in i- and j-direction respectively. This equation has been found to give good values of the relaxation parameter by Son and Hanratty (30). The finite difference equations with over-relaxation parameter ω are thus expressed as follows:

In rectangular coordinates, from Equation 4-43,

$$\psi^{k+1}_{i,m} = (1-\omega)\psi^{k}_{i,m} + \frac{\omega}{h^2 + y_i y_{i-1}} \left[\frac{y_i y_{i-1}}{2} (\psi^{k}_{i,m+1} + \psi^{k+1}_{i,m-1}) + \frac{h^2}{y_i + y_{i-1}} (y_{i-1}\psi^{k}_{i+1,m} + y_i \psi^{k+1}_{i-1,m}) - \frac{h^2 y_i y_{i-1}}{2} \zeta^{k+1}_{i,m} \right] \qquad (4\text{-}50)$$

and in polar coordinates, from Equation 4-47,

$$\psi^{k+1}_{i,m} = (1-\omega)\psi^{k}_{i,m} + \frac{\omega h^2 l_j^2}{2(h^2 + l_j^2)} \left[\frac{\psi^{k}_{i,j+1} + \psi^{k+1}_{i,j-1}}{h^2} + \frac{\psi^{k}_{i,j+1} - \psi^{k+1}_{i,j-1}}{2rh} + \frac{\psi^{k}_{i+1,j} + \psi^{k+1}_{i-1,j}}{l_j^2} - \zeta^{k+1}_{i,j} \right] \qquad (4\text{-}51)$$

Equations 4-44 and 4-50 in rectangular coordinate systems and Equations 4-48 and 4-51 in polar coordinates constitute the working formulae for inner mesh points of the system.

No quantitative test of this successive over-relaxation method against the ordinary iterative computation has been made, but from preliminary computations Equations 4-50 and 4-51 seemed to give definite indication of convergence with fewer iterations required than the iterative computation by Equations 4-43 and 4-47.

Coordinate Arrangement

Rectangular and polar coordinate systems are conveniently arranged in such a way that calculated values of stream function and vorticity at the boundary in one unit cell can be most easily transmitted to another at the matching plane. The coordinate arrangement is illustrated in Figure 14. Table I gives the field definition of variable parameters and constants in Figure 14 for Re = 100 and P_t = 1.50 as a representative case.

The detailed description of the working equations used at the matching planes as well as at the boundary regions is presented in Appendix I.

Computer Program

Flow Chart

The general computational sequence of the program for numerical iterative solution of the Navier-Stokes equations of tube bank flow is shown in the schematic diagram of Figure 15. The basic feature of the program is that the computation is broken down into sub-calculations with specific and independent functions, which allows debugging and major

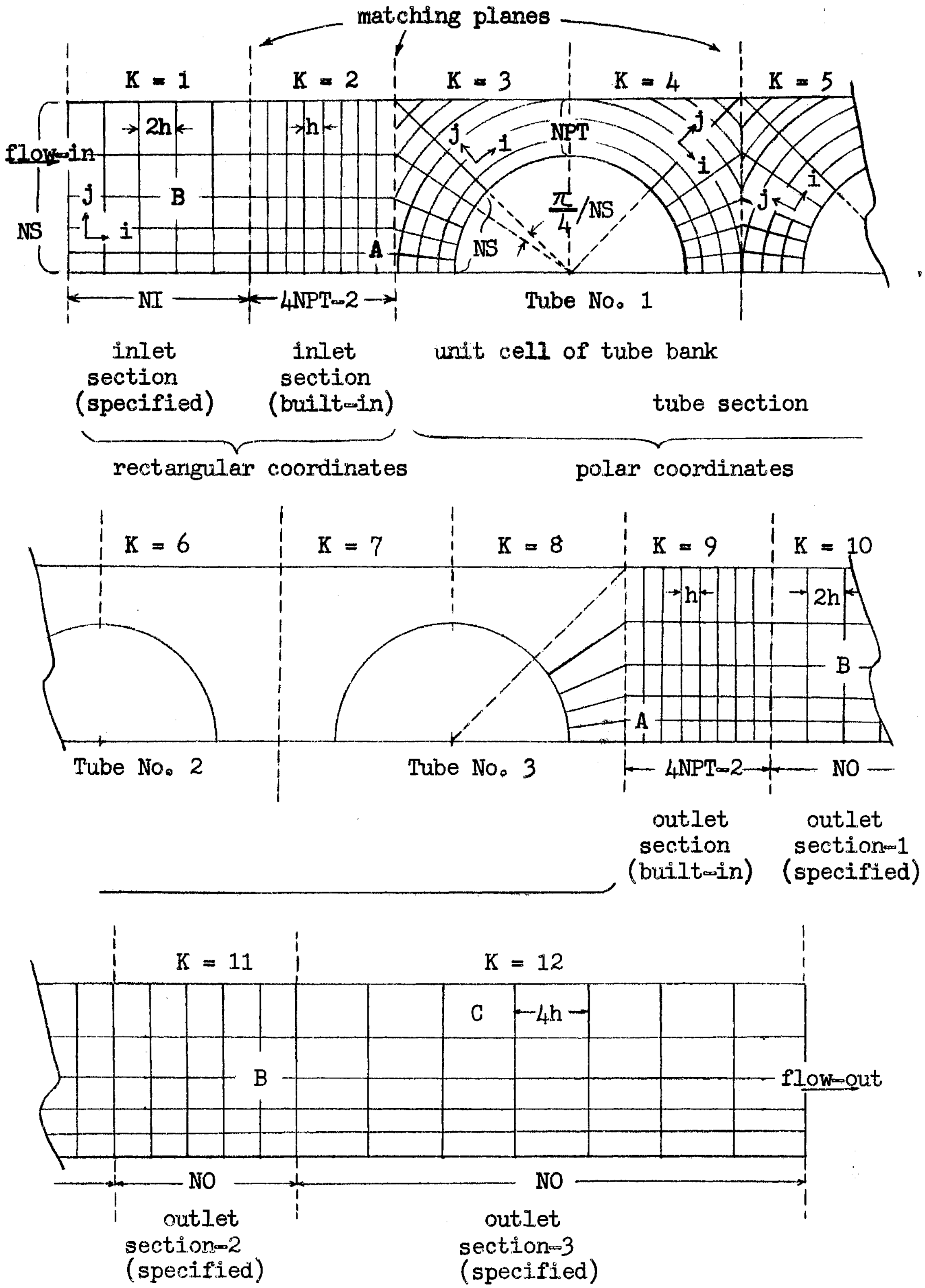

Figure 14. Coordinate Arrangement

TABLE I

FIELD DEFINITION OF VARIABLE PARAMETERS AND CONSTANTS FOR Re = 100 and P_t = 1.50

Section I.D. number K	Number of increments in i-direction	Number of increments in j-direction	total field points in a section	Mesh size in x- or r-direction
1	NI = 10	NS = 18	153	2h=0.1
2	4NPT-2= 38	NS = 18	646	h=0.05
3 - 8	2NS+1= 39	Variable: NPT $\sim 2P_t/h$ = 10 $\sim$ 23	470 (for each of 6 sections)	h=0.05
9	4NPT-2= 38	NS = 18	646	h=0.05
10	NO = 39	NS = 18	646	2h=0.1
11	NO = 39	NS = 18	646	2h=0.1
12	NO = 39	NS = 18	646	4h=0.2

Total field points in entire system = 6203

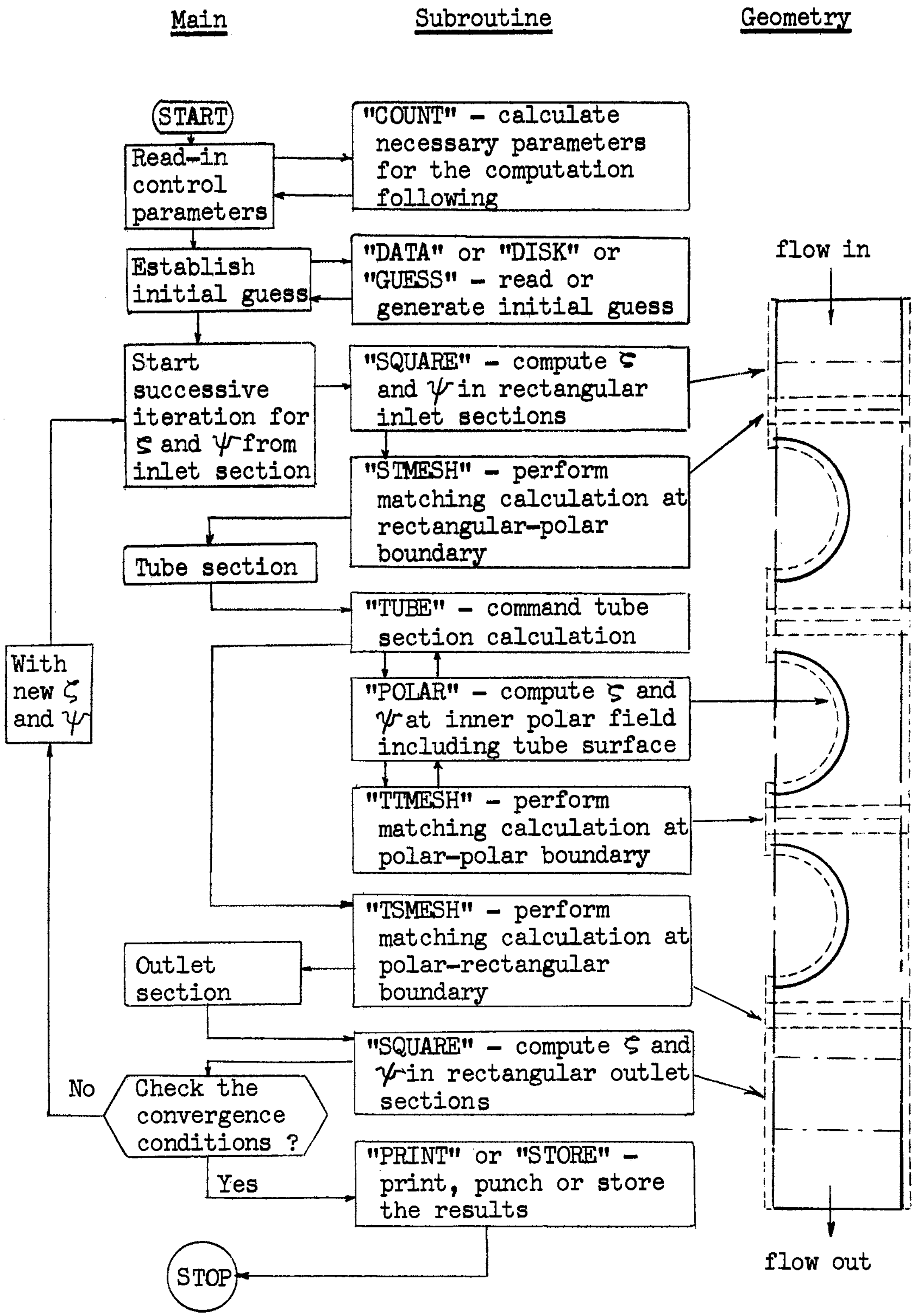

Figure 15. Computer Block Diagram for Vorticity and Stream Function Calculation

changes in working formulae without disturbing the over-all program.

The complete description of the main program, the subroutine functions, the required input data and format, and the control parameters for the operation of the program are presented in Appendix I.

Computational Procedure

Initialization of a computation consists of reading the necessary control parameters of the program operation as first input data and defining a set of constants based on the parameters. Then a tagged array is established to define every mesh point in rectangular and polar coordinate sections. The format of the subsequent calculation at each point of various parts of the solution is determined by the tag values of the point to be calculated.

In order to reduce the number of iterations needed, the initial guess should be as close as possible to the expected solution. The initial guess used at Re = 1 for $P_t = 1.50$ and 1.25 with h = 0.10 and also at Re = 10 for $P_t = 1.50$ with h = 0.05 was the Poiseulle flow profile between infinite parallel flat plates applied for non-uniform tube bank channel.

The computation proceeded from rectangular inlet section to the rectangular outlet section, marching down through series of three unit cells of the tube bank in polar coordinates by alternative computation of ζ and then ψ at every mesh point utilizing Equations 4-36, 4-44, 4-50, 4-47, 4-51 and also their boundary point formulae with iterative field values and prescribed boundary values. Once a solution is obtained for a given Reynolds number, then this is used as starting solution for the next higher value of Reynolds number.

Convergence Criterion

Thom and Apelt (37) have studied the effect of small computational disturbance introduced into a two-dimensional vorticity field and obtained a convergence criterion for a square mesh. Lester (38) has generalized this work to include a rectangular mesh and shown the disturbance will not grow in magnitude provided that

$$\frac{h}{L}\,\mathrm{Re} < \sqrt{8\left(3q^2 + 4 + \frac{3}{q^2}\right)} \qquad (4\text{-}52)$$

where L is the characteristic length of the system and q is the ratio of the mesh length in y-direction to that in the x-direction. Lester also found that a convergence criterion based on stream function is less stringent than that on vorticity field. It has been found that the condition given by Equation 4-52 gives some indication as to where divergence is likely to occur.

In polar coordinate sections, mesh sizes are generally smaller than those in rectangular sections as is seen in Figure 14. The computational stability for the entire tube bank is therefore safely defined in rectangular sections alone, provided that the condition given by Equation 4-52 is valid in polar coordinate systems.

As the order-of-magnitude indication test of condition given by Equation 4-52, the maximum attainable Reynolds number was calculated from the equation for the basic mesh size in the x- or r-direction, that is, h = 0.05. This mesh size was used in all the computations but Re = 1, 5, and 10 for P_t = 1.50.

There are three regions in rectangular sections which give representative mesh size for comparison (Figure 14).

A. Smallest mesh size region at the lower corner of sections $K = 2$ and $K = 9$ of built-in inlet and outlet section, where $h = 0.05$ and

$$Re < \sqrt{40}\left(\frac{h}{L}\right) = \sqrt{40}\left(\frac{0.05}{1.0}\right) = 127$$

B. Medium mesh size region at the middle field of sections $K = 1$, $K = 10$ and $K = 11$, where $h = 0.10$ and

$$Re < 63.4$$

C. Largest mesh size region at the upper corner of section $K = 12$, where $h = 0.20$ and

$$Re < 31.7$$

For the above system with basic mesh size of 0.05, actual converged solutions have been obtained at Reynolds number up to 100, but the computation diverged at the second iteration when $Re = 150$ for $P_t = 1.50$ was attempted using the solution at $Re = 100$.

The condition to be observed for a stable converged solution is that the fractional change on the vorticity and stream function at any point over a iterative step is small. Termination of iterative computation is set by the following arbitrary empirical condition:

$$\sum_{i,j} \left(\psi^{k+1}_{i,j} - \psi^{k}_{i,j}\right) < 0.5 \qquad (4\text{-}53)$$

and

$$\sum_{i,j} (\zeta^{k+1}_{i,j} - \zeta^{k}_{i,j}) < 0.5 \tag{4-54}$$

It was found that in this particular problem $\sum_{i,j}(\psi^{k+1}_{i,j} - \psi^{k}_{i,j})$ was about one-fifth of $\sum_{i,j}(\zeta^{k+1}_{i,j} - \zeta^{k}_{i,j})$.

At the most severe case for convergence of the solution at Re = 100 and P_t = 1.50, the maximum difference in the vorticity at a middle-field mesh point of about one radius downstream from the last tube row was found to be 0.0038 between the fiftieth iteration and the ninety-second iteration at which the convergence conditions were reached. The maximum vorticity in the entire field, ζ_{max}, was 10.1 at a surface point of the first tube row, thus giving

$$\frac{[\zeta^{92} - \zeta^{50}]_{max}}{\zeta_{max}} = 0.0004 \tag{4-55}$$

Considering the number of iterative steps covered, this would indicate the stringent conditions imposed by Equations 4-53 and 4-54 compared with the convergence conditions used elsewhere; e.g., by Mills (32)

$$\frac{\zeta^{k+1}_{i,j} - \zeta^{k}_{i,j}}{\zeta_{max}} < 0.0001 \tag{4-56}$$

and

$$\frac{\psi^{k+1}_{i,j} - \psi^{k}_{i,j}}{\psi_{max}} < 0.00003 \tag{4-57}$$

where the changes on vorticity and stream function are taken over a single iterative step, and by Hung and Macagno (31),

$$\frac{\zeta_{i,j}^{k+10} - \zeta_{i,j}^{k}}{\zeta_{max}} < 0.0001 \tag{4-58}$$

and

$$\frac{\psi_{i,j}^{k+10} - \psi_{i,j}^{k}}{\psi_{max}} < 0.000015 \tag{4-59}$$

where ten iterative steps are taken for calculating the fractional changes.

CHAPTER V

PRESENTATION AND DISCUSSION OF RESULTS

Converged Solutions

The series of calculations were started at Re = 1 in both cases of $P_t = 1.50$ and $P_t = 1.25$, in which the Poiseuille flow profile between infinite flat plates applied for non-uniform tube bank channel was used to generate the initial guess of the stream function and the vorticity.

A series of resulting flow patterns and their corresponding vorticity contours are shown in Figures 16 to 28 at Reynolds numbers 1 to 100 for pitch ratios of 1.50 and 1.25. The plotting of the contours was done by the CALCOMP 565 digital plotter hooked up to the IBM 360 Model 65 computer. The computer programs developed for plotting instructions are presented in Appendix J. The mesh size of x- and r-direction was 0.10 at Re = 1, 5 and 10 for $P_t = 1.50$ and h = 0.05 for the rest of the cases. At Re = 10 of $P_t = 1.50$, the two solutions with both mesh sizes were obtained for comparison and found that the two results were almost identical except minor details in the eddy regions. The mesh size of 0.05 was sufficiently small for resolving the detailed flow patterns in the eddy regions and in the wake-bubble (i.e., eddy region enclosed by contour of zero stream function appearing behind the last tube row).

Figure 16 and Figure 23 show that, even for Re = 1, small eddies exist between tubes in the tube. The stream functions at each corresponding mesh point in two eddies formed between tube number 1 and tube

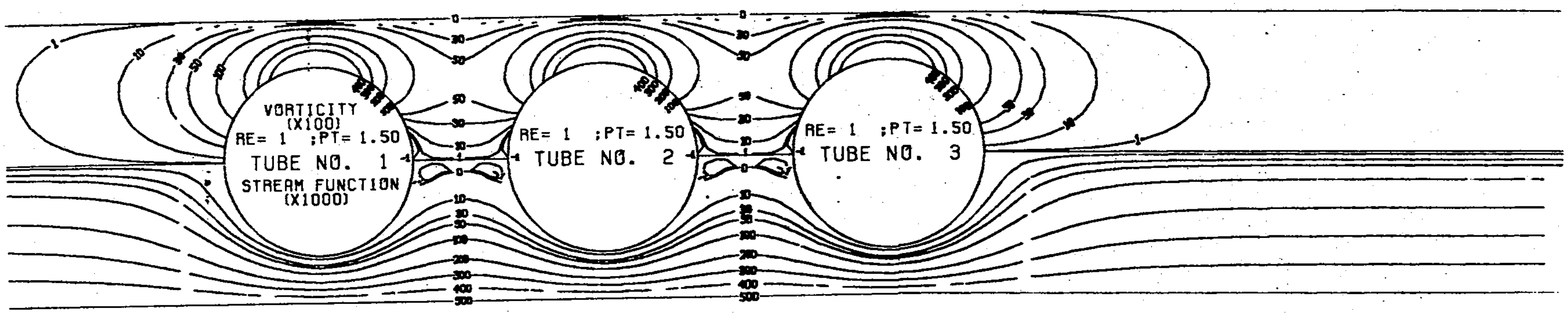

Figure 16. Contours of Vorticity and Stream Function (Re=1;P_t=1.50;h=0.10)

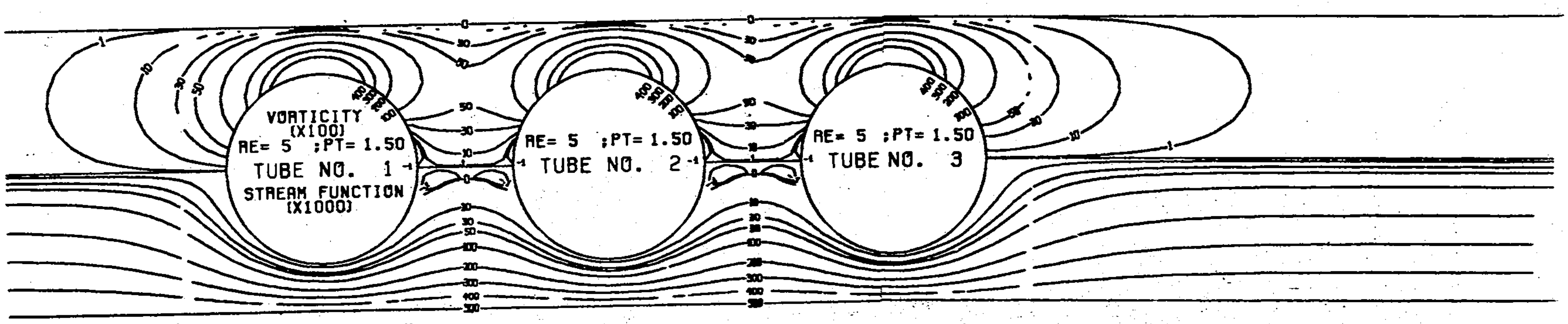

Figure 17. Contours of Vorticity and Stream Function (Re=5;P_t=1.50;h=0.10)

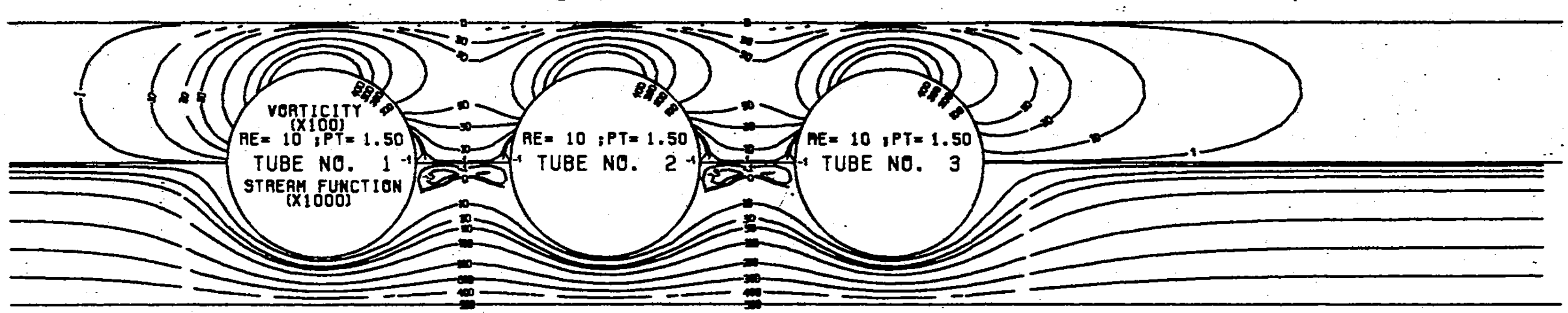

Figure 18. Contours of Vorticity and Stream Function (Re=10;P_t=1.50;h=0.10)

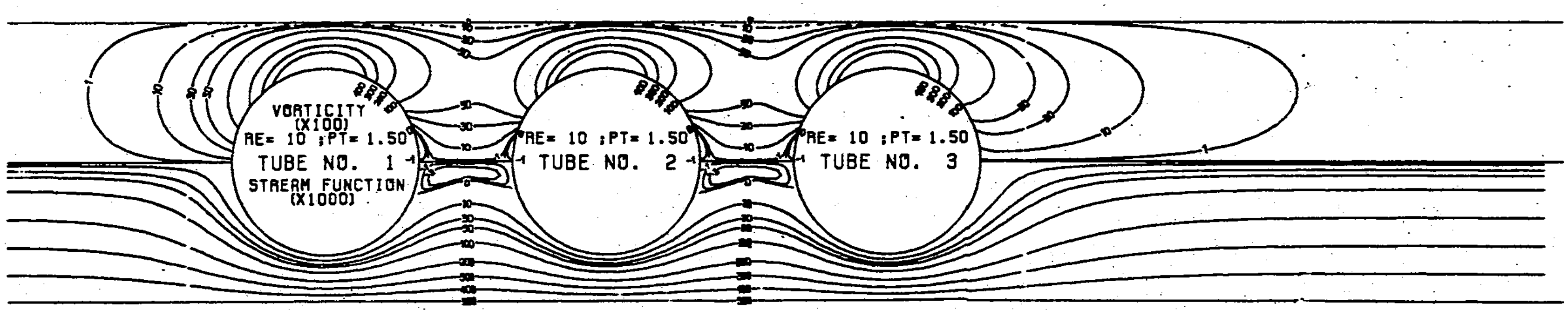

Figure 19. Contours of Vorticity and Stream Function (Re=10;P_t=1.50;h=0.05)

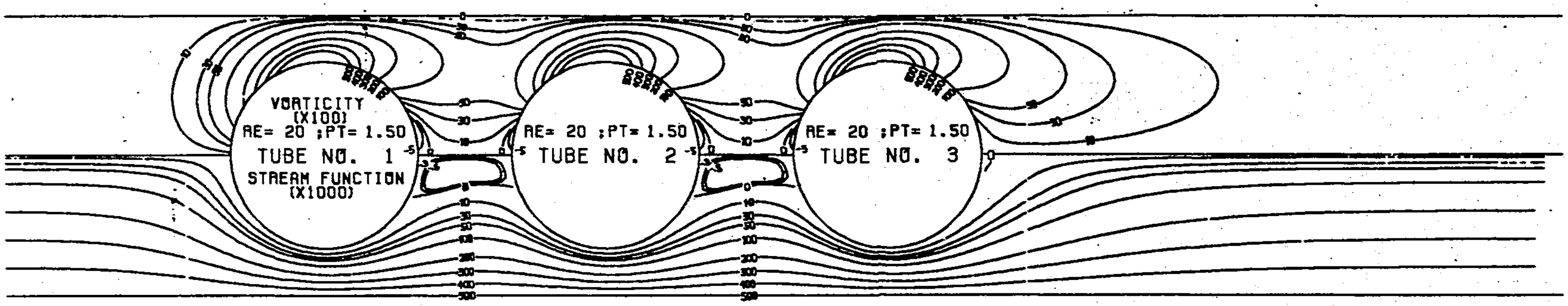

Figure 20. Contours of Vorticity and Stream Function (Re=20;P_t=1.50;h=0.05)

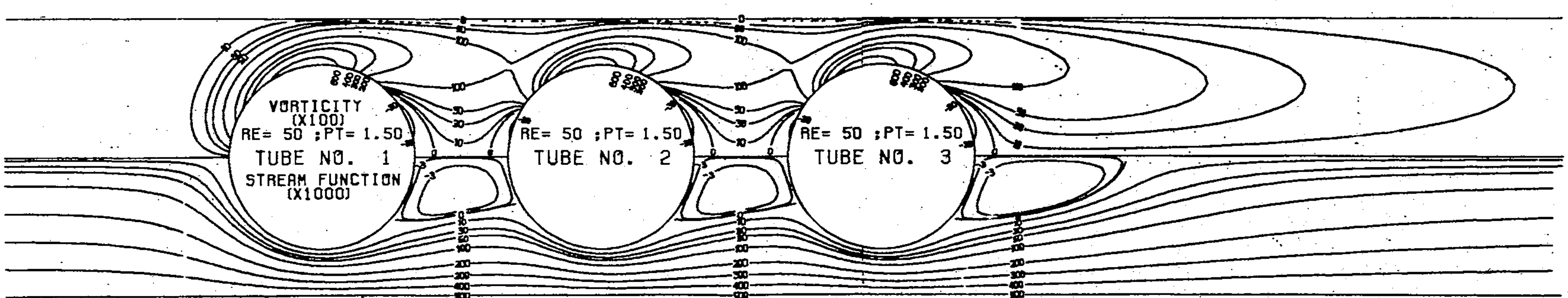

Figure 21. Contours of Vorticity and Stream Function (Re=50;P_t=1.50;h=0.05)

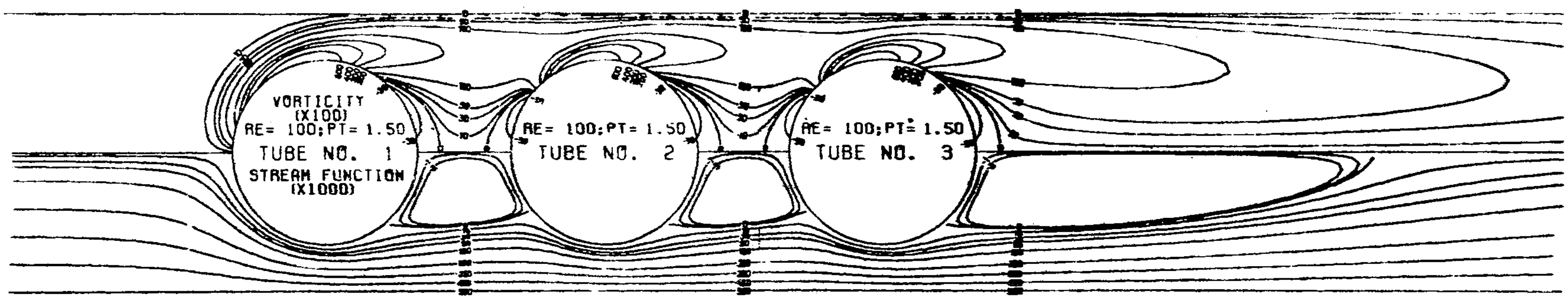

Figure 22. Contours of Vorticity and Stream Function (Re=100;P_t=1.50;h=0.05)

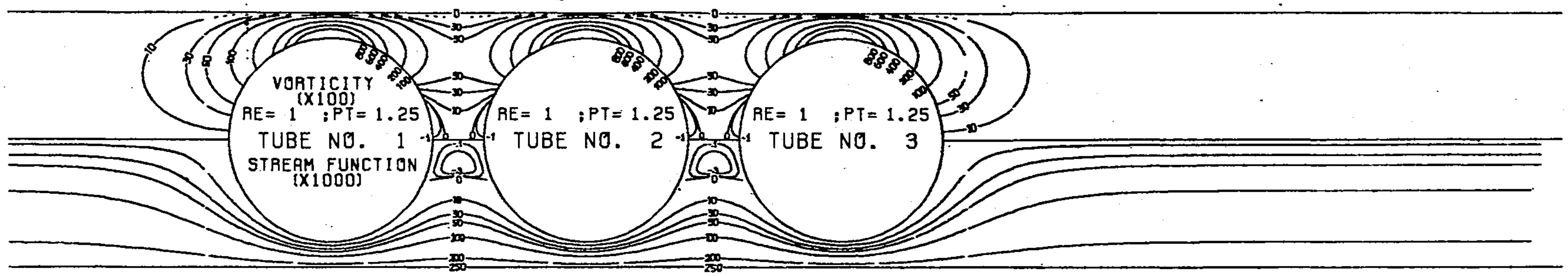

Figure 23. Contours of Vorticity and Stream Function (Re=1;P_t=1.25;h=0.05)

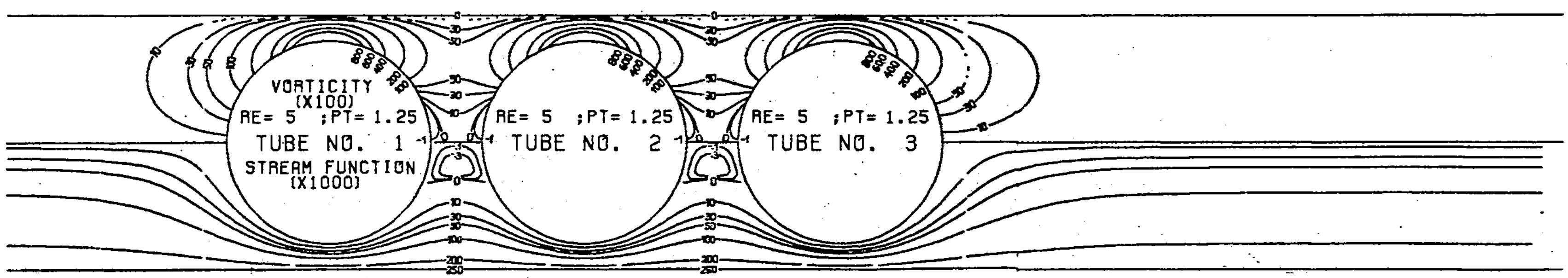

Figure 24. Contours of Vorticity and Stream Function (Re=5;P_t=1.25;h=0.05)

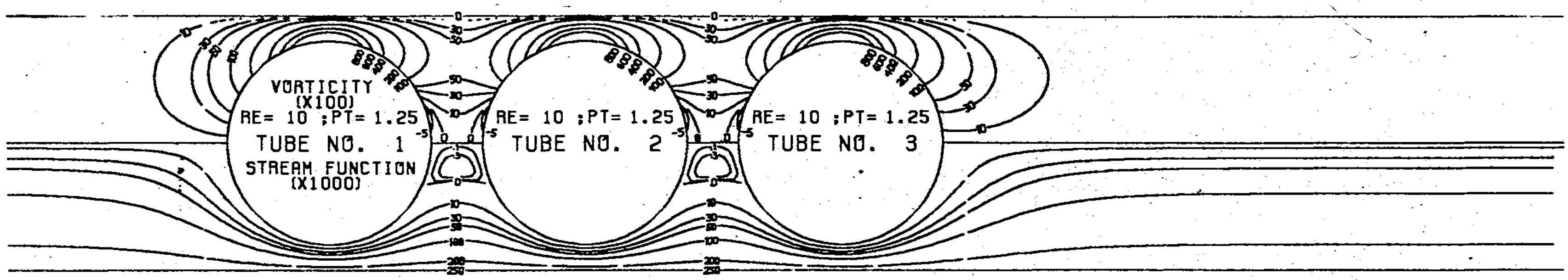

Figure 25. Contours of Vorticity and Stream Function (Re=10; P_t=1.25; h=0.05)

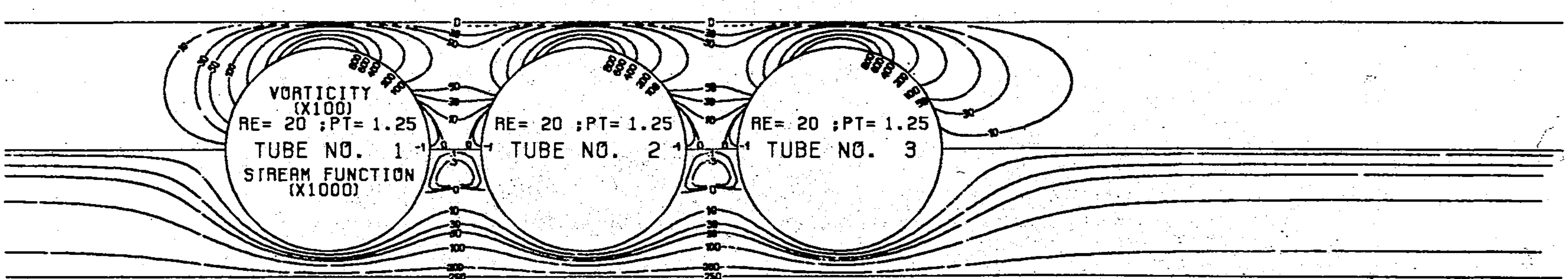

Figure 26. Contours of Vorticity and Stream Function (Re=20; P_t=1.25; h=0.05)

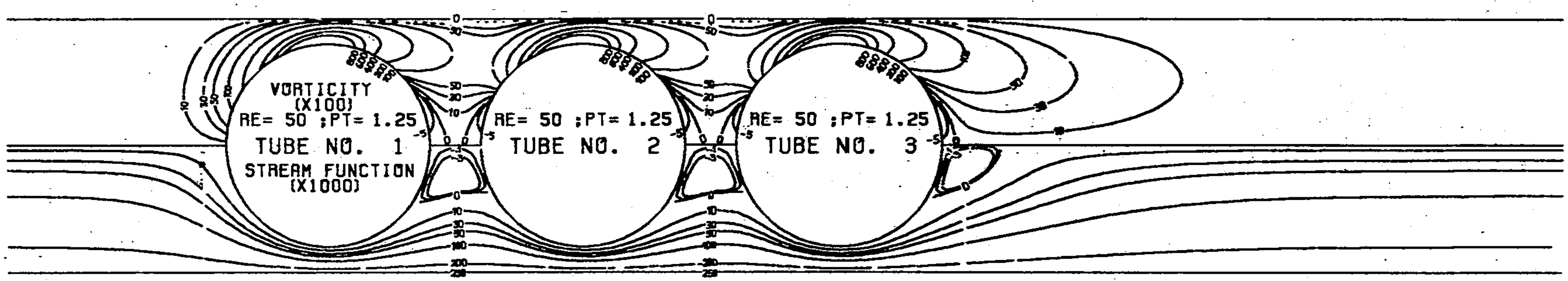

Figure 27. Contours of Vorticity and Stream Function (Re=50; P_t=1.25; h=0.05)

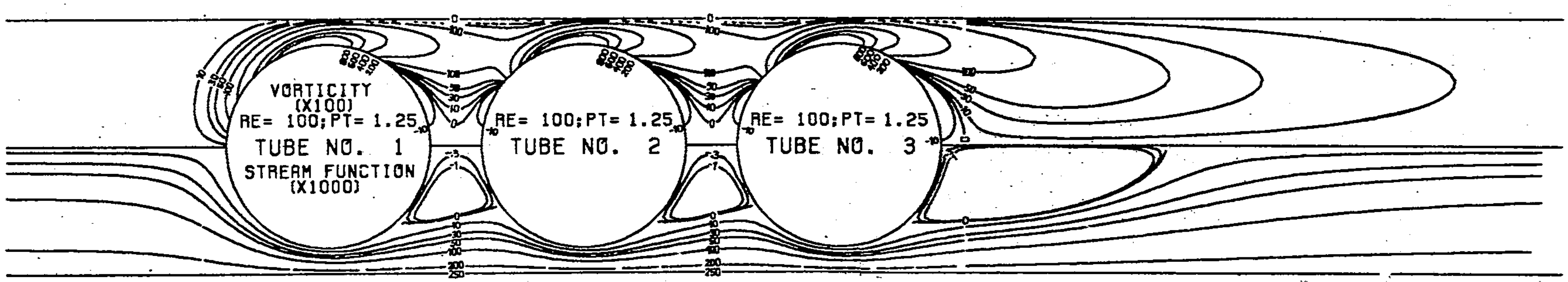

Figure 28. Contours of Vorticity and Stream Function (Re=100; P_t=1.25; h=0.05)

number 2, and between tube number 2 and tube number 3 are found to be almost identical. As the Reynolds number is increased, the eddies grow in size and the point of detachment on the leeward part of the tube and the point of reattachment on the front part of the next tube (Figure 29) creeps up toward the point of minimum clearance of tube bank flow channel. The angles of detachment and reattachment on the second tube are given in Table II and also plotted in Figure 30 and Figure 31 as a function of Reynolds number.

Although there has been no reported experimental visual evidence in this Reynolds number range of eddies formed between tubes in the tube bank, Acrivos et al.(39) have obtained photographed flow patterns of the confined cavity formed between two backward facing steps perpendicular to the free stream at relatively low Reynolds numbers. Their pictures give some qualitative evidence to the calculated stream line profiles of eddies in the tube bank flow.

The wake behind the last tube row in the tube bank does not appear until Reynolds number exceeds 20, which compares with the first appearance of wake at the Reynolds number of 5 in case of a uniform flow past a cylinder (40) where the Reynolds number defined is based on the velocity of undisturbed flow. The sizes of the wake-bubbles in tube bank flow at Re = 50 and Re = 100 are smaller than those observed behind a single cylinder in a uniform flow at the corresponding Reynolds numbers. This may be explained by the presence of straight downstream channel of tube bank where the flow is contained in the narrow region into which the wake has to expand, thus suppressing the wake growth and formation. On the other hand, in case of uniform flow past a cylinder the flow field is infinite and the wake-bubble behind the cylinder is unconstrained.

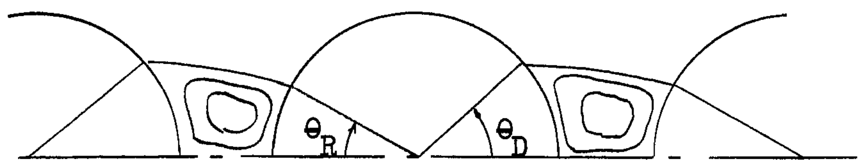

Figure 29. Angles of Separation on a Tube

TABLE II

ANGLES OF SEPARATION FOR THE SECOND TUBE

Pitch ratio P_t	Reynolds number Re	Angles of detachment (degrees) θ_D	Angles of reattachment (dergees) θ_R
1.50	1	17	16
	5	19	17
	10	21	18.5
	20	28	21
	50	44	30
	100	52	38
1.25	1	24	23
	5	24	23.5
	10	25	24
	20	26	24
	50	34	28
	100	50	36

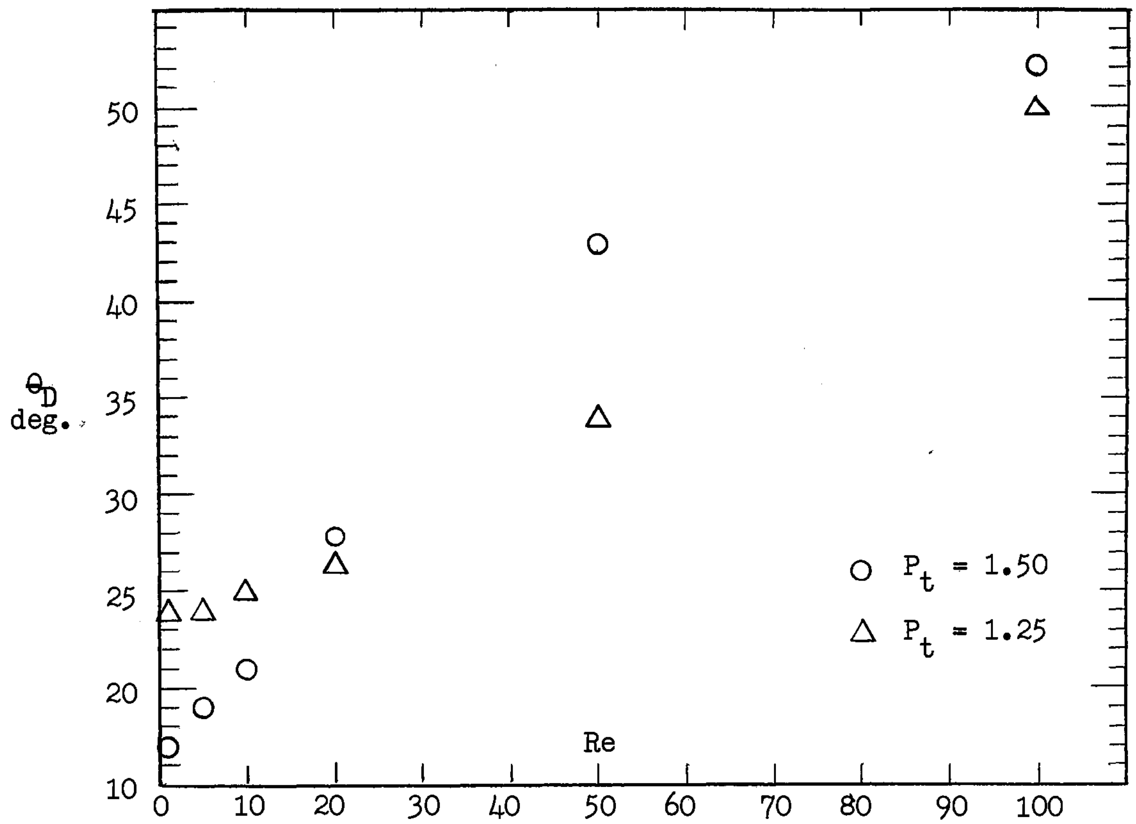

Figure 30. Angle of Detachment vs. Reynolds Number for the Second Tube

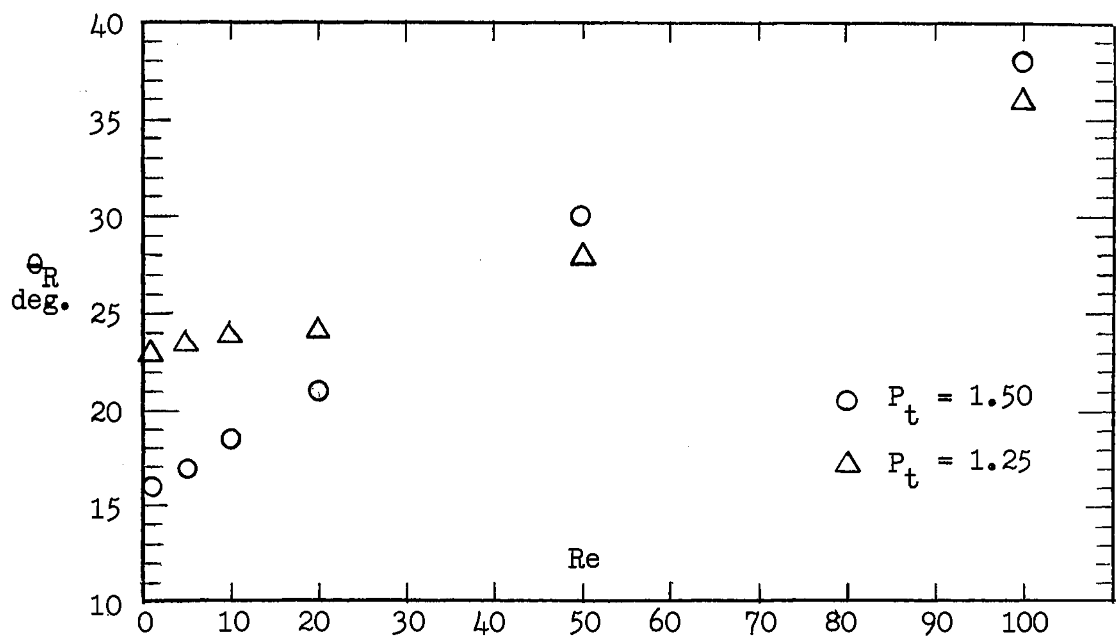

Figure 31. Angle of Reattachment vs. Reynolds Number for the Second Tube

As the Reynolds number increases, the vorticity is carried away further downstream by convection, while the diffusion of vorticity upstream toward the entrance from the first tube row of the tube bank becomes smaller. In general, the shape of wake-bubble and the corresponding vorticity contours behind the last tube row of the tube bank are more elongated in the direction of flow than those in case of uniform flow past a single cylinder.

Figures 32 to 44 show the vorticity around the tube surfaces of three tube rows for all the Reynolds numbers and pitch ratios covered. The point of maximum vorticity appears about on the tube surface of minimum clearance of tube bank while in case of flow past a single cylinder the point of maximum vorticity is situated on the forward part of the cylinder.

Form Drag and Friction Drag

Once the converged numerical solution is obtained, the pressure variation along the tube surface, the form drag coefficient and the friction drag coefficient can be calculated from the tube surface vorticity and its gradient around the tube surface. The full derivation of the equations used in this section is presented in Appendix G.

The final expression of pressure variation around the tube surface is given as

$$P^*(\theta) = P_o^* + \frac{4}{Re}\int_0^\theta \left[\frac{\partial \zeta}{\partial r}\right]_{r=R} R \, d\theta \qquad (5\text{-}1)$$

where pressure has been normalized with respect to $\frac{1}{2}\rho\bar{u}^2$ and P_o^* is the normalized pressure at the front stagnation point.

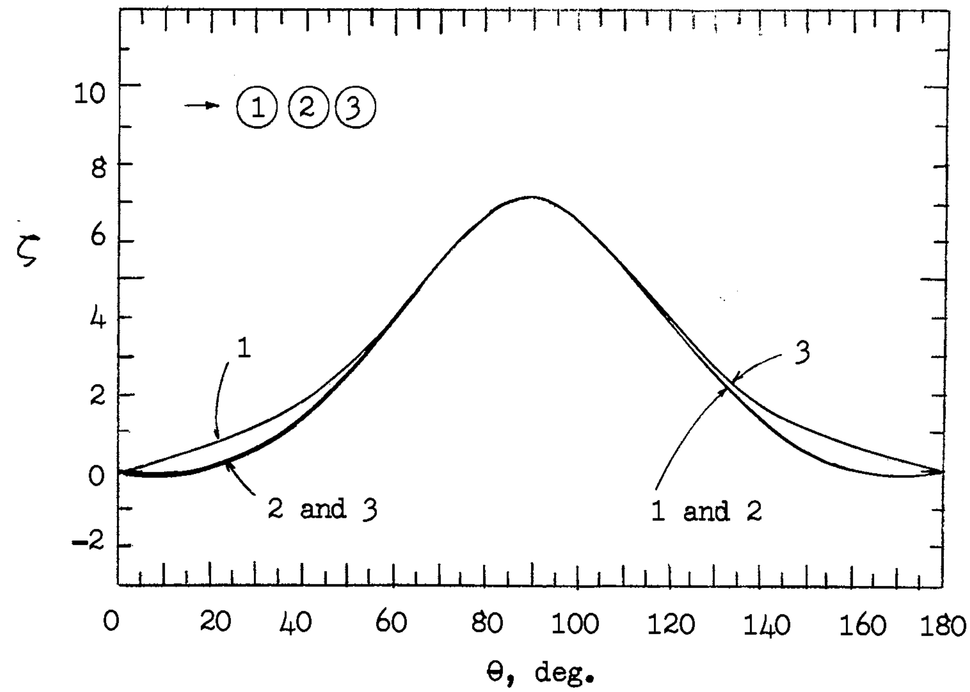

Figure 32. Vorticity Around the Tube
($Re = 1$; $P_t = 1.50$; $h = 0.10$)

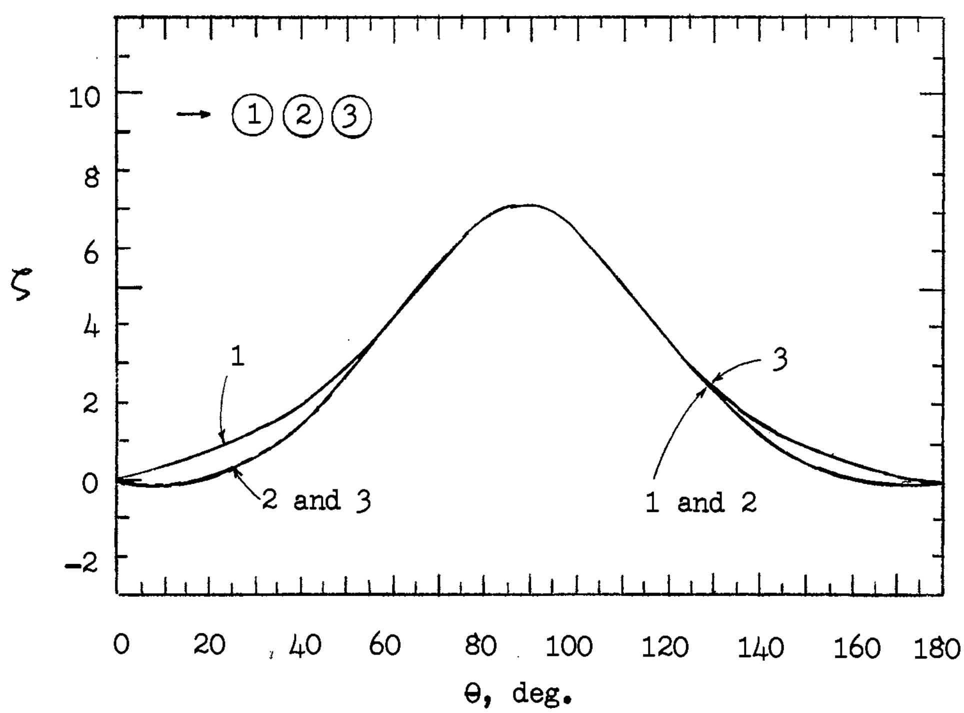

Figure 33. Vorticity Around the Tube
($Re = 5$; $P_t = .150$; $h = 0.10$)

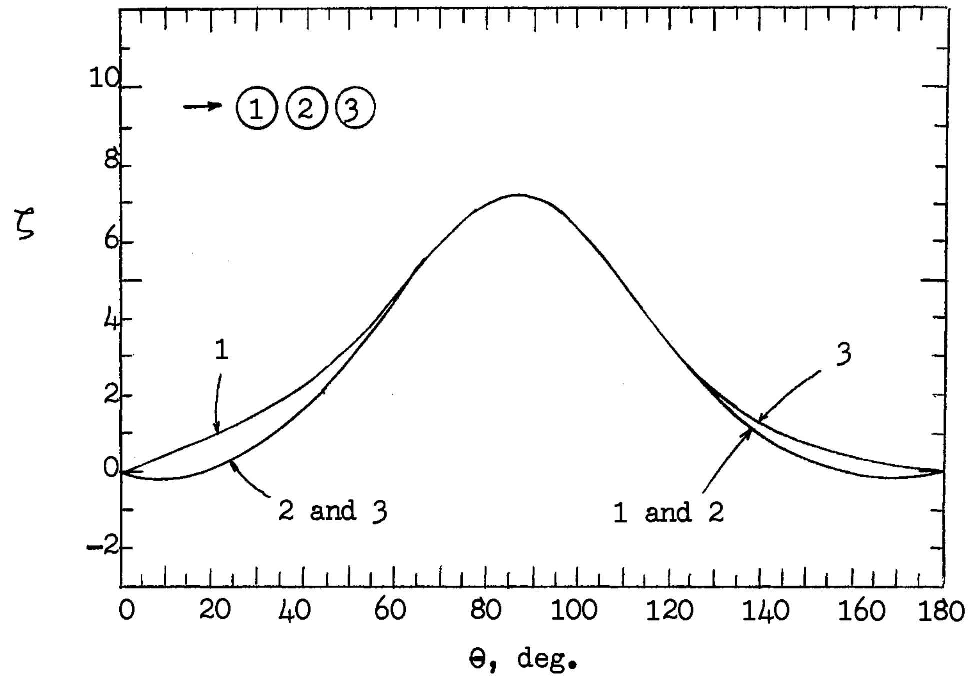

Figure 34. Vorticity Around the Tube
($Re = 10$; $P_t = 1.50$; $h = 0.10$)

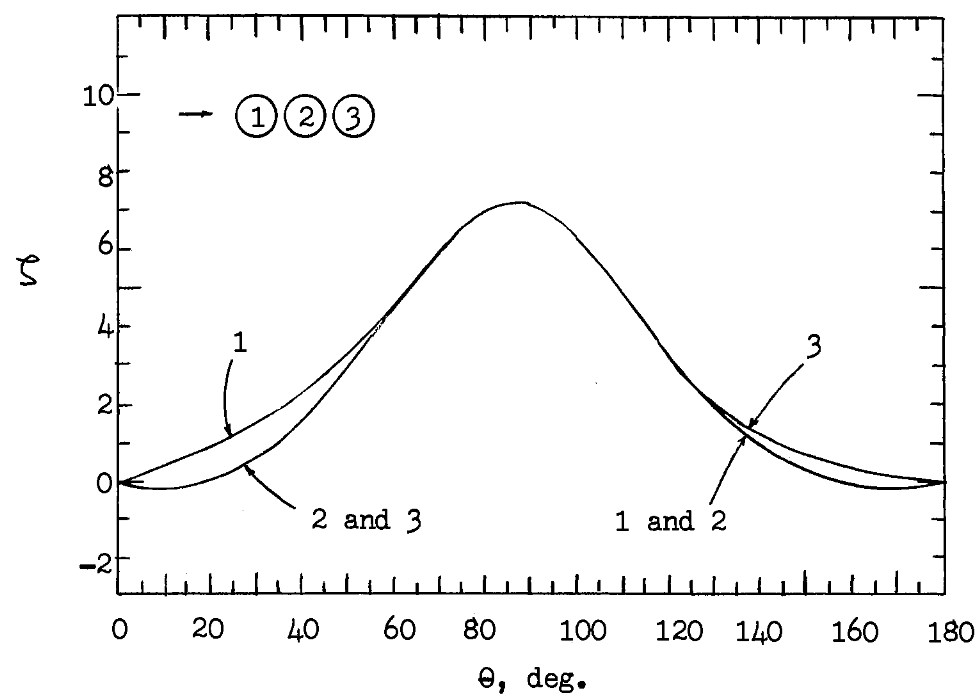

Figure 35. Vorticity Around the Tube
($Re = 10$; $P_t = 1.50$; $h = 0.05$)

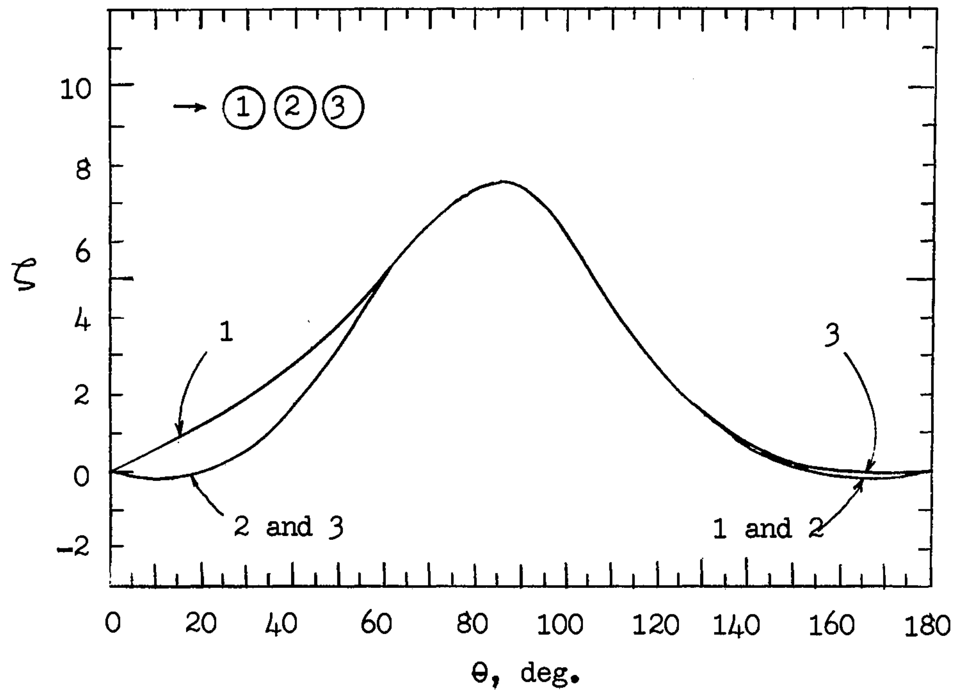

Figure 36. Vorticity Around the Tube
(Re = 20; P_t = 1.50; h = 0.05)

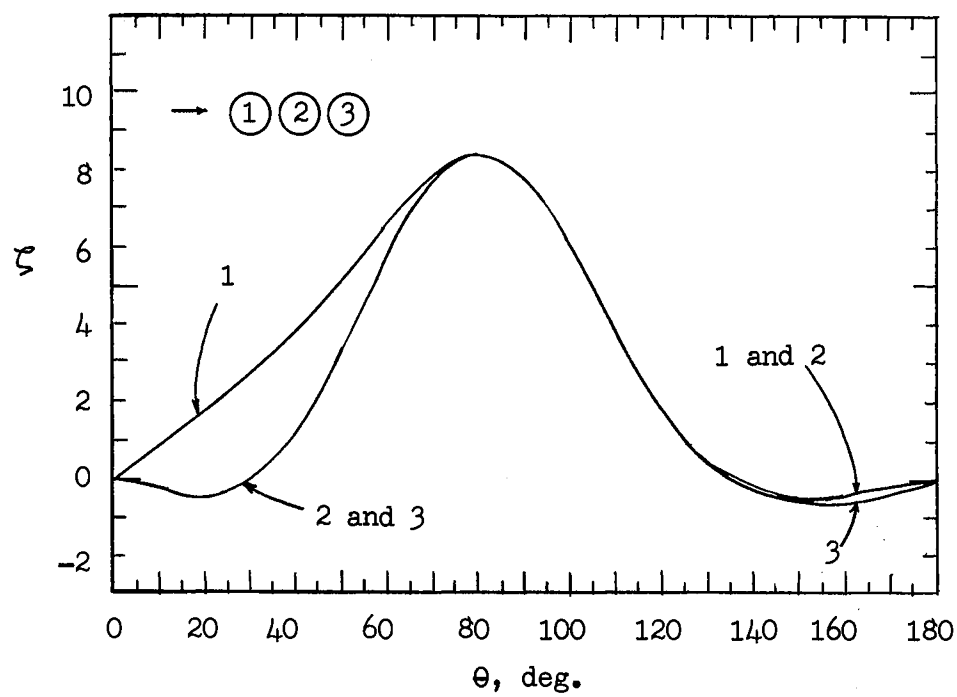

Figure 37. Vorticity Around the Tube
(Re = 50; P_t = 1.50; h = 0.05)

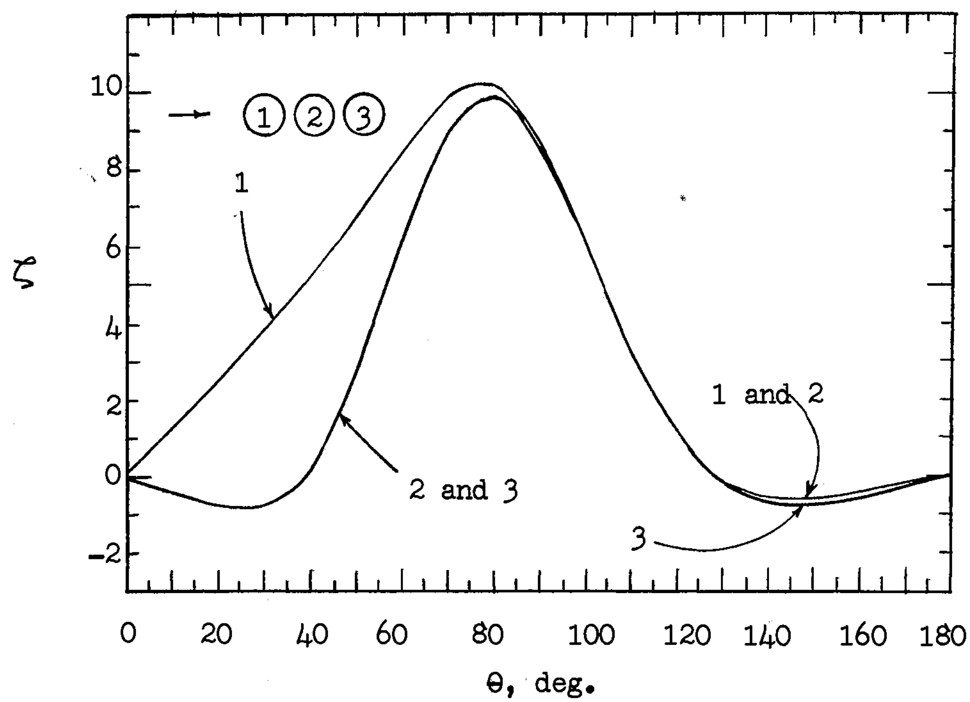

Figure 38. Vorticity Around the Tube
($Re = 100$; $P_t = 1.50$; $h = 0.05$)

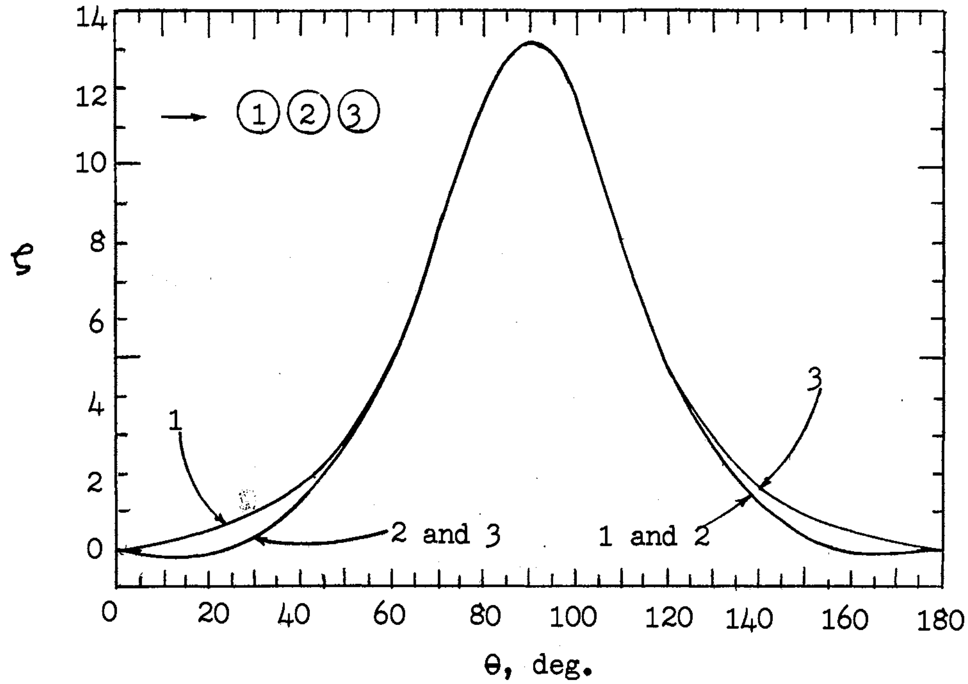

Figure 39. Vorticity Around the Tube
($Re = 1$; $P_t = 1.25$; $h = 0.05$)

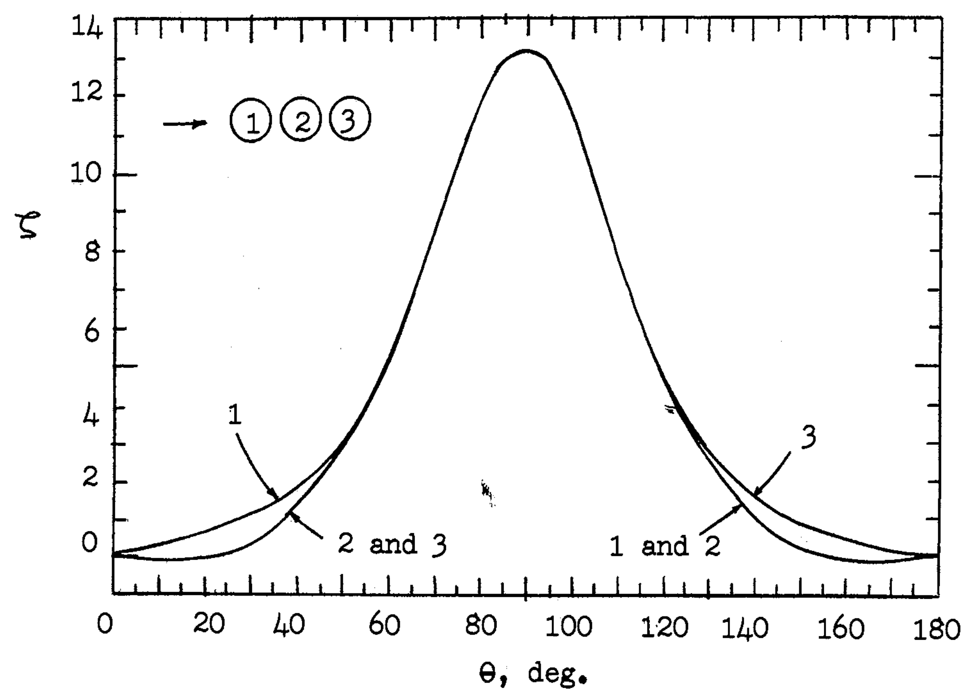

Figure 40. Vorticity Around the Tube
($Re = 5$; $P_t = 1.25$; $h = 0.05$)

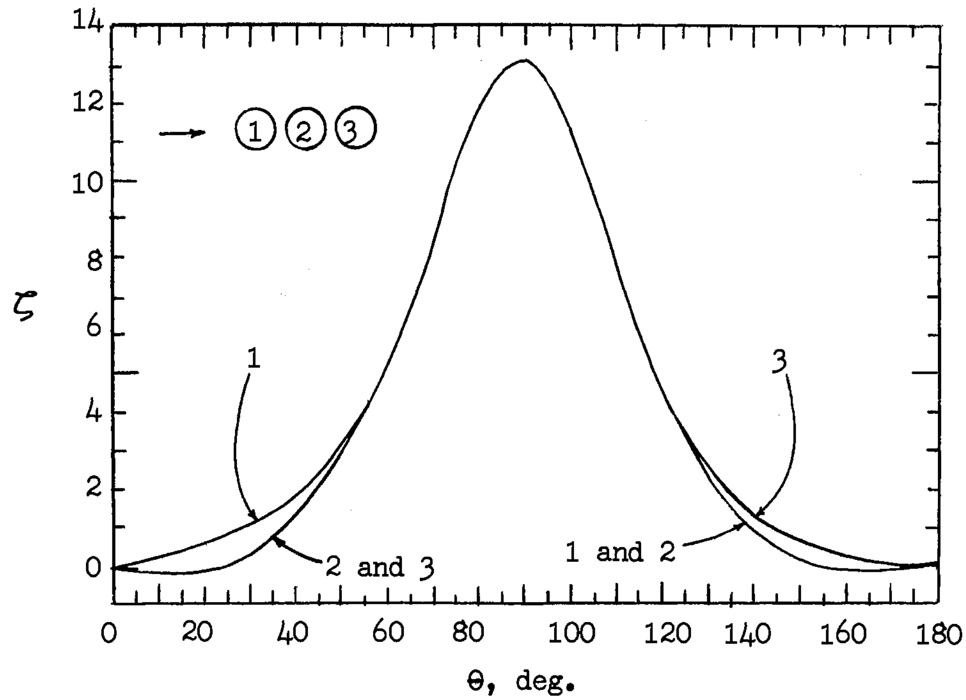

Figure 41. Vorticity Around the Tube
($Re = 10$; $P_t = 1.25$; $h = 0{,}05$)

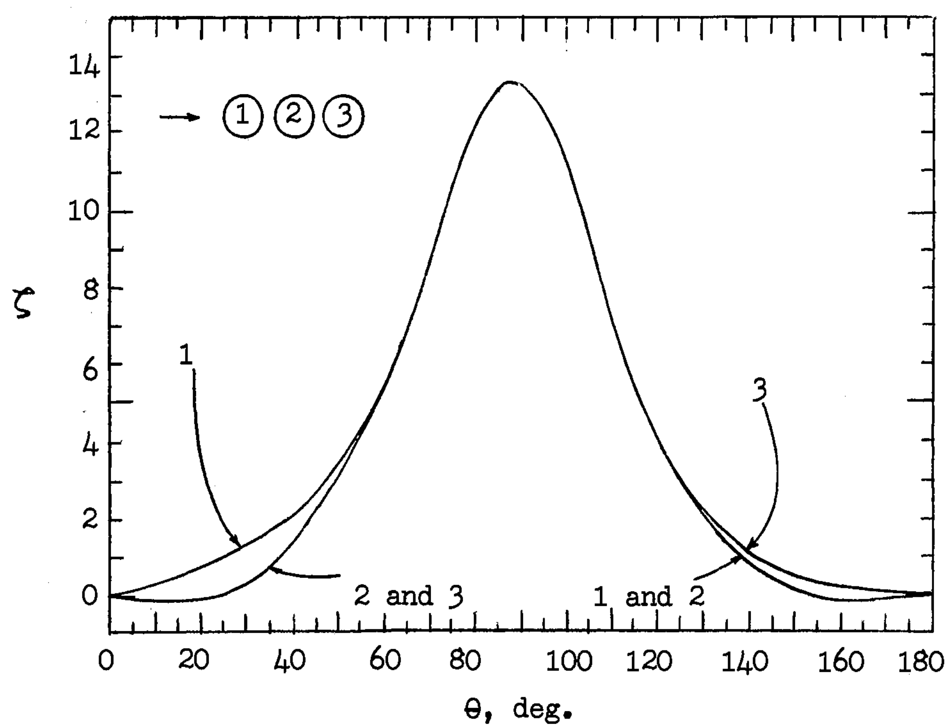

Figure 42. Vorticity Around the Tube
($Re = 20$; $P_t = 1.25$; $h = 0.05$)

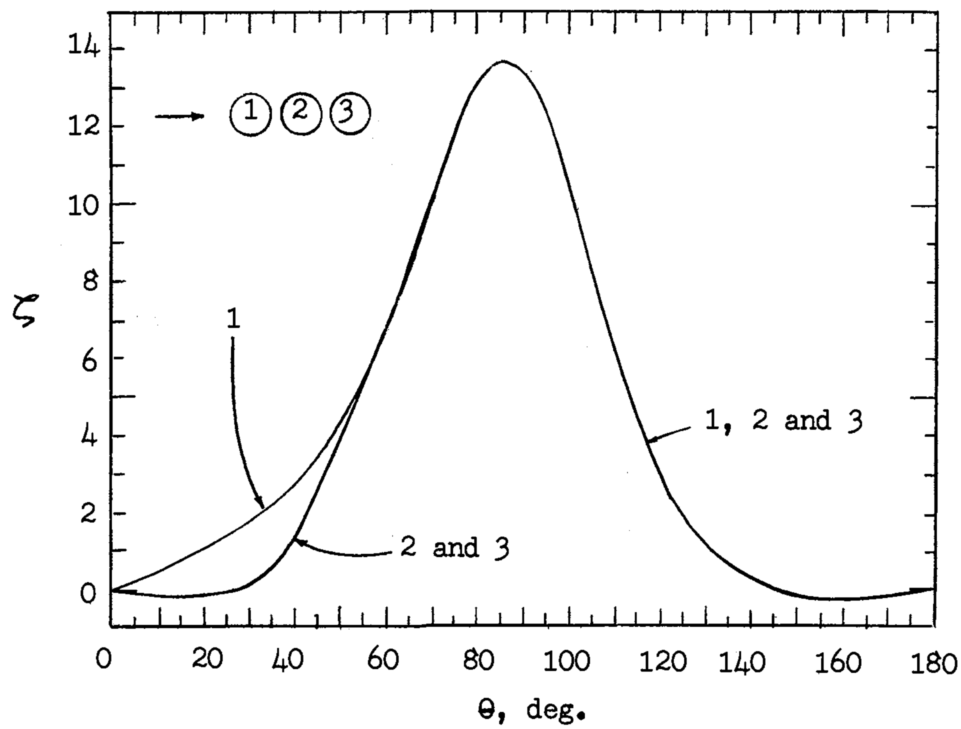

Figure 43. Vorticity Around the Tube
($Re = 50$; $P_t = 1.25$; $h = 0.05$)

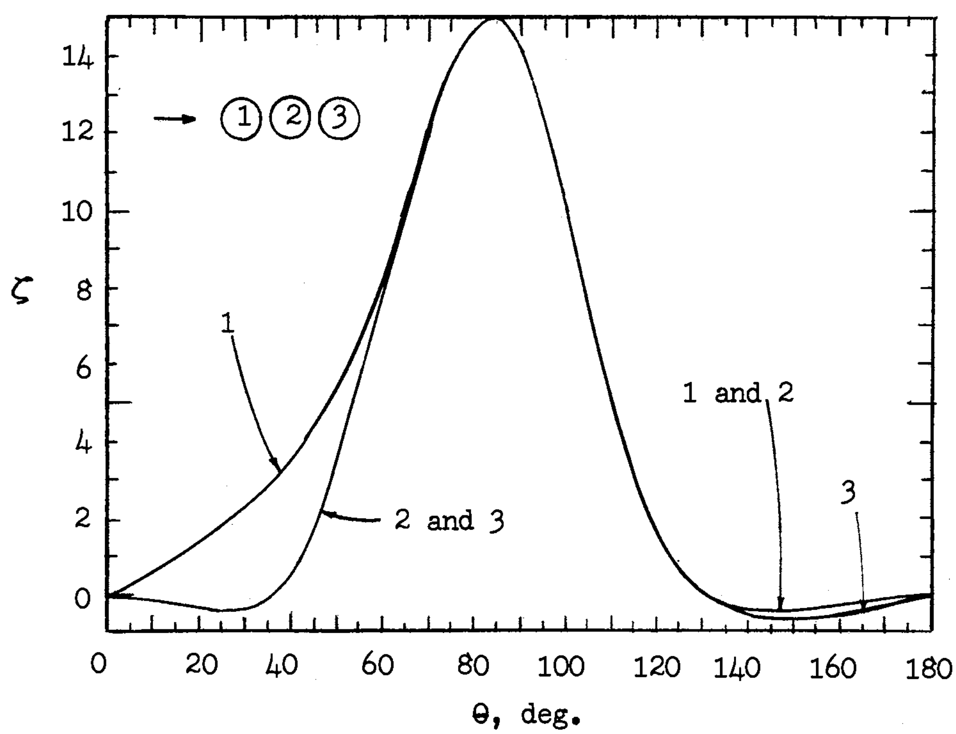

Figure 44. Vorticity Around the Tube
($Re = 100$; $P_t = 1.25$; $h = 0.05$)

The contribution of the pressure forces, i.e., form drag, to the total drag is therefore

$$C_p = \int_0^{\pi} P^*(\theta) \cos \theta \, d\theta \qquad (5\text{-}2)$$

The vorticity gradient $[\frac{\partial \zeta}{\partial r}]_{r=R}$ at a point on a tube surface in Equation 5-1 may be estimated from an appropriate expression of ζ as a function of r at that point. A parabolic function of r was used to approximate the radial distribution of ζ at a point on the tube surface. The derivation of the equation used is presented in Appendix G. The vorticity gradient equation used in the numerical integration of Equation 5-1 is

$$[\frac{\partial \zeta}{\partial r}]_{r=R} = \frac{1}{h}(2\zeta_{i,2} - \frac{1}{2}\zeta_{i,3} - \frac{3}{2}\zeta_{i,1}) \qquad (5\text{-}3)$$

where $\zeta_{i,1}$ = vorticity on the tube surface point (i,1)

$\zeta_{i,2}$ = vorticity on the tube surface point (i,2)

$\zeta_{i,3}$ = vorticity on the tube surface point (i,3)

The tube surface points mentioned above should be referred to Figure 67 of Appendix G.

The contribution of the shear forces, i.e., friction drag, to the total drag is calculated from

$$C_f = \frac{4}{Re}\int_0^{\pi} \zeta_{r=R} \sin \theta \, d\theta \qquad (5\text{-}4)$$

Total drag coefficient for a tube, C_D, is thus

$$C_D = C_p + C_f \tag{5-5}$$

In tube bank fluid flow experiments, the drag coefficient is reported in terms of the friction factor, f, defined by Equation 2-4. In order to compare the results obtained from numerical solutions with experimental data, the relationship between drag coefficient C_D and the ideal tube bank friction factor f must be derived.

Considering the momentum balance on a control volume of inline square tube bank with three tube rows of Figure 45, one can write the force balance

$$2\, P_t\, g_c \Delta P = (\Delta F + \Delta\tau)\, g_c \tag{5-6}$$

where ΔF = pressure drag contribution to total pressure drop

$\Delta\tau$ = friction drag contribution to total pressure drop

$\Delta P = P_1 - P_2$

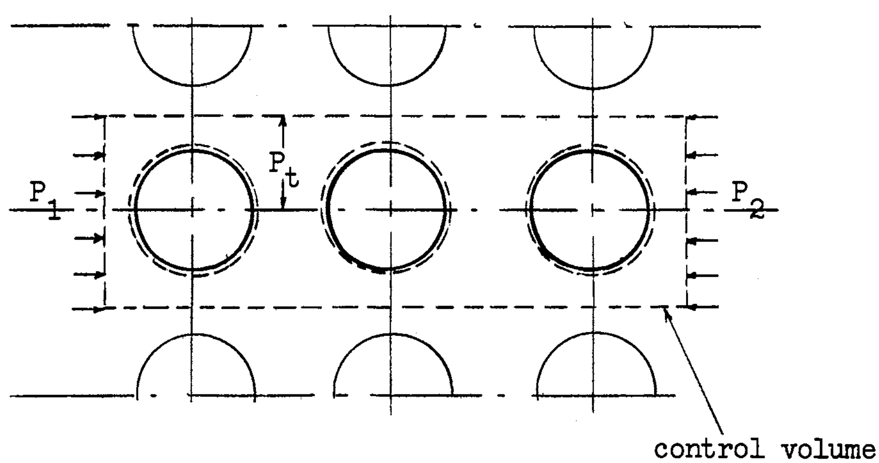

Figure 45. Tube Bank Force Balance

In the Delaware correlations, the isothermal friction factor is defined by Equation 2-4 or

$$f = \frac{2\ g_c \Delta P}{4\ N_t \rho \bar{u}^2} \tag{5-7}$$

where N_t = number of tubes in a tube row in inline tube bank. Eliminating ΔP from Equation 5-6 and 5-7, one obtains

$$f = \frac{(\Delta F + \Delta \tau)\ g_c}{4\ N_t\ 2\ P_t\ \frac{1}{2}\rho \bar{u}^2} \tag{5-8}$$

But computed pressure drag and friction drag on the tube bank is expressed, respectively, as

$$C_p = \frac{(\Delta F/2)\ g_c}{\frac{1}{2}\rho \bar{u}^2\ N_t} \tag{5-9}$$

and

$$C_f = \frac{(\Delta \tau/2)\ g_c}{\frac{1}{2}\rho \bar{u}^2\ N_t} \tag{5-10}$$

From Equations 5-8, 5-9 and 5-10, one finds

$$f = \frac{C_p + C_f}{4\ P_t} \tag{5-11}$$

or

$$f = \frac{C_D}{4\ P_t} \tag{5-12}$$

The detailed description of computer program for calculating the form drag coefficient, the friction drag coefficient and the ideal tube bank friction factor, together with the required input data and control parameters, is given in Appendix K.

The computed pressure variation around the tubes at Re = 1, 5, 10, 20, 50 and 100 for pitch ratios of 1.50 and 1.25 is shown in Figures 46 to 58. Although no experimental data have been reported on pressure distribution around the tubes in tube banks at these low Reynolds numbers, the measured pressure distribution obtained by Kitaura et al. (41) at Re = 16,000 and 20,200 for an inline tube layout are indicative of the computed results we obtained. Kitaura et al. have observed that (i) pressure variations around the third tube and thereafter are about identical; (ii) for the second tube and thereafter the pressure first increases due to momentum recovery at the rear stagnation region of the preceding tube and then decreases steadily again after detachment of flow in the leeward part of the tube; (iii) effect of tube proximity on pressure appears as the maximum pressure drop which is greater for smaller pitch ratios and occurs around the point of minimum clearance of tube bank flow channel, i.e., an angular position of about 90^{o} from the stagnation point.

The calculated form drag coefficients, friction factor coefficients, total drag coefficients, tube bank friction factors and the ratio of form drag to total drag coefficient are listed in Table III for both pitch ratios of 1.50 and 1.25 at Reynolds numbers 1 to 100. Unlike a uniform flow past a single cylinder (30), the ratio of C_p/C_D for all the tubes in three tube rows is almost constant at the order of 0.7 for P_t = 1.50 and 0.8 for P_t = 1.25 over the Reynolds number range covered.

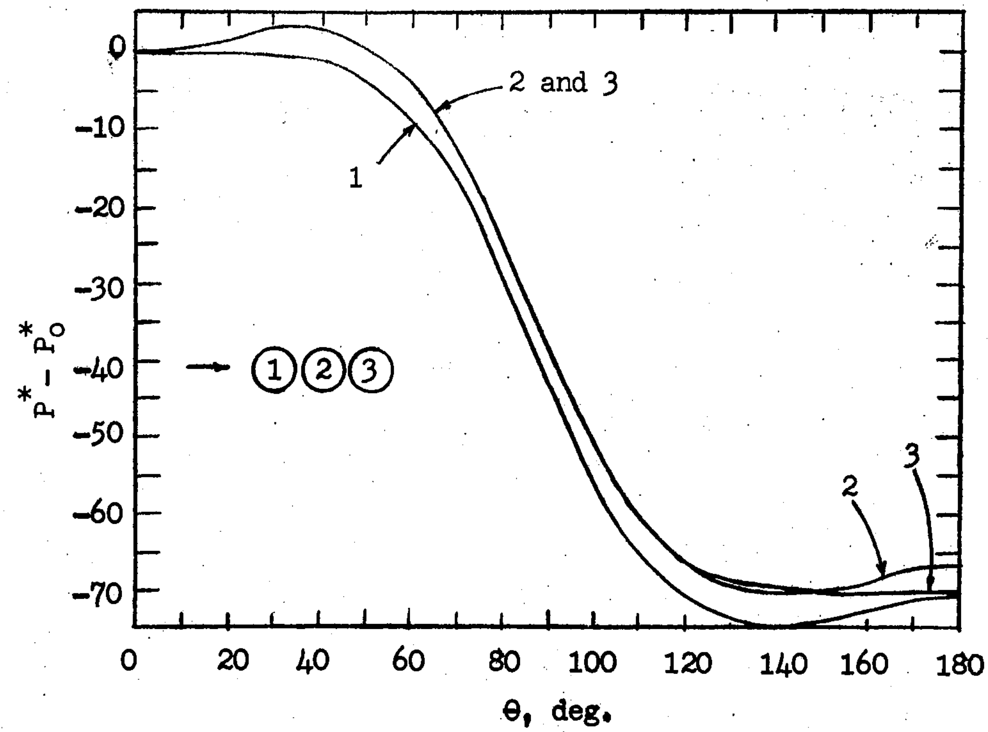

Figure 46. Pressure Variation Around the Tube
($Re = 1$; $P_t = 1.50$; $h = 0.10$)

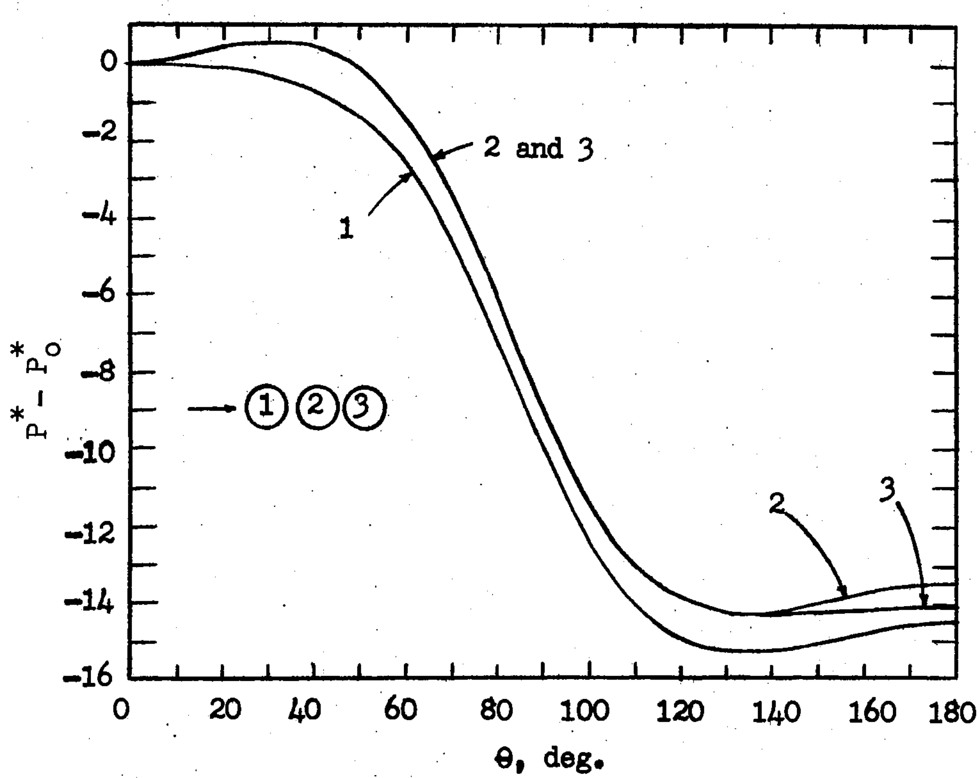

Figure 47. Pressure Variation Around the Tube
($Re = 5$; $P_t = 1.50$; $h = 0.10$)

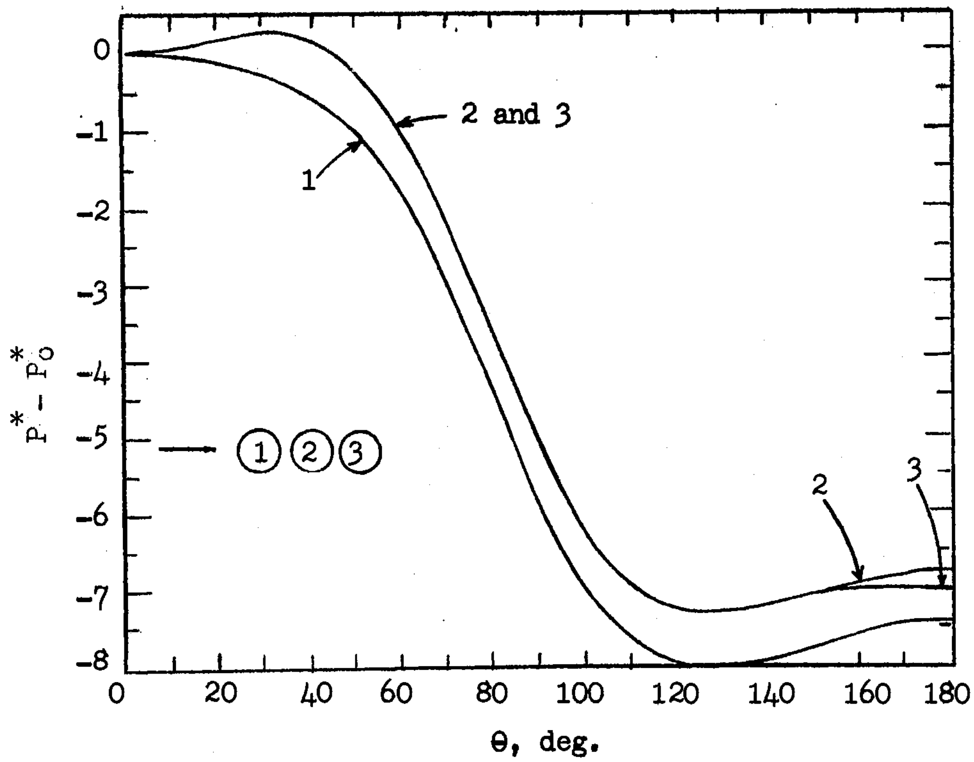

Figure 48. Pressure Variation Around the Tube
(Re = 10; P_t = 1.50; h = 0.10)

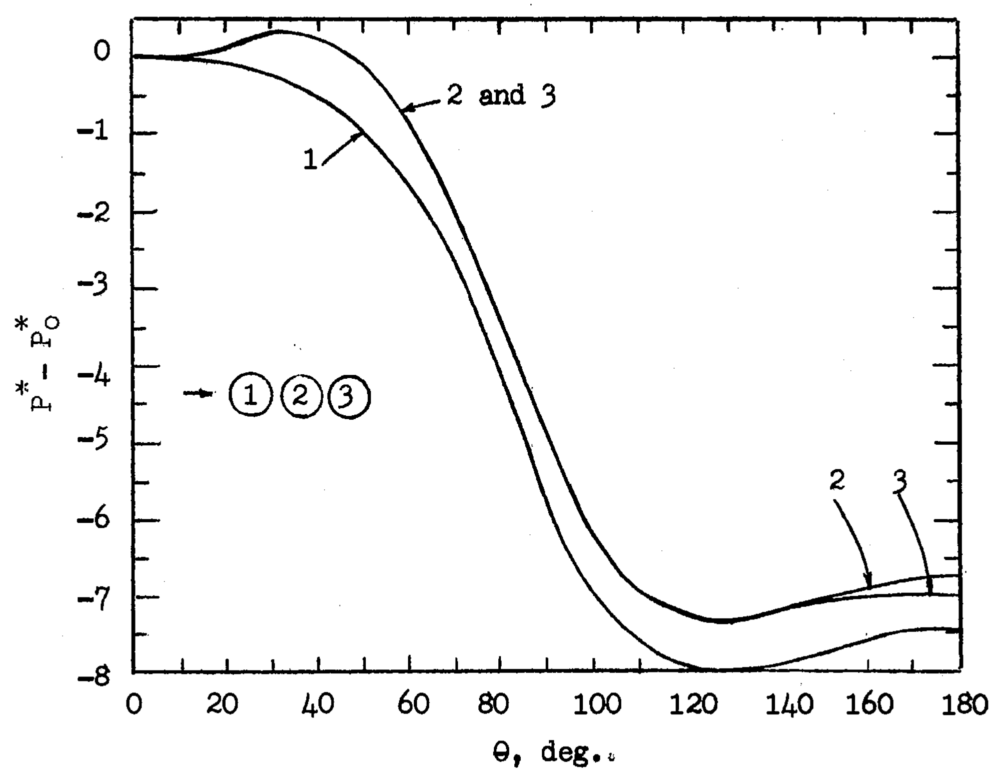

Figure 49. Pressure Variation Around the Tube
(Re = 10; P_t = 1.50; h = 0.05)

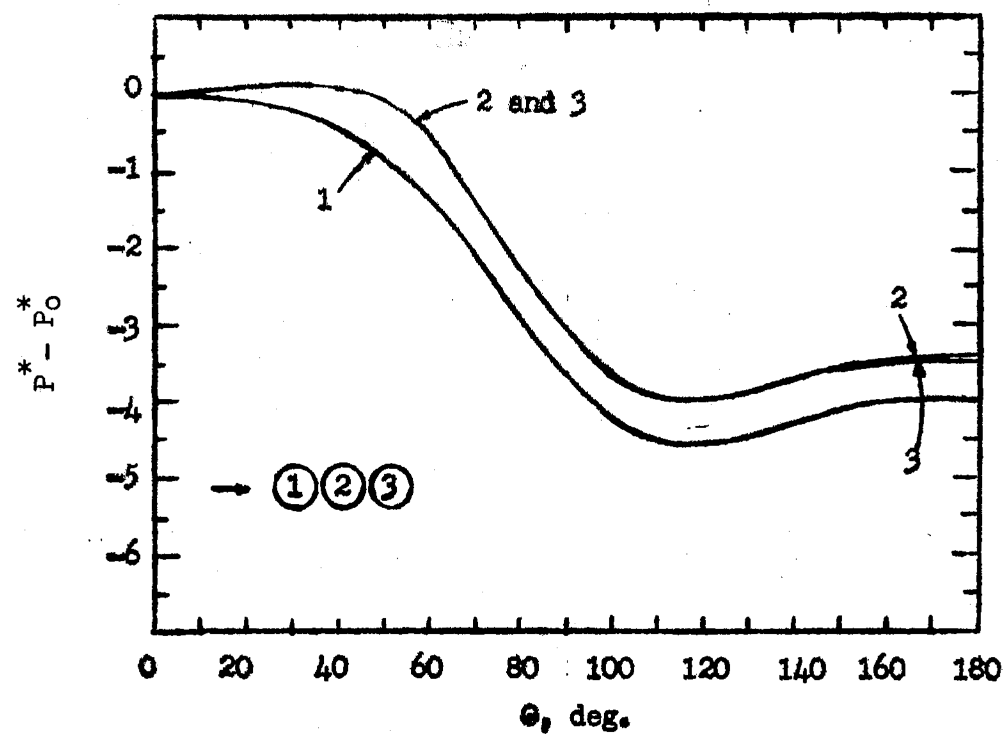

Figure 50. Pressure Variation Around the Tube
(Re =20; P_t = 1.50; h = 0.05)

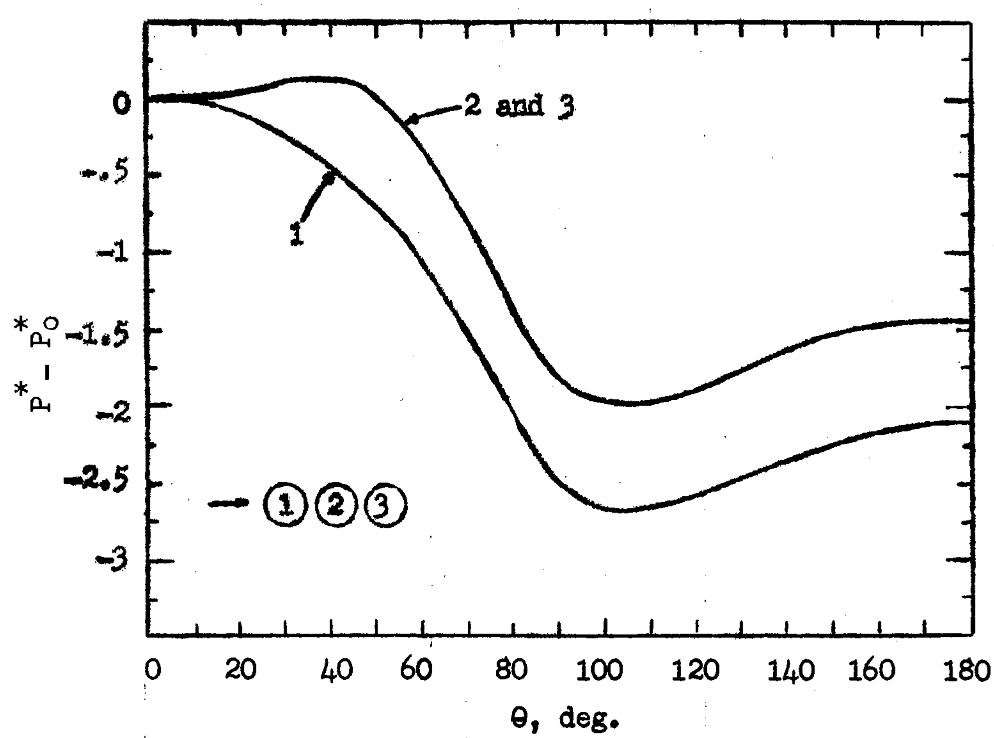

Figure 51. Pressure Variation Around the Tube
(Re = 50; P_t = 1.50; h = 0.05)

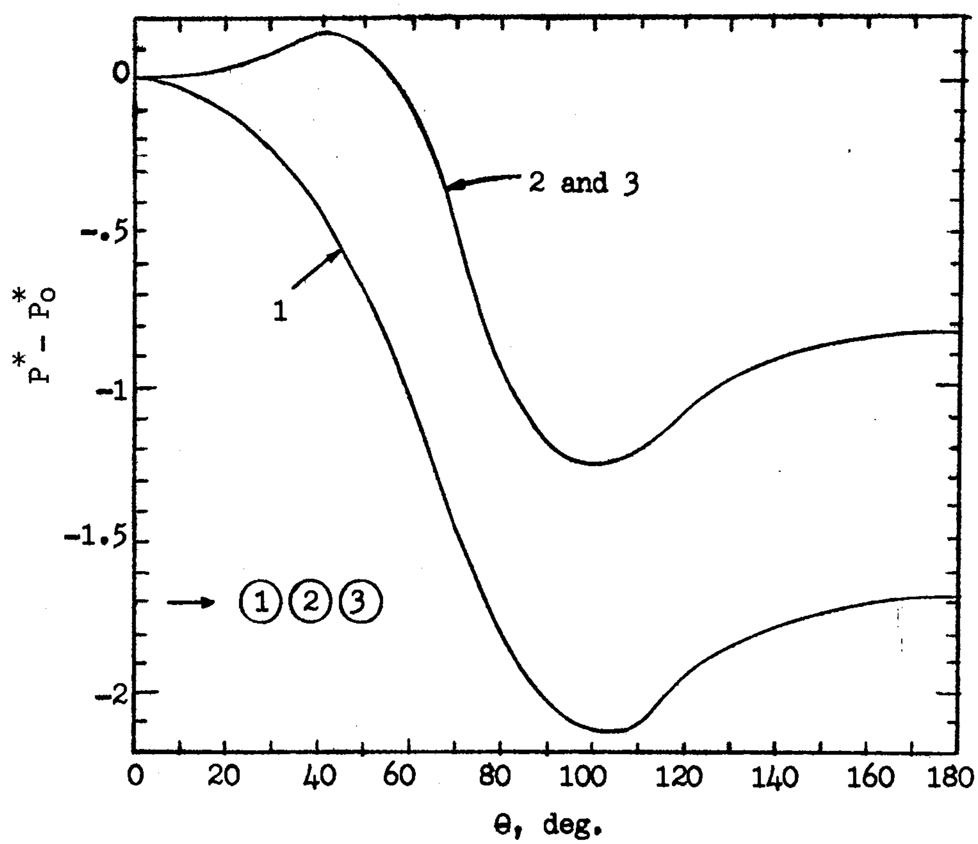

Figure 52. Pressure Variation Around the Tube
(Re = 100; P_t = 1.50; h = 0.05)

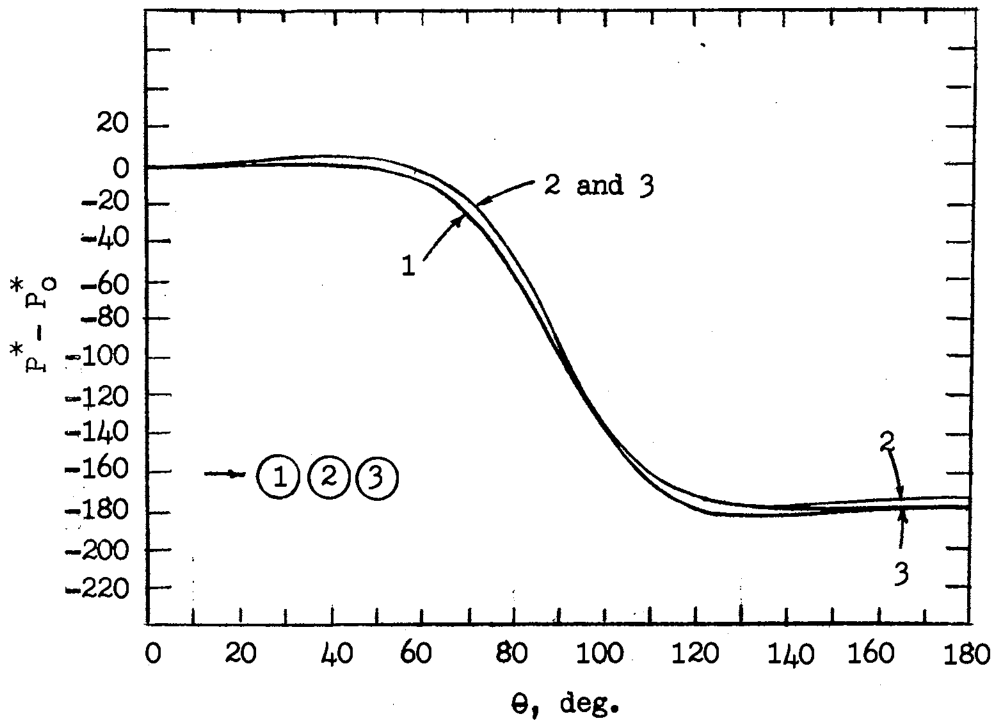

Figure 53. Pressure Variation Around the Tube
(Re = 1; P_t = 1.25; h = 0.05)

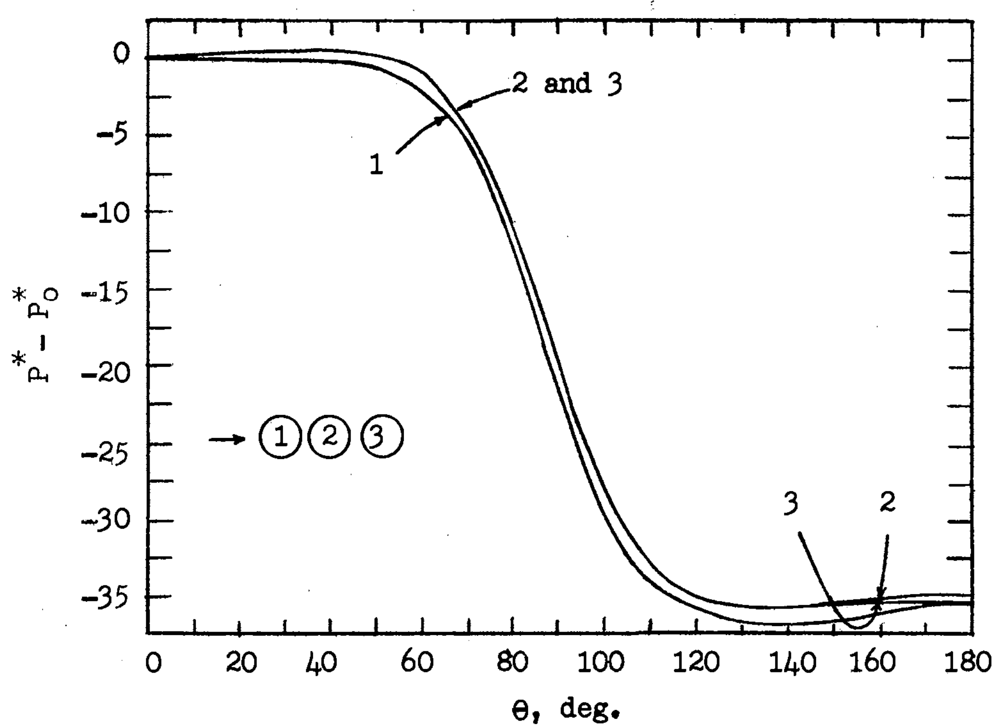

Figure 54. Pressure Variation Around the Tube
(Re = 5; P_t = 1.25; h = 0.05)

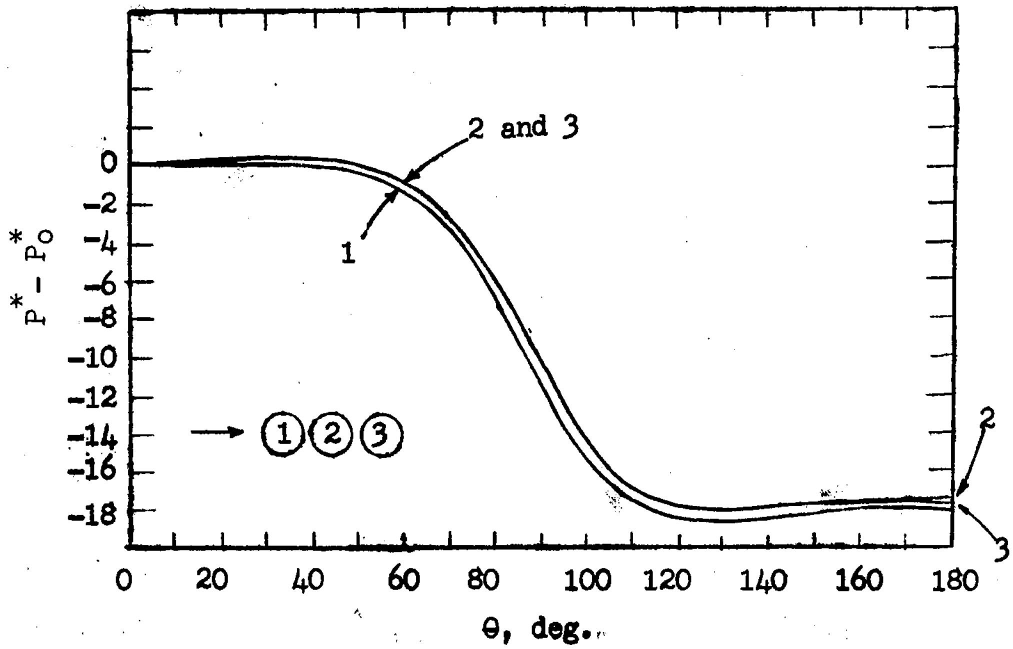

Figure 55. Pressure Variation Around the Tube
(Re = 10; P_t = 1.25; h = 0.05)

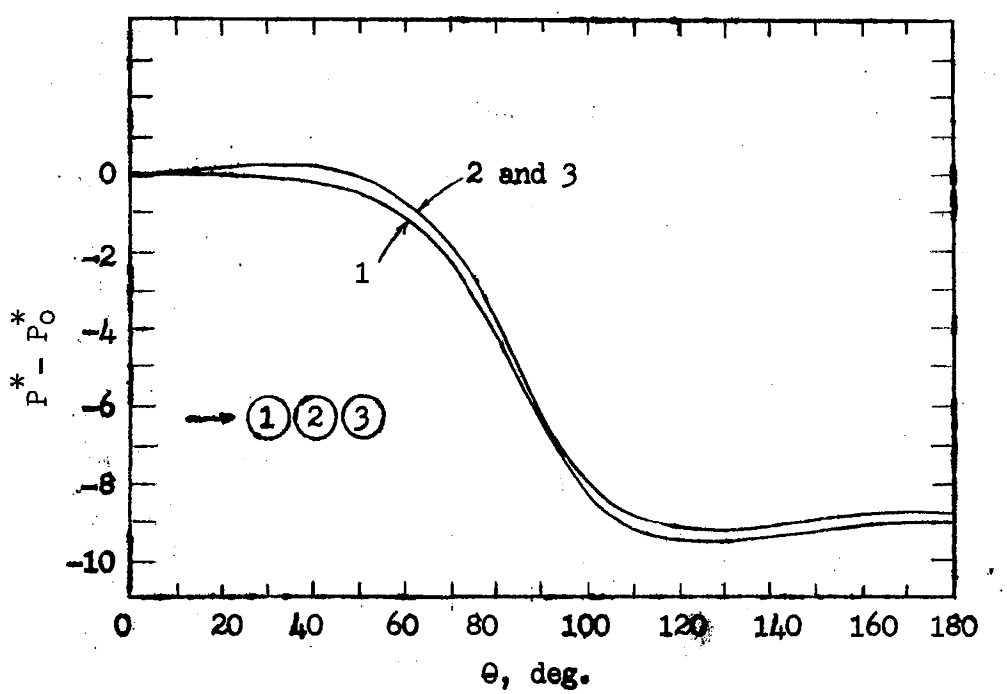

Figure 56. Pressure Variation Around the Tube
(Re = 20; P_t = 1.25; h 0.05)

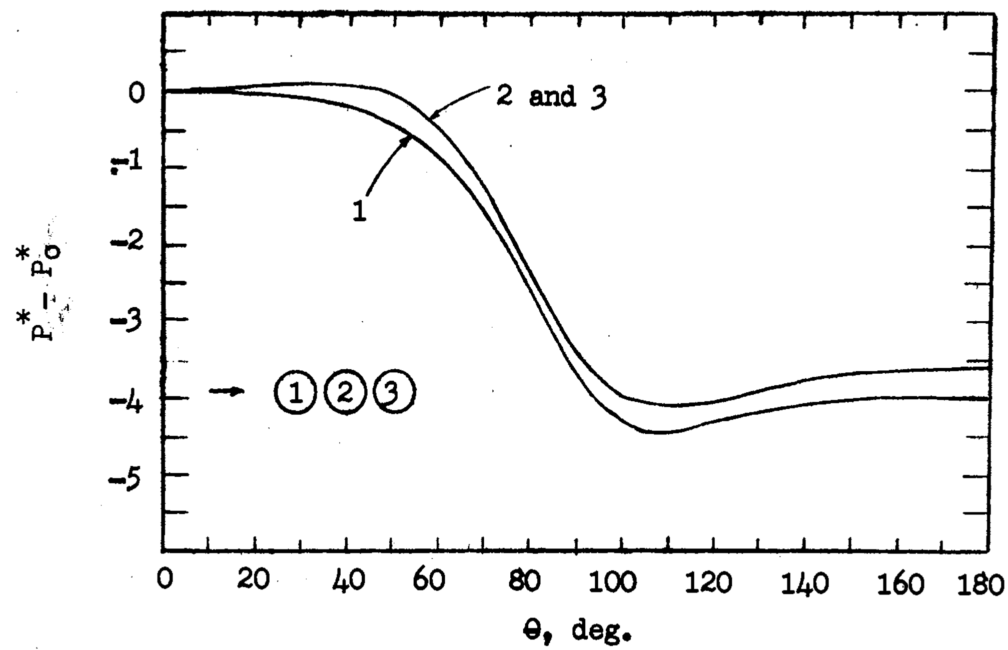

Figure 57. Pressure Variation Around the Tube (Re = 50; P_t = 1.25; h = 0.05)

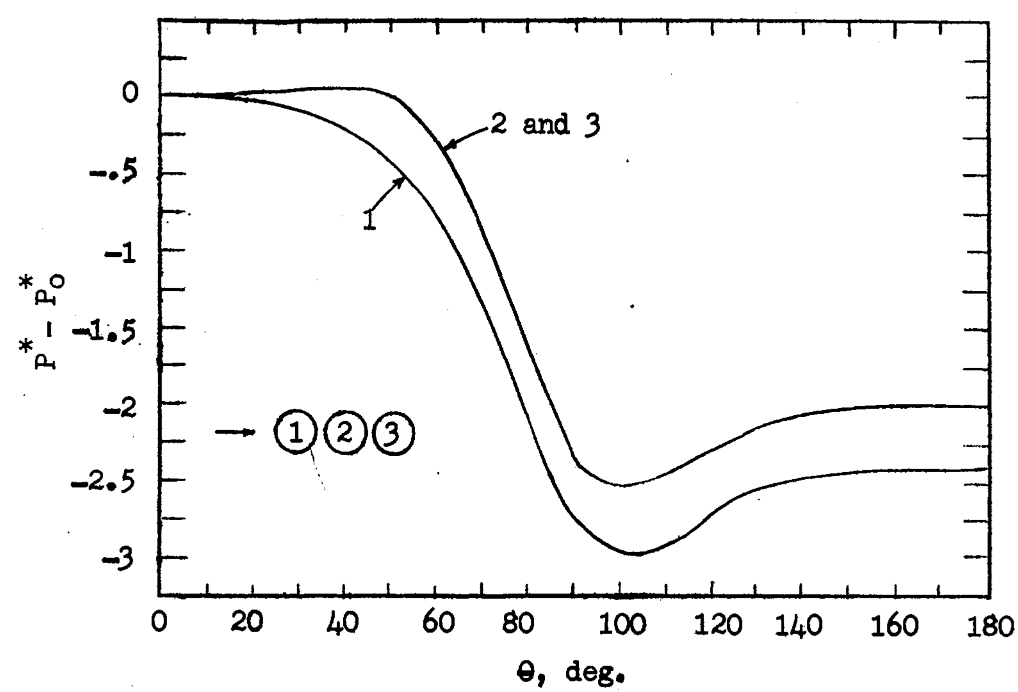

Figure 58. Pressure Variation Around the Tube (Re = 100; P_t = 1.25; h = 0.05)

TABLE III

CALCULATED FRICTION FACTORS (P_t = 1.50)

Re	NPT/h	Tube number	C_f	C_p	C_D	f	C_p/C_D
		1	30.9	71.6	102.5	17.1	0.700
1		2	30.3	70.0	100.3	16.7	0.700
		3	30.9	71.8	102.7	17.1	0.700
	5/0.10	1	6.21	14.4	20.6	3.43	0.700
5		2	6.06	14.0	20.1	3.34	0.696
		3	6.16	14.3	20.4	3.41	0.701
	5/0.10 10/0.05	1	3.12 3.12	7.28 7.20	10.4 10.3	1.73 1.72	0.700 0.698
10		2	3.03 3.02	7.04 6.95	10.1 9.96	1.68 1.66	0.697 0.697
		3	3.07 3.06	7.15 7.05	10.2 10.1	1.70 1.68	0.701 0.698
		1	1.58	3.78	5.36	0.893	0.705
20		2	1.51	3.56	5.07	0.844	0.702
		3	1.52	3.58	5.10	0.850	0.702
		1	0.679	1.91	2.59	0.432	0.738
50	10/0.05	2	0.597	1.59	2.19	0.365	0.725
		3	0.597	1.59	3.19	0.365	0.725
		1	0.389	1.39	1.78	0.297	0.780
100		2	0.295	0.928	1.22	0.204	0.760
		3	0.293	0.922	1.22	0.203	0.755

TABLE III (Continued)

CALCULATED FRICTION FACTORS ($P_t = 1.25$)

Re	NPT/h	Tube number	C_f	C_p	C_D	f	C_p/C_D
1	$\frac{5}{0.05}$	1	46.6	178.3	224.9	45.0	0.793
		2	46.0	176.4	222.3	44.5	0.794
		3	46.6	178.4	224.9	45.0	0.793
5		1	9.33	35.7	45.0	9.00	0.793
		2	9.19	35.6	44.5	8.89	0.793
		3	9.30	35.6	44.9	8.89	0.793
10		1	4.67	17.9	22.6	4.51	0.792
		2	4.59	17.6	22.2	4.45	0.793
		3	4.63	17.8	22.4	4.49	0.795
20		1	2.34	9.07	11.4	2.27	0.791
		2	2.30	8.86	11.2	2.23	0.791
		3	2.31	8.92	11.2	2.25	0.796
50		1	0.947	3.80	4.75	0.950	0.800
		2	0.913	3.67	4.58	0.916	0.801
		3	0.915	3.67	4.58	0.916	0.801
100		1	0.490	2.24	2.73	0.546	0.820
		2	0.451	2.03	2.48	0.496	0.818
		3	0.450	2.03	2.48	0.495	0.818

The calculated tube bank friction factors are compared with the Delaware isothermal data for inline square tube layout in Figure 59.

In both pitch ratios, the first tube contributes the largest pressure loss of total tube bank pressure drop, and the second and the third tube shows near-identical values of friction factors. The entrance effect and the exit effect for tube banks appear in the difference of calculated friction factors between the first and the second tubes, and the second and the third tubes, respectively. As is seen in Figure 59, the entrance effect becomes more distinctive as the Reynolds number increases, while the difference between the second and the third tubes is negligibly small over the entire Reynolds number range covered.

In order to compare the computed friction factors of tube bank three tube rows deep with the Delaware experimental data based on ten rows deep, it is assumed that the friction factor can be estimated by

$$f = \frac{1}{10}(f^1 + 8f^2 + f^3) \tag{5-13}$$

where the superscript for f is the tube number in the rows counted from the inlet. This may be justified because of the fact that the exit effect on the friction factor is negligibly small so that the friction factor for the second tube can represent that of all the inner tubes in ten rows deep. The calculated results are given in Table IV and compared with the experimental friction factors read from the Delaware data.

The computed average friction factors are within -7 to -13% of the Delaware data for P_t = 1.50 and -7 to -10% for P_t = 1.25 over the Reynolds number range studied.

The most plausible explanation of the difference between the

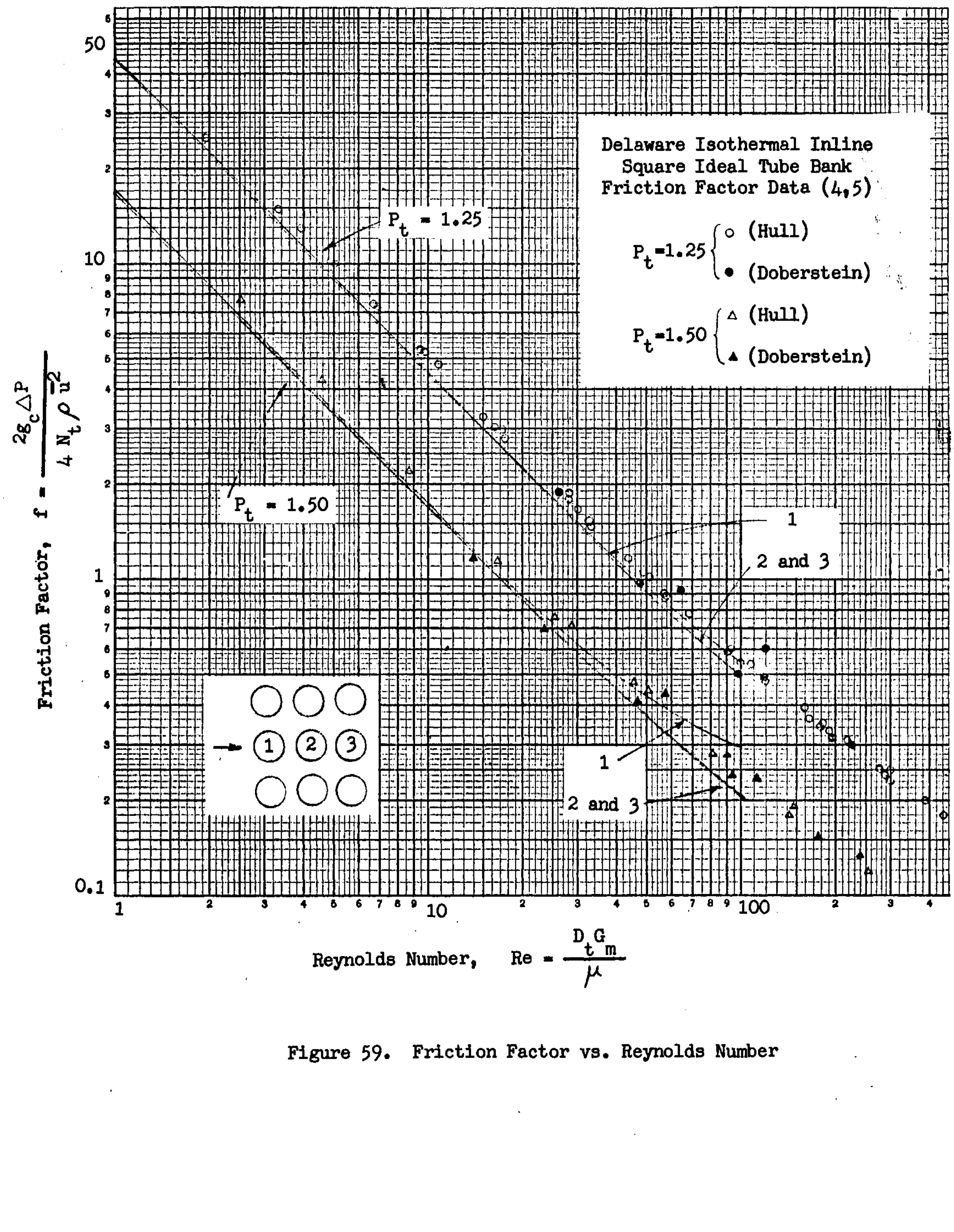

Figure 59. Friction Factor vs. Reynolds Number

TABLE IV

COMPARISON BETWEEN CALCULATED AND EXPERIMENTAL FRICTION FACTORS

Reynolds number	Pitch ratio 1.50			Pitch ratio 1.25		
Re	f^{cal}	f^{exp}	difference %(c)	f^{cal}	f^{exp}	difference %(c)
1	16.8	18.0 (b)	-6.7	44.6	48.0 (b)	-7.5
5	3.36	3.75	-10	8.90	9.90	-10
10	1.67 (a)	1.90	-13	4.46	4.90	-9.0
20	0.850	0.94	-9.6	2.24	2.40	-6.7
50	0.372	0.42	-12	0.919	1.00	-8.1
100	0.213	0.24	-12	0.501	0.55	-8.9

(a) finer mesh size, i.e., h = 0.05

(b) extrapolated

(c) % difference = $(f^{cal} - f^{exp})/ f^{exp} \times 100$

calculated and the experimental friction factors in which the calculated f-factor is smaller than the experimental on an average of -10% is that the calculated friction factor is based on tube bank of infinite tube length and infinite number of tubes in a row normal to the direction of flow. The effect of the two side walls parallel to the long side of the tube may be negligible because of the tube bank construction of the Delaware ideal tube banks in which the outer-most tubes of the tube banks are half-way imbedded on the side walls to minimize the side wall effect. The amount of increased pressure drop due to the presence of the other two side walls (top and bottom) may be calculated using the Graetz solution for flow through rectangular channel (14) with values of the height-width ratio of tube bank flow channel. The discussion and calculation of the Graetz correction factors are given in Appendix H. From Table V, the increase in friction factor due to side wall effect should be from +4.3 to +12% for $P_t = 1.50$ and from +2.1 to +10% for $P_t = 1.25$.

CHAPTER VI

CONCLUSIONS AND RECOMMENDATIONS

The initial purpose of this study was to investigate the fluid dynamics and heat transfer mechanisms during flow across tube banks. However, the latter objective was not achieved because of the great effort required to solve the fluid dynamics problem.

CONCLUSIONS

No simplified flow model attempted was found satisfactory in predicting tube bank friction factors. Numerical solutions of the Navier-Stokes equations have been obtained for two-dimensional, incompressible, viscous Newtonian flow across banks of tubes of inline square tube layout at Reynolds numbers of 1, 5, 10, 20, 50 and 100 for pitch ratios of 1.50 and 1.25. An attempted solution at Re = 150 utilizing the solution at Re = 100 diverged at the second iteration.

It has been found that there are eddy regions between tube rows at all Reynolds numbers studied, while the wake-bubble behind the last tube row appears only after the Reynolds number exceeds 20. As the Reynolds number increases, the size of the eddy between the tube rows grows and the wake-bubble lengthens.

The ratio of computed form drag to total drag has been found almost constant at the order of 0.7 for $P_t = 1.50$ and of 0.8 for $P_t = 1.25$ on all the tube rows over the Reynolds number range covered. It also has been found that the contribution of the first tube row to the total pressure drop is the largest of three tube rows for both pitch ratios and at all the Reynolds numbers calculated. The calculated tube bank friction factors has been found within -7 to -13% for $P_t = 1.50$ and from -7 to -10% for $P_t = 1.25$ of the Delaware isothermal data of inline square tube bank over the Reynolds number range covered in this study.

RECOMMENDATIONS

The following recommendations are made based on the results of this exploratory study:

1. Semi-empirical flow models should be reconsidered in the light of the numerical solutions obtained in this study. The goal would be to represent tube bank flow mechanisms by analytical expressions and thereby enable us to predict pressure drops and heat transfer coefficients as direct functions of Reynolds number.
2. Numerical as well as analytical and/or semi-empirical solutions should be sought for other tube layouts, i.e., equilateral triangular and rotated square configurations.
3. In order to attain solutions at higher Reynolds numbers, the unsteady state equations as well as a finer mesh size should be attempted. The unsteady state approach or time-dependent method of numerical solution of the Navier-Stokes equations takes into account the time derivative of velocity. The incremental time steps which appear in the denominator of the finite difference expression provide greater stability in numerical computations. For the time-dependent method, the finite difference equations

become:

In rectangular coordinates;

$$\zeta^{n+1}_{i,m} = \left(\frac{1}{\frac{h^2 y_i y_{i-1} Re}{8\delta s} + y_i y_{i-1} + h^2}\right)\Big[\frac{y_i y_{i-1}}{2}(\zeta^n_{i,m+1} + \zeta^n_{i,m-1})$$

$$+ \frac{h^2}{y_i + y_{i-1}}(y_{i-1}\zeta^n_{i+1,m} + y_i\,\zeta^n_{i-1,m}) + \frac{Re\ h\ y_i y_{i-1}}{8(y_i + y_{i-1})}$$

$$\left\{\frac{h(y_i + y_{i-1})}{\delta s}\zeta^{n-1}_{i,m} + (\psi^n_{i,m+1} - \psi^n_{i,m-1})(\zeta^n_{i+1,m} - \zeta^n_{i-1,m})\right.$$

$$\left. - (\psi^n_{i+1,m} - \psi^n_{i-1,m})(\zeta^n_{i,m+1} - \zeta^n_{i,m-1})\right\}\Big] \qquad (6\text{-}1)$$

and

$$\psi^{n+1}_{i,m} = \left(\frac{1}{h^2 + y_i y_{i-1}}\right)\Big[\frac{y_i y_{i-1}}{2}(\psi^{n+1}_{i,m+1} + \psi^{n+1}_{i,m-1}) + \frac{h^2}{y_i + y_{i-1}}$$

$$(y_{i-1}\psi^{n+1}_{i+1,m} + y_i\ \psi^{n+1}_{i-1,m}) - \frac{h^2 y_i y_{i-1}}{2}\zeta^{n+1}_{i,m}\Big] \qquad (6\text{-}2)$$

In polar coordinates;

$$\zeta^{n+1}_{i,j} = \left(\frac{1}{\frac{h^2\ l_j^2\ Re}{8\delta s} + l_j^2 + h^2}\right)\Big[\frac{h^2 l_j^2}{2}\left\{\frac{\zeta^n_{i,j+1} + \zeta^n_{i,j-1}}{h^2}\right.$$

$$\left. + \frac{\zeta^n_{i,j+1} - \zeta^n_{i,j-1}}{2rh} + \frac{\zeta^n_{i+1,j} + \zeta^n_{i-1,j}}{l_j^2}\right\} + \frac{Re\ h\ l_j}{16r}$$

$$\left\{\frac{2rhl_j}{s}\zeta^{n-1}_{i,j} + (\psi^n_{i+1,j} - \psi^n_{i-1,j})(\zeta^n_{i,j+1} - \zeta^n_{i,j-1})\right.$$

$$\left. - (\psi^n_{i,j+1} - \psi^n_{i,j-1})(\zeta^n_{i+1,j} - \zeta^n_{i-1,j})\right\}\Big] \qquad (6\text{-}3)$$

and

$$\psi_{i,j}^{n+1} = \frac{h^2 l_j^2}{2(h^2 + l_j^2)} \left[\frac{\psi_{i,j+1}^{n+1} + \psi_{i,j-1}^{n+1}}{h^2} + \frac{\psi_{i,j+1}^{n+1} - \psi_{i,j-1}^{n+1}}{2rh} + \frac{\psi_{i+1,j}^{n+1} + \psi_{i-1,j}^{n+1}}{l_j^2} - \zeta_{i,j}^{n+1} \right] \tag{6-4}$$

where the superscript n is the time step index and δs denotes the incremental time step.

The computation for higher Reynolds number with the time-dependent method starts with the results of the steady state solutions at one Reynolds number. With a time step of δs, the vorticity ζ at the time $(n + 1)\delta s$ can be calculated from the settled values of ζ and ψ at the time $n\delta s$ and $(n - 1)\delta s$ using Equations 6-1 and 6-3. Equations 6-2 and 6-4 are then used to obtain new values of ψ at $(n + 1)\delta s$ applying a single iterative process in which new values of ζ at the time $(n + 1)\delta s$ are utilized. This computational process with next time step δs is repeated until the settled solution of ζ and ψ with respect to time are reached.

4. Finally, but not least urgently, heat transfer calculations should be carried out, first with constant physical properties and ultimately with temperature dependent viscosity, thermal conductively, heat capacity and density. If constant physical properties are assumed, the energy equations and the equations of motion can be decoupled. The equations of energy in terms of nondimensionalized temperature T and stream function ψ become exactly similar to the vorticity transport equations or

the Navier-Stokes equations in terms of ζ except the Reynolds number, Re, is replaced by the Prandtl number, Pr.

In rectangular coordinates, the energy equation is written as

$$\frac{\partial \psi}{\partial y}\frac{\partial T}{\partial x} - \frac{\partial \psi}{\partial x}\frac{\partial T}{\partial y} = \frac{1}{Pr}\left(\frac{\partial^2 T}{\partial x^2} + \frac{\partial^2 T}{\partial y^2}\right) \qquad (6\text{-}5)$$

and in polar coordinates,

$$\frac{\partial \psi}{\partial r}\frac{\partial T}{r\partial \theta} - \frac{\partial \psi}{r\partial \theta}\frac{\partial T}{\partial r} = \frac{1}{Pr}\left(\frac{\partial^2 T}{\partial r^2} + \frac{\partial T}{r\partial r} + \frac{\partial^2 T}{r^2\partial \theta^2}\right) \qquad (6\text{-}6)$$

where

$$T = \frac{t - t_i}{t_B - t_i} \quad \text{for constant wall temperature} \qquad (6\text{-}7)$$

t_i = temperature of incoming flow

t_B = temperature of tube wall

Boundary conditions for tube bank heat transfer for constant wall temperature, e.g., condensing vapor on tube-side, may be best illustrated in Figure 60.

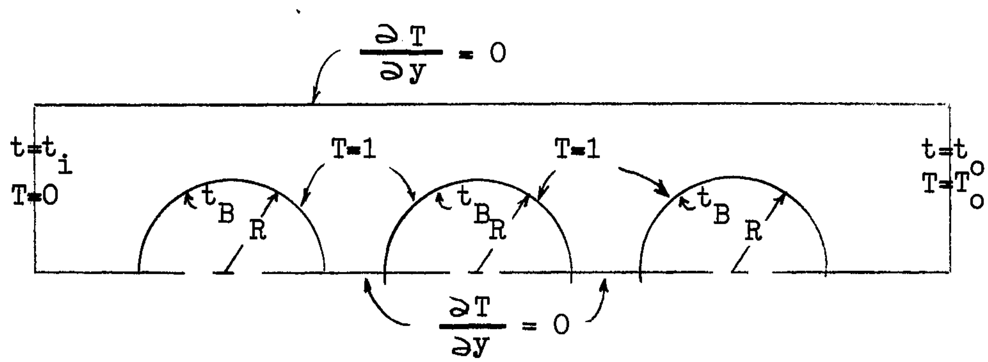

Figure 60. Tube Bank Heat Transfer Boundary Conditions

Knowing that stream function has been solved a priori, the temperature distribution can be calculated by a single T-field iteration with finite difference approximations of Equations 6-5 and 6-6. Computational procedure is shown by the block diagram of Figure 61.

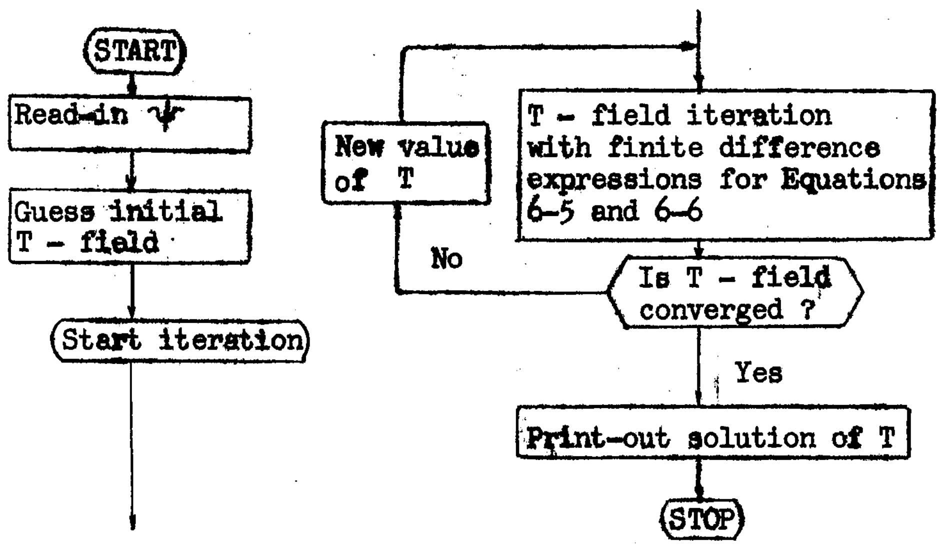

Figure 61. Computer Block Diagram of Temperature Profile Calculation

Once the temperature distribution is obtained, the local Nusselt number around the tube may be computed from

$$Nu(\theta) = -2 \left[\frac{\partial T}{\partial r} \right]_{r=R} \tag{6-8}$$

The Nusselt number for the tube is then calculated from

$$Nu = \frac{1}{\pi} \int_0^{\pi} Nu(\theta) \, d\theta = f(Re, Pr) \tag{6-9}$$

Ultimately, tube bank heat transfer coefficient or j-factor would be calculated from the Nusselt number obtained above.

NOMENCLATURE

For the Text

a	= width-length ratio; Equation H-4
a_i, a_m	= length parameters; Figures 70, 71 and 73
"a"	= a point on a contour surface; Figure 65
A_1, A_2, A_3	= parameters in radial velocity distribution equation; Equation G-17
b_i	= length parameter; Figures 70, 71 and 73
B, B+1	= tube surface node and field mesh point next to the point B and also scale factor; Equation E-2
C_D, C_f, C_p	= total drag, friction drag and form drag coefficients
$C_i(C_1, C_2, C_3)$	= parameters in laminar velocity profiles in variational method; Equations 3-24, 3-26, 3-27 and 3-34
ΔC_i	= incremental change in parameter C_i
C_l	= distance between tube walls of two adjacent tubes in transverse direction [ft]
D_c	= minimum clearance between two tubes in transverse direction [ft]
Det	= determinant; Equation D-21
D_t	= tube diameter [ft]
$\delta\delta\theta$	= angular length parameter [rad]; Figure 70
E_1, E_2	= integration constants; Equations A-10 and A-11
F	= variational function; Equation 3-18
$F(\theta)$	= dimensionless velocity profile; Equation 3-2
ΔF	= pressure drop due to form drag [lb_f/ft^2]; Equation 5-9
f	= tube bank friction factor

f^1, f^2, f^3 = tube bank friction factor for the first, second and third tube row, respectively; Equation 5-13

$f_1, f_2, \ldots f_9$ = coefficients in the dissipation integral I; Equation D-14

$f(a)$ = function of $a = Z_1/Z_2$; Equation H-7

$f(P_t)$ = function of pitch ratio; Equation 3-10

$f_\theta(P_t, \theta)$ = function of pitch ratio and θ; Equation 3-17

f_n = tube bank friction factor for power-law fluid; Equation C-9

G_m = mass velocity at the minimum clearance in tube bank $[lb_m/ft^2\text{-sec}] = \rho \bar{u}$

$\vec{g}$, g_x, g_y = conservative body force vector, x- and y-component of $\vec{g}$ $[lb_f/lb_m]$

g_c = conversion factor $[lb_f\text{-}ft^2/lb_m\text{-}sec^2]$

h = mesh size in x- and r- direction

h_i, h_o = length parameters; Figures 70, 71 and 73

I = dissipation integral; Equation 3-18, and also the number of increments in i-direction; Equation 4-49

I_1, I_2, I_3, I_4 = components of dissipation integral; Equation D-14

J = number of increments in j-direction; Equation 4-49

K = tube section identification number; Figure 14, and also power-law fluid consistency index; Equation C-1

L = characteristic length of the system

L^* = length used in Rayleigh flow problem; Equation B-7

l_i = length parameter; Figures 70, 71 and 73

l_j = mesh size in j-direction

M = parameter; Equation H-2

m = dummy index in summation notation; Equation H-1

N_t = number of major restrictions encountered in flow through a tube bank

Nu = Nusselt number; Equation 6-8

n = power-law fluid index of shear stress-strain expression;

Equation C-1; and also time step index; Equation 6-1

n_p = number of parameters in trial velocity profiles

"O" = irregular star point; Figure 71

O(h) = order of magnitude of h

P, P_1, P_2 = pressures $[lb_f/ft^2]$

P_o = pressure at stagnation point $[lb_f/ft^2]$

P_l, P_t = longitudinal and transverse pitch ratio, respectively

Pr = Prandtl number

Q = volumetric flow rate $[ft^3/sec]$

q = ratio of the mesh length in y-direction to that in the x-direction; Equation 4-52

r = independent space variable in polar coordinates

R = radius of tube

R_j, R_t = length parameters; Figure 70

"R" = irregular star point; Figures 70, 71 and 73

Re = tube bank Reynolds number based on D_t; Equations 2-6 and 4-24

Re_c = tube bank Reynolds number based on D_c; Equation 2-5

Re_n = Reynolds number for power-law fluid; Equation C-8

Re_r = Reynolds number on symmetry line between tubes; Equation 3-3

s = time [sec]

"S" = irregular star; Figure 70, 71 and 73

"SD" = irregular star; Figure 73

δs = incremental time step [sec]

T = dimensionless temperature; Equation 6-7

t = temperature $[^oF]$; Figure 6-1

t_B = tube wall temperature $[^oF]$; Figure 6-1

t_i = temperature of incoming fluid $[^oF]$; Figure 6-1

U,V	= dimensionless velocities
$\bar{v}$	= velocity vector
u,v,u^*	= velocities [ft/sec or dimensionless]
v_r, v_θ	= velocity in r- and θ -directions [ft/sec or dimensionless]
v_o	= velocity on symmetry line [ft/sec]
$\bar{u}$	= mean velocity at minimum tube clearance [ft/sec]
W	= mass flow rate per unit depth of tube in tube bank [lb_m/sec-ft]; Equation 3-7
X,Y	= dimensionless independent space variables in rectangular coordinates
YI_i, y_i	= length parameters; Figure 70
Z_1	= short side of a duct of rectangular cross section [ft]
Z_2	= long side of a duct of rectangular cross section [ft]

Greek Letters

μ = viscosity [lb_m/ft-sec]

ρ = density [lb_m/ft^3]

ν = kinematic viscosity [ft^2/sec]

ψ = stream function

$\vec{\nabla}$ = vector gradient

∇^2 = $\vec{\nabla} \cdot \vec{\nabla}$

∇^4 = biharmonic operator

Δ = rate of deformation tensor

η = similarity variable; Equation B-2

ζ = vorticity

θ = independent space variable in polar coordinates [rad]

θ_D, θ_R = angle of detachment and angle of reattachment [$^\circ$]: Table II

Φ = Re•f

ϕ = independent space variable in polar coordinates [rad]

$\vec{\tau}, \tau$ = shear stress vector and shear stress [lb_f/ft^2]

$\Delta\tau$ = pressure drop due to friction drag [lb_f/ft^2]

ω = over-relaxation parameter; Equation 4-49

ξ = parameter; Equation E-7

Subscript

i,j,m	= indices of space variables
duct	= of the duct
max	= of the maximum
vortex	= of the vortex
r	= of the r-direction
θ	= of the θ -direction
l	= of the longitudinal direction
t	= of the transverse direction
$\mathbb{C}$	= of the centerline (symmetry line)
∞	= undisturbed or at infinity

Superscript

$1,2,3$	= tube row number counted from inlet
k	= iteration index
n	= time step index
$'$	= physical quantities in the definition of the non-dimensionalization
cal	= calculated
exp	= experimental
$*$	= normalized values by deviding by $\frac{1}{2}\rho\bar{u}^2$

Notation Cited from Computer Programs

EPSMAX	= limit to be specified for $\sum_{i,j}(\zeta^{k+1}_{i,j}-\zeta^{k}_{i,j})$ and $\sum_{i,j}(\psi^{k+1}_{i,j}-\psi^{k}_{i,j})$
ITMAX	= maximum number of iterations for one computer run
K	= section identification number; Figure 14
N2	= number of increments in x-direction at the section K=12
NI,NO	= numbers of increments in x-direction at the inlet and outlet sections, respectively; Figure 14
NJ	= number of j-increments
NPT	= number of increments at the minimum clearance of tube bank flow channel; Figure 14
NS	= number of increments in θ-direction per an angle of $\pi/4$; Figure 14
NT	= number of tube rows; Figure 14
RE	= tube bank Reynolds number
PT	= transverse pitch ratio
F(M)	= contour values of vorticity or stream function to be plotted
NCOUNT	= number of contour values to be plotted
Q(1,J),Q(2,J)	= values of vorticity or stream function read at every two i-incremental steps
F(K,I,J)	= stream function
V(K,I,J)	= vorticity

A SELECTED BIBLIOGRAPHY

1. Bell, K. J., "Final Report - Cooperative Research Program on Shell and Tube Heat Exchangers", University of Delaware Experiment Station Bulletin No. 5 (1963)

2. Huge, E. C., "Experimental Investigation of Effects of Equipment Size on Convection Heat Transfer and Flow Resistance in Cross Flow of Gases over Tube Banks", Transactions A.S.M.E. 59, 573 -572 (1937)

3. Pierson, O. L., "Experimental Investigation of the Influence of Tube Arrangement on Convection Heat Transfer and Flow Resistance in Cross Flow Over Tube Banks", Transactions A.S.M.E. 59, 563 -572 (1937)

4. Bergelin, O. L., A. P. Colburn, and H. L. Hull, "Heat Transfer and Fluid Friction During Viscous Flow Across Banks of Tubes", University of Delaware Experiment Station Bulletin No. 2 (1950)

5. Bergelin, O. L., M. D. Leighton, W. L. Lafferty Jr, and R. L. Pigford, "Heat Transfer and Pressure Drop During Viscous and Turbulent Flow Across Baffled and Unbaffled Tube Banks", University of Delaware Experiment Station Bulletin No. 4 (1958)

6. Bell, K. J., "Exchanger Design Based on the Delaware Research Program", Petro-Chem Eng. 32, C26-C40c (1960)

7. Chilton, T. H. and R. P. Genereaux, "Pressure Drop Across Tube Banks", Transactions A.I.Ch.E. 29, 161-173 (1933)

8. Grimison. E. D., "Correlation and Utilization of New Data on Flow Resistance and Heat Transfer for Cross Flow of Gases Over Tube Banks", Transactions A.S.M.E. 59, 583-594 (1937)

9. Gunter, A. Y. and W. A. Shaw, "A General Correlation of Friction Factors for Various Types of Surfaces in Cross Flow", Transactions A.S.M.E. 67, 643-660 (1945)

10. Boucher, D. F. and C. F. Lapple, "Pressure Drop Across Tube Banks: Critical Comparison of Available Data and the Proposed Methods of Correlation", Chem. Eng. Prog. 44, 117-134 (1948)

11. Tamada, K. and H. Fujikawa, "The Steady Two-dimensional Flow of Viscous Fluid at Low Reynolds Numbers Passing Through an Infinite Row of Equal Parallel Circular Cylinders", Quart. Journ. Mech. and Applied Math. 10, 425-432 (1957)

12. Happel, J., "Viscous Flow Relative to Arrays of Cylinders", A.I.Ch.-E. Journal 5, 174-177 (1959)

13. Friedl, P. J. and K. J. Bell, "Approximate Solution for Creeping Flow in Complex Geometries: Flow Across Banks of Tubes", presented at December, 1960, meeting of American Institute of Chemical Engineers, Washington, D.C.

14. Graetz, L. Z., "Uber die Bewegung von Flussigkeiten in Rohren", Z. fur Math. und Phys. 25, 316 (1880)

15. Schlichting, H., Boundary Layer Theory, McGraw-Hill, New York (1959)

16. Pohlhausen, K., "Zur Naherungsweisen Integration der Differentialgleichung der Grenzschicht", Zeitschrift fur agew. Math. und Mech. 1, 252 (1921)

17. Millsaps, K. and K. Pohlhausen, "Thermal Distributions in Jeffery-Hamel Flow Between Nonparallel Plane Walls", Journ. Aero. Science 20, 187-196 (1953)

18. Bergelin, O. P., K. J. Bell, and M. D. Leighton, "Heat Transfer and Fluid Friction During Flow Across Banks of Tubes: VII. Bypassing Between Tube Bandle and Shell", Chem. Eng. Prog. Symposium Series 29, 129-145 (1959)

19. Bird, R. B., W. E. Stewart, and E. N. Lightfoot, Transport Phenomena, John Willey & Sons, New York (1960)

20. Schechter, R. S., The Variational Method in Engineering, McGraw-Hill, New York (1967)

21. Schechter, R. S., "On the Steady Flow of a Non-Newtonian Fluid in Cylinder Ducts", A.I.Ch.E. Journal 7, 445-448 (1961)

22. Delleur, J. W. and A. A. Sooky, "Variational Methods in Fluid Dynamics", Proc. Amer. Soc. Civ. Engrs. 87, EM 6, 57-77 (1961)

23. Bird, R. B., "New Variational Principle for Incompressible Non-Newtonian Flow", Physics of Fluids 3, 539-541 (1960)

24. Booth, A. D., "An Application of the Method of Steepest Descents to the Solution of Systems of Non-Linear Simultaneous Equations", Quart. Journ. Mech. and Applied Math. 2, 460-468 (1949)

25. Simon, R. and J. E. Briggs, "Application of Benedict-Webb-Rubin Equation of State to Hydrogen Sulfide-Hydrocarbon Mixtures", A.I.Ch.E. Journal 10, 548-550 (1964)

26. Thom, A., "The Flow Past Circular Cylinders at Low Speed", Proc. Roy. Soc. 131, Ser. A, 651-668 (1933)

27. Kawaguchi, M., "Numerical Solution of the Navier-Stokes Equations for the Flow Around a Circular Cylinder at Reynolds Number 40", Journ. Phys. Soc. Japan 8, 747 (1953)

28. Allen, D. N. de. G. and R. V. Southwell, "Relaxation Methods Applied to Determine the Motion, in Two Dimensions, of a Viscous Fluid Past a Fixed Cylinder", Quart. Journ. Mech. and Applied Math. 8, 129-145 (1955)

29. Keller, H. B. and H. Takami, "Numerical Studies of Steady Viscous Flow About Cylinders", Proc. Symp. on Numerical Solution of Nonlinear Differential Equations, 115-140, University of Wisconsin (1966)

30. Son, J. S. and T. J. Hanratty, "Numerical Solution for the Flow Around a Cylinder at Reynolds Numbers of 40, 200, and 500", Journ. Fluid Mech. 35, 369-386 (1969)

31. Hung, W. T. K. and E. O. Macagno, "Laminar Eddies in a Two Dimensional Conduit Expansion", La Houille Blanche 21, 391-400 (1966)

32. Mills, R. D., "Numerical Solutions of Viscous Flow Through a Pipe Orifice at Low Reynolds Numbers", Journ. Mech. Eng. Sci. 10, 133-140 (1968)

33. Mills, R. D., "Numerical Solutions of the Viscous Flow Equations for a Class of Closed Flows", Journ. Roy. Aero. Soc. 69, 714-718 (1965)

34. Milne, W. E., Numerical Solution of Differential Equations, John Willey & Sons, New York (1953)

35. Carnahan, B., J. O. Wilkes, and H. A. Luter, Applied Numerical Solutions of the Navier-Stokes Equations, John Willey & Sons, New York (1969)

36. Russel, D..B., "On Obtaining Solution to the Navier-Stokes Equations with Automatic Digital Computers", Rep. Memo. Aero. Res. Coun. No. 3331 (1962)

37. Thom, A. and C. J. Apelt, "Note on the Convergence of Numerical Solutions of the Navier-Stokes Equations", Rep. Memo. Aero. Res. Coun. No. 3061 (1956)

38. Lester, W. G..S., "Some Convergence Probles in Numerical Solution of the Navier-Stokes Equations", Rep. Memo. Aero. Coun. No. 3239 (1961)

39. Acrivos, A., L. G. Leal, D. D. Snowden, and F. Pan, "Further Experiments on Steady Separated Flows Past Bluff Objects", Journ. Fluid Mech. 34, 25-48 (1968)

40. Taneda, S., "Experimental Investigation of the Wakes Behind Cylinders and Plates at Low Reynolds Numbers", Journ. Phys. Soc. Japan 11, 302-307 (1956)

41. Kitaura, Y., H. Tanaka, H. Tanaka, and T. Miura, "Fluid Flow and Pressure Drop in Tube Banks", Kagaku Kogaku (Chem. Eng. Japan) 92, 883-889 (1968)

APPENDIX A

VELOCITY PROFILE IN CONVERGING

AND DIVERGING CHANNELS

For the radial flow between converging and diverging walls (Figure 62), the Navier-Stokes equations in polar coordinates may be written:

Continuity condition;

$$\frac{\partial [rv_r]}{\partial r} = 0 \tag{A-1}$$

Equations of motion;

r-component $$v_r \frac{\partial v_r}{\partial r} = -\frac{1}{\rho}\frac{\partial P}{\partial r} + \frac{\nu}{r^2}\frac{\partial^2 v_r}{\partial \theta^2} \tag{A-2}$$

θ - component $$\frac{2\mu}{r}\frac{\partial v_r}{\partial \theta} = \frac{\partial P}{\partial \theta} \tag{A-3}$$

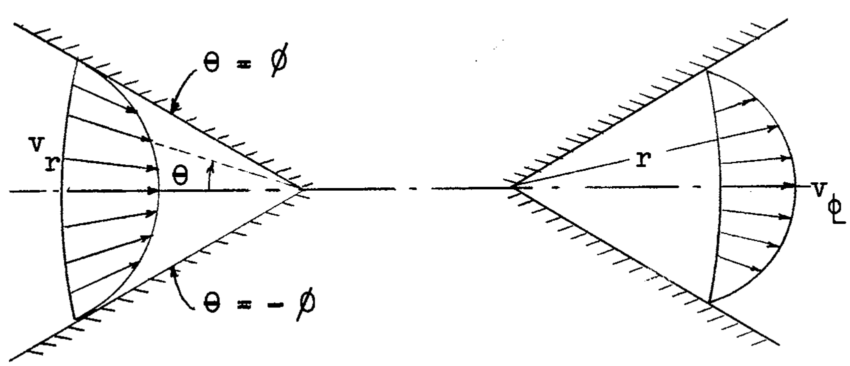

Figure 62. Flows in Converging and Diverging Channels

Here, the boundary conditions are

$$\left.\begin{array}{ll} v_r = 0 & \text{at } \theta = \phi \\ \left.\begin{array}{l} v_r = v_\phi \\ \dfrac{\partial v_r}{\partial \theta} = 0 \end{array}\right\} & \text{at } \theta = 0 \end{array}\right\} \tag{A-4}$$

<u>General Equation</u>

The equation of continuity, Equation A-1, is satisfied by introducing the similarity variable, $F(\theta)$, a function of θ given by

$$v_r = \left(\frac{\nu \, Re_r}{r}\right) F(\theta) \tag{A-5}$$

where Re_r is defined by

$$Re_r = \frac{r \, v_\phi}{\nu} \tag{A-6}$$

and v_o is the radial velocity along the centerline of the channel. Since the flow is radial, the velocity is inversely proportional to the radius and hence the Reynolds number Re_r is invariant along the channel. Differentiating Equation A-2 and A-3, with respect to θ and r respectively, and subtracting one from the other to eliminate pressure terms, one gets

$$\frac{\partial v_r}{\partial \theta} \frac{\partial v_r}{\partial r} + v_r \frac{\partial^2 v_r}{r \partial \theta \partial r} = \frac{\nu}{r}\left[- 2 \frac{\partial^2 v_r}{\partial r \partial \theta} + \frac{1}{r} \frac{\partial^2 v_r}{\partial \theta^2} + \frac{4 \partial v_r}{r \partial \theta}\right] \tag{A-7}$$

Differentiating Equation A-5 with respect to Θ and r, and substituting into Equation A-7, one obtains, after rearrangement, the ordinary differential equation of $F(\Theta)$

$$F'''(\Theta) + 4\,F'(\Theta) + 2\,F(\Theta)F'(\Theta) = 0 \tag{A-8}$$

Boundary conditions, Equation A-4, may be rewritten

$$\begin{aligned} F(\pm \phi) &= 0 \\ F'(0) &= 0 \\ F(0) &= 1 \end{aligned} \tag{A-9}$$

<u>High Reynolds Number Approximation</u>

At high Reynolds number a potential flow exists in the core region and a boundary layer flow is expected at the region adjacent to the wall. The solution of the boundary layer equation for the converging flow has been obtained by Pohlhausen (16).

Integrating Equation A-8 with respect to Θ, one gets

$$[F(\Theta)]^2 + 4\,F(\Theta) + F''(\Theta) + E_1 = 0 \tag{A-10}$$

Multiplying Equation A-10 by $6F'(\Theta)$ and integrating again, one finds

$$2[F(\Theta)]^3 + 12[F(\Theta)]^2 + 3[F'(\Theta)]^2 + 6E_1F(\Theta) + 2E_2 = 0 \tag{A-11}$$

where E_1 and E_2 denote the integration constants.

Solving Equation A-11 for $F'(\theta)$, and after rearrangement, the following expression is obtained

$$\theta = \sqrt{\frac{3}{2}} \int \frac{dF(\theta)}{E_2 - 3E_1 F(\theta) - 6[F(\theta)]^2 - [F(\theta)]^3} \tag{A-12}$$

For high Reynolds number, Equation A-12 has been integrated to yield (17)

$$F(\theta) = 3 \tanh^2[\sqrt{\frac{Re_r}{2}}(\theta - \phi) + 1.1462] - 2 \tag{A-13}$$

Shear stress at the angular position ϕ in the converging section of the channel (Figure 5) may be given by

$$\tau = \frac{\mu}{r}\left(\frac{\partial v_r}{\partial \theta}\right)_{\theta=\phi} \tag{A-14}$$

From Equation A-5, one gets

$$\frac{\partial v_r}{\partial \theta} = \frac{\nu \, Re_r}{r} F'(\theta) \tag{A-15}$$

Differentiating Equation A-13 with respect to θ, $F'(\theta)$ is found

$$F'(\theta) = 6\sqrt{\frac{Re_r}{2}} \frac{\sinh[\frac{Re_r}{2}(\theta - \phi) + 1.1462]}{\cosh^3 [\frac{Re_r}{2}(\theta - \phi) + 1.1462]} \tag{A-16}$$

Thus,

$$F'(\phi) = 1.155\sqrt{Re_r} \tag{A-17}$$

From Equations A-14, A-15 and A-17, one obtains the local shear stress at angular position of ϕ on a tube surface in the converging channel section,

$$\frac{\tau}{\frac{1}{2}\rho v_o^2} = \frac{2.31}{\sqrt{Re_r}} \tag{A-18}$$

Since the continuity condition gives

$$\bar{u}\,(P_t - 1)\,D_t = \int_{-\phi}^{\phi} v_r \, r \, d\theta \tag{A-19}$$

or after rearrangement,

$$Re(P_t - 1) = 2\,Re_r \int_0^{\phi} F(\theta)\, d\theta \tag{A-20}$$

Substituting Equation A-13 into Equation A-20, one finds after integration

$$Re\left(\frac{P_t - 1}{2}\right) = \sqrt{2Re_r}\left[\,2\phi + 3\sqrt{\frac{Re_r}{2}}\,\phi + 3\left\{\tanh(1.1462) - \tanh\left(\sqrt{\frac{Re_r}{2}}\,\phi + 1.1462\right)\right\}\right] \tag{A-21}$$

For high Reynolds number ϕ and the term $3[\tanh(1.1462)-\tanh(\sqrt{Re_r/2}\,\phi + 1.1462)]$ are negligible compared with the term $\sqrt{Re_r/2}\,\phi$. Hence, Equation A-21 can be approximated by

$$Re\left(\frac{P_t - 1}{2}\right) \doteq 3\,Re_r\,\phi \tag{A-22}$$

Substituting Equation A-22 into Equation A-18, the normalized shear stress becomes

$$\frac{\tau}{\frac{1}{2}\rho v_o^2} = \frac{2.31}{\sqrt{Re\left(\frac{P_t - 1}{6\theta}\right)}} \tag{A-23}$$

The friction factor around the converging part of channel between tubes is then calculated by integrating Equation A-23 from 0 to $\pi/2$,

$$f = \frac{(2)(2.31)(6)}{\sqrt{Re\ (P_t - 1)}} \int_0^{\pi/2} \sqrt{\phi}\ d\phi$$

$$= \frac{14.7}{\sqrt{(P_t-1)Re}} \tag{A-24}$$

APPENDIX B

ENERGY DISSIPATION DUE TO VORTEX MOTION

The Rayleigh flow which describes the flow induced by a sudden motion of flat plate originally at rest at time s = 0 (Figure 63), may be expressed in terms of velocity profile of fluid at time s

$$U = 1 - \frac{2}{\sqrt{\pi}} \int_0^{\eta} \exp(-\eta^2)\, d\eta \tag{B-1}$$

where

$$\eta = \frac{y}{2\sqrt{\nu s}} \tag{B-2}$$

$$U = u/u^*$$

u^* = constant velocity of flat plate

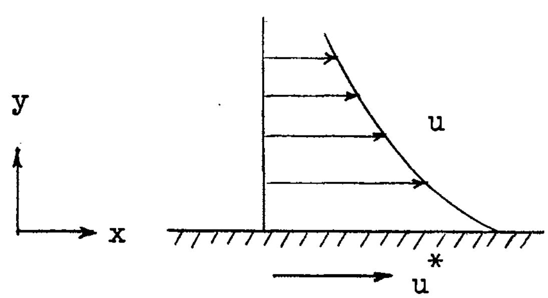

Figure 63. Rayleigh Flow

The shear stress acting on the surface of a plate is given by

$$\tau = -\frac{\mu}{g_c}\left.\frac{du}{dy}\right|_{y=0} \tag{B-3}$$

Upon substitution of Equation B-1 into Equation B-3, the shear stress is obtained after integration

$$\tau = \frac{\mu u^*}{g_c\sqrt{\pi\nu s}} \tag{B-4}$$

Work required to move the flat plate from x = 0 at standstill to $x = L^*$ at the constant velocity of u^* may be calculated from

$$\int_0^{L^*} \tau \, dx = \frac{\mu u^*}{g_c}\sqrt{\frac{u^*}{\pi\nu}}\, 2\, L^{*\frac{1}{2}} \tag{B-5}$$

where the use is made of $s = L^*/u^*$ in the process of integration.

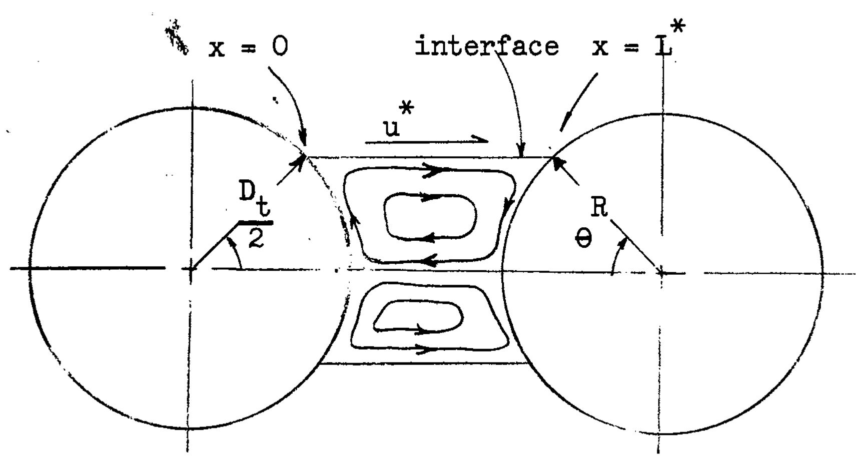

Figure 64. Vortex Flow Between Tubes

The vortex motion in the eddy between tubes (Figure 64) is assumed to be induced by the main flow which accelerates a sheet of fluid in the eddy at the point of detachment, $x = 0$, to the point of reattachment, $x = L^*$, where the fluid is then turned back along the tube surfaces and the velocity dies out where the sheet of fluid returns the original point around the neighborhood of the point of detachment, and then new cycle starts. All the energy transfered from the main flow to the wake at the interface which is then dissipated by the vortex motion in the wake may be calculated from Equation B-5. The pressure drop to the energy lost is then given by

$$\Delta P_{vortex} = \frac{2}{L^*} \int_0^{L^*} \tau \, dx$$

$$= \frac{4}{g_c \sqrt{\pi}} \sqrt{\frac{\rho \mu}{L^*}} \; u^{*\frac{3}{2}} \qquad \text{(B-6)}$$

Rearranging with the following expressions

$$L^* = D_t (P_t - \cos\theta) \qquad \text{(B-7)}$$

$$u^* = \frac{u^* (P_t - \sin\theta)}{P_t - 1} \qquad \text{(B-8)}$$

into the form of friction factor, Equation B-6 results in

$$f_{vortex} = \frac{1.13}{Re} \; \frac{(P_t - 1)^{3/2}}{(P_t - \cos\theta)(P_t - \sin\theta)} \qquad \text{(B-9)}$$

APPENDIX C

VARIATIONAL FUNCTION FOR TWO-DIMENSIONAL POWER-LAW FLUID FLOW

The power-law (Ostwald-dewaele) model of non-Newtonian fluid flow characteristic may be expressed in terms of tensor notation (19) by

$$\vec{\tau} = - K \left(\frac{|\Delta : \Delta|}{2} \right)^{\frac{n-1}{2}} \Delta \qquad \text{(C-1)}$$

where Δ is the rate of deformation tensor, K is the consistency index of a fluid expressing the physical property of the fluid, and n is the power-law index characterizing the degree of non-Newtonian behavior of the fluid.

For the steady flow of an incompressible power-law fluid through the unit cell of tube bank (Figure 9), where the boundary condition specifies the velocity on one part of the boundary and the stresses on the other part of the boundary, the energy change per unit volume of fluid may be given (22, 23) by the dimensional expression

$$F' = \frac{K}{n+1} \left(\Delta : \Delta \right)^{\frac{n+1}{2}} - 2 \vec{\nabla} \cdot P \vec{v} \qquad \text{(C-2)}$$

The first term in the right hand side of Equation C-2 is the rate of irreversible conversion to internal energy and for the power-law fluid this term reduces to the following expression (19, 22) in the two-dimensional rectangular coordinates,

$$\tfrac{1}{2}(-\vec{\tau}\cdot\nabla\vec{\tau}) = \frac{1}{2}\left[2\left\{(\frac{\partial u'}{\partial x'})^2 + (\frac{\partial v'}{\partial y'})^2\right\} + (\frac{\partial v'}{\partial x'} + \frac{\partial u'}{\partial y'})^2\right] \tag{C-3}$$

The second term in Equation C-2 turns out to be

$$2(\vec{\nabla}\cdot P\vec{v}) = 2\left[(-\frac{\partial P'}{\partial x'})\, u' + (-\frac{\partial P'}{\partial y'})\, v'\right] \tag{C-4}$$

Substituting Equation C-3 and Equation C-4 into Equation C-2, one gets

$$F' = \frac{K}{n+1}\left[2(\frac{\partial u'}{\partial x'})^2 + 2(\frac{\partial v'}{\partial y'})^2 + (\frac{\partial u'}{\partial y'} + \frac{\partial v'}{\partial x'})^2 \right]^{\frac{n+1}{2}}$$

$$- \left\{(-\frac{\partial P'}{\partial x'})\, u' + (-\frac{\partial P'}{\partial y'})\, v' \right\} \tag{C-5}$$

The following variables are introduced to non-dimensionalize Equation C-5:

$$X = x'/R', \quad Y = y'/R'$$

$$U = u'/\,\bar{u}', \quad V = v'/\,\bar{u}' \tag{C-6}$$

and

$$F = \frac{F'}{(\frac{K}{n+1})(\frac{\bar{u}'}{R'})^{n+1}}$$

Substituting these into Equation C-5, one finds

$$F = \left[2(\frac{\partial U}{\partial X})^2 + (\frac{\partial V}{\partial Y})^2 + (\frac{\partial U}{\partial Y} + \frac{\partial V}{\partial X})^2 \right]^{\frac{n+1}{2}}$$

$$- \left\{(-\frac{\partial P}{\partial X})(\frac{2R}{\rho\bar{u}^2})\frac{(2R)^n\,\bar{u}^{2-n}}{\frac{2^n}{n+1}K} + (-\frac{\partial P}{\partial Y})(\frac{2R}{\rho\bar{u}^2})\frac{(2R)^n\,\bar{u}^{2-n}}{\frac{2^n}{n+1}K}\right\} \tag{C-7}$$

Rearranging further with the definition given by

$$Re_n = \frac{(2R)^n \ \bar{u}^{2-n}}{\frac{2^n}{n+1} K} \tag{C-8}$$

and

$$f_n = \left(-\frac{\partial P}{\partial X}\right) \frac{2R}{\frac{2^n}{n+1} K} \tag{C-9}$$

and also assuming that

$$\frac{\left(-\frac{\partial P}{\partial Y}\right)}{\left(-\frac{\partial P}{\partial X}\right)} = \frac{\partial X}{\partial Y} \tag{C-10}$$

one obtains the final formula for F,

$$F = \left[2\left(\frac{\partial U}{\partial X}\right)^2 + 2\left(\frac{\partial V}{\partial Y}\right)^2 + \left(\frac{\partial U}{\partial Y} + \frac{\partial V}{\partial X}\right)^2 \right]^{\frac{n+1}{2}}$$

$$- Re_n \ f_n\left(U + \frac{\partial X}{\partial Y} V\right) \tag{C-11}$$

APPENDIX D

INTEGRATION AND MINIMIZATION OF THE DISSIPATION INTEGRAL

The dissipation integral, Equation 3-23, may be written for the case of Newtonian fluid (n = 1) as

$$I = I_1 + I_2 + I_3 + I_4 \tag{D-1}$$

where

$$I_1 = \int_{-P_t}^{P_t}\int_{-P_1}^{P_1} 2\left(\frac{\partial U}{\partial X}\right)^2 dX\, dY \tag{D-2}$$

$$I_2 = \int_{-P_t}^{P_t}\int_{-P_1}^{P_1} 2\left(\frac{\partial V}{\partial Y}\right)^2 dX\, dY \tag{D-3}$$

$$I_3 = \int_{-P_t}^{P_t}\int_{-P_1}^{P_1} \left(\frac{\partial U}{\partial Y} + \frac{\partial V}{\partial X}\right)^2 dX\, dY \tag{D-4}$$

and

$$I_4 = \int_{-P_t}^{P_t}\int_{-P_1}^{P_1} - \Phi \left(U + \frac{\partial X}{\partial Y} V\right) dX\, dY \tag{D-5}$$

Since the integrands in Equations D-2, D-3 and D-4 are always positive, the symmetry condition can be applied to simplify the integration of these equations. And considering the non-uniform boundary of the integration, Equations D-2, D-3 and D-4 become

$$I_1 = 8\int_{X=0}^{X=1}\int_{Y=\sqrt{1-X^2}}^{Y=P_t} \left(\frac{\partial U}{\partial X}\right)^2 dY\, dX + 8\int_{X=1}^{X=P_1}\int_{Y=0}^{Y=P_t} \left(\frac{\partial U}{\partial X}\right)^2 dY\, dX \tag{D-2'}$$

$$I_2 = 8\int_{X=0}^{X=1}\int_{Y=\sqrt{1-X^2}}^{Y=P_t} \left(\frac{\partial V}{\partial Y}\right)^2 dY\, dX + 8\int_{X=1}^{X=P_1}\int_{Y=0}^{Y=P_t} \left(\frac{\partial V}{\partial Y}\right)^2 dY\, dX \tag{D-3'}$$

$$I_3 = 8\int_{X=0}^{X=1}\int_{Y=\sqrt{1-X^2}}^{Y=P_t} \left(\frac{\partial U}{\partial Y} + \frac{\partial V}{\partial X}\right)^2 dY\, dX + 8\int_{X=1}^{X=P_1}\int_{Y=0}^{Y=P_t} \left(\frac{\partial U}{\partial Y} + \frac{\partial V}{\partial X}\right)^2 dY\, dX \tag{D-4'}$$

<u>With the First Trial Velocity Profile</u>

The velocity gradients from Equation 3-26 and Equation 3-27 are calculated as:

$$\frac{\partial U}{\partial X} = 2\,X\,[C_1 + C_2(2\,X^2 - 1 + Y^2)] \tag{D-6}$$

$$\frac{\partial V}{\partial Y} = C_3\,X\,[-5\,Y^4 - 3(X^2 - 1 - P_t^2)Y^2 + P_t^2(X^2 - 1)\,] \tag{D-7}$$

$$\frac{\partial U}{\partial Y} = 2\,(C_1 + C_2X^2)Y \tag{D-8}$$

$$\frac{\partial V}{\partial X} = C_3[\,-Y^5 + (P_t^2 + 1 - 3X^2)Y^3 + P_t^3(3X^2 - 1)Y\,] \tag{D-9}$$

Substituting Equation D-6 into Equation D-2' and integrating with respect to Y, one gets

$$\frac{1}{32} I_1 = \int_{X=0}^{X=1} X^2[C_1^2(P_t - \sqrt{1-X^2}) + 2C_1C_2\Big\{(2X^2-1)(P_t - \sqrt{1-X^2})$$

$$+ \frac{P_t^3 - (\sqrt{1-X^2})^3}{3}\Big\} + C_2^2\Big\{(2X^2-1)^2(P_t - \sqrt{1-X^2}) + 2(2X^2-1)$$

$$\frac{P_t^3 - (\sqrt{1-X^2})^3}{3} + \frac{1}{5}(P_t^5 - (\sqrt{1-X^2})^5)\Big\}]\,dX$$

$$+ \int_{X=1}^{X=P_1} X^2[C_1^2 P_t + 2C_1C_2\Big\{(2X^2-1)P_t + \frac{P_t^3}{3}\Big\}$$

$$+ C_2^2\Big\{(2X^2-1)^2 P_t + 2(2X^2-1)\frac{P_t^3}{3} + \frac{P_t^5}{5}\Big\}]\,dX \tag{D-10}$$

Introducing new variable θ defined by

$$\sin\theta = X,\ \cos\theta = \sqrt{1 - X^2} \text{ and } dX = \cos\theta\,d\theta \tag{D-11}$$

Equation D-10 may be written as

$$\frac{1}{32} I_1 = \int_0^{\frac{\pi}{2}} \sin^2\theta\,\cos\theta\,[C_1^2(P_t - \cos\theta) + 2C_1C_2\Big\{(2\sin^2\theta)(P_t - \cos\theta)$$

$$+ \frac{P_t^3 - \cos\theta}{3} \Big\} + C_2^2 \Big\{ (2\sin\theta - 1)^2 (P_t - \cos\theta) + 2(2\sin\theta - 1) \frac{P_t^3 - \cos^3\theta}{3}$$

$$+ \frac{1}{5}(P_t^5 - \cos\theta) \Big\}]\, d\theta + \int_1^{P_1} X^2 \, [C_1^2 P_t + 2C_1 C_2 \Big\{ (2X^2-1)P_t + \frac{P_t^3}{3} \Big\}$$

$$+ C_2^2 \Big\{ (2X^2-1)^2 P_t + 2(2X^2-1)\frac{P_t^3}{3} + \frac{P_t^5}{5} \Big\}]\, dX \qquad \text{(D-12)}$$

After tedious piece-wise integration, one finds

$$I_1 = C_1^2 \left(\frac{32}{3} P_t P_1^3 - 2\pi\right) + 2C_1 C_2 \left[\frac{32}{9} P_t^3 P_1^3 + 32 P_t P_1^3 \left(\frac{2}{3} P_1^2 - \frac{1}{3}\right) - \frac{\pi}{3} \right]$$

$$+ C_1^2 \left[\frac{32}{15} P_t^5 P_1^3 + \frac{64}{3} P_t^3 P_1^3 \left(\frac{2}{5} P_1^2 - \frac{1}{3}\right) + 32 P_t P_1^3 \left(\frac{4}{7} P_1^4 - \frac{4}{5} P_1^2 + \frac{1}{3}\right) - \frac{11}{24}\pi \right] \qquad \text{(D-13)}$$

Similar expressions are obtained for I_2, I_3 and I_4, and then substituted into Equation D-1 and rearranged to result in

$$I = I_1 + I_2 + I_3 + I_4$$

$$= f_1 C_1^2 + f_2 C_1 C_2 + f_3 C_2^2 + f_4 C_3^2 + f_5 C_1 C_3 + f_6 C_2 C_3$$

$$-(f_7 C_1 + f_8 C_2 + f_9 C_3)\, \Phi \qquad \text{(D-14)}$$

where

$$f_1 = \frac{16}{3} P_t^3 P_1 + \frac{32}{3} P_t P_1^3 - 3\pi$$

$$\left.\begin{aligned}
f_2 &= \frac{32}{3}P_t^3P_1^3 + 64P_tP_1^3\left(\frac{2}{5}P_1^2 - \frac{1}{3}\right) - \pi \\
f_3 &= \frac{32}{15}P_t^3P_1^3 + \frac{16}{3}P_t^3P_1^3\left(\frac{9}{5}P_1^2 - \frac{4}{3}\right) + 32P_tP_1^3\left(\frac{4}{7}P_1^4 - \frac{4}{5}P_1^2 + \frac{1}{3}\right) - \frac{25}{48}\pi \\
f_4 &= \frac{32}{693}P_t^{11}P_1 + \frac{32}{315}P_t^9P_1^3\left(\frac{29}{3}P_1^2 - 2\right) + \frac{32}{35}P_t^7P_1\left(\frac{9}{5}P_1^4 - \frac{8}{3}P_1^2 + \frac{1}{3}\right) \\
&\quad + \frac{32}{5}P_t^5P_1^3\left(\frac{P_1^4}{7} - \frac{2}{5}P_1^2 + \frac{1}{3}\right) - \frac{3\pi}{16}P_t^4 + \frac{345}{1280}\pi P_t^2 - \frac{713}{7680}\pi \\
f_5 &= \frac{32}{35}P_t^7P_1 + \frac{32}{15}P_t^5P_1(P_1^2 - 1) \\
f_6 &= \frac{32}{105}P_t^7P_1^3 + \frac{32}{5}P_t^5P_1^3\left(\frac{P_1^2}{5} - \frac{1}{9}\right) - \frac{\pi}{12}P_t^2 - \frac{\pi}{40} \\
f_7 &= \frac{4}{3}P_t^3P_1 + \frac{4}{3}P_tP_1^3 - 4P_tP_1 + \frac{\pi}{2} \\
f_8 &= \frac{4}{9}P_t^3P_1^3 + \frac{4}{5}P_tP_1^5 - \frac{4}{3}P_tP_1^3 - \frac{\pi}{12} \\
f_9 &= 0
\end{aligned}\right\} \quad \text{(D-15)}$$

It should be noted here that, in the process of integration of Equation D-5, the $\frac{\partial X}{\partial Y}V$ term was neglected so that f_9 become zero in Equation D-15. This should be justifiable since V should not be important in steady uniform flow compared with U.

Applying the set of conditions for minimization of I, Equation 3-24, one gets

$$\frac{\partial I}{\partial C_1} = 2\,f_1C_1 + f_2C_2 + f_5C_3 - f_7\,\Phi = 0$$

$$\frac{\partial I}{\partial C_2} = f_2 C_1 + 2\, f_3 C_2 + f_6\, C_3 - f_8\, \Phi = 0 \tag{D-16}$$

$$\frac{\partial I}{\partial C_3} = f_5 C_1 + f_6 C_2 + 2\, f_4 C_3 - f_9\, \Phi = 0$$

However the continuity condition, Equation 3-25, predetermines C_1 as

$$1 = \frac{1}{P_t - 1} \int_1^{P_t - 1} C_1 (Y^2 - 1)\, dY$$

or

$$C_1 = \frac{3}{P_t^2 + P_t - 2} \tag{D-17}$$

The set of equations in Equation D-16 are then solved for C_2, C_3 and Φ:

$$C_2 = \frac{C_1}{\text{Det}} \begin{vmatrix} 2f_1 & f_7 & f_5 \\ f_2 & f_8 & f_6 \\ f_5 & f_9 & 2f_4 \end{vmatrix} \tag{D-18}$$

$$C_3 = \frac{C_1}{\text{Det}} \begin{vmatrix} 2f_1 & f_2 & f_7 \\ f_2 & 2f_3 & f_8 \\ f_5 & f_6 & f_9 \end{vmatrix} \tag{D-19}$$

and

$$\Phi = \frac{C_1}{\text{Det}} \begin{vmatrix} 2f_1 & f_2 & f_5 \\ f_2 & 2f_3 & f_6 \\ f_5 & f_6 & 2f_4 \end{vmatrix} \tag{D-20}$$

where

$$\mathrm{Det} = \begin{vmatrix} f_7 & f_2 & f_5 \\ f_8 & 2f_3 & f_6 \\ f_9 & f_6 & 2f_4 \end{vmatrix} \tag{D-21}$$

When $P_t = P_l = 1.50$ and $P_t = P_l = 1.25$ (inline square layout) are substituted into Equations D-17, D-20 and D-21, the following friction factor vs. Reynolds number relationships are obtained, respectively:

$$f = \frac{18.4}{Re} \qquad \text{for } P_t = 1.50 \tag{D-22}$$

$$f = \frac{45.5}{Re} \qquad \text{for } P_t = 1.25 \tag{D-23}$$

If the term $\frac{\partial X}{\partial Y} V$ is not neglected but assumed to be

$$\frac{\partial X}{\partial Y} V = \frac{X}{Y} V \tag{D-24}$$

the coefficient f_9 of Equation D-15 becomes

$$f_9 = \frac{8}{3} P_t^3 P_l^3 \left(\frac{P_t^2}{15} + \frac{P_l^2}{5} - \frac{1}{3} \right) + \frac{\pi}{12} P_t^2 - \frac{\pi}{96} \tag{D-25}$$

and the following results,

$$f = \frac{21.7}{Re} \qquad \text{for } P_t = 1.50 \tag{D-26}$$

and

$$f = \frac{52.8}{Re} \quad \text{for } P_t = 1.25 \tag{D-27}$$

<u>With the Second Trial Velocity Profile</u>

Exactly the same procedure will be followed:

The velocity gradients from Equations 3-34 and 3-27 are;

$$\frac{\partial U}{\partial X} = 2X \left[2C_1(X^2 + P_t^2 - 1) - C_2 \left\{ Y^4 - 2P_t^2Y^2 - 3X^2 - 4(P_t^2 - 1)X^2 + (2P_t^2 - 1) \right\} \right] \tag{D-28}$$

$$\frac{\partial V}{\partial Y} = C_3X \left[-5Y^4 - 3(X^2 - 1 - P_t^2)Y^2 + P_t^2(X^2 - 1) \right] \tag{D-29}$$

$$\frac{\partial U}{\partial Y} = 4Y(C_1 + C_2X^2)(P_t^2 - Y^2) \tag{D-30}$$

and

$$\frac{\partial V}{\partial X} = C_3\left[-Y^5 + (P_t^2 + 1 - 3X^2)Y^3 + P_t^2(3X^2 - 1)Y \right] \tag{D-31}$$

Substituting Equation D-28 into Equation D-2' and first integrating with respect to Y and introducing new variable θ defined by Equation D-11, one finds

$$\frac{1}{32} I_1 = (2P_t^2-1)\int_0^{\frac{\pi}{2}} \sin^2\theta \cos\theta\Big[C_1^2(P_t-\cos\theta)+2C_1C_2\Big\{(2\sin^2\theta-1)(P_t-\cos\theta) + \frac{P_t^3-\cos^3\theta}{3}\Big\}+C_2^2\Big\{(2\sin^2\theta-1)^2(P_t-\cos\theta)+2(2\sin^2\theta$$

$$- 1)\frac{P_t^3 - \cos^3\theta}{3} + \frac{P_t^5 - \cos^5\theta}{5}\Big\}\Big]\, d\theta + (2P_t^2-1)^2 \int_0^{P_1} \Big[C_1^2 P_t X^2$$

$$+ 2C_1C_2\Big\{(2X^4 - X^2)P_t + \frac{P_t^3}{3} X^2\Big\} + C_1^2\Big\{(4X^6 - 4X^4 + X^2)P_t$$

$$+ \frac{2}{3}P_t^3(2X^4 - X^2) + \frac{P_t^5}{5} X^2\Big\}\Big]\, dX \tag{D-32}$$

After considerable manipulation in the integration process, one obtains

$$I_1 = C_1^2\Big\{\Big(\frac{32}{3}P_t P_1^3 - 2\pi\Big)(2P_t^2-1)^2 - 2(2P_t^2-1)\Big(\frac{32}{9}P_t^3P_1^3 - \frac{\pi}{3}\Big) + \frac{32}{15}P_t^5P_1^3 - \frac{\pi}{8}\Big\}$$

$$+ 2C_1C_2\Big[\Big\{\frac{32}{9}P_t^3P_1^3 + 32P_tP_1^3\Big(\frac{2}{5}P_1^2 - \frac{1}{3}\Big) - \frac{\pi}{3}\Big\}(2P_t^2-1)^2 - 2(2P_t^2-1)$$

$$\Big\{\frac{32}{15}P_t^5P_1^3 + \frac{32}{3}P_t^3P_1^3\Big(\frac{2}{5}P_1^2 - \frac{1}{3}\Big) - \frac{\pi}{24}\Big\} + \frac{32}{21}P_t^7P_1^3 + \frac{32}{5}P_t^5P_1^3\Big(\frac{2}{5}P_1^2 - \frac{1}{3}\Big)$$

$$- \frac{21}{80}\pi\Big] + C_2^2\Big[\Big\{\frac{32}{15}P_t^5P_1^3 + \frac{64}{3}P_t^3P_1^3\Big(\frac{2}{5}P_1^2 - \frac{1}{3}\Big) + 32P_tP_1^3\Big(\frac{4}{7}P_1^4 - \frac{4}{5}P_1^2 + \frac{1}{3}\Big)$$

$$- \frac{11}{24}\pi\Big\}(2P_t^2-1)^2 - 2(2P_t^2-1)\Big\{\frac{32}{21}P_t^7P_1^3 + \frac{64}{5}P_t^5P_1^3\Big(\frac{2}{5}P_1^2 - \frac{1}{3}\Big) + \frac{32}{3}P_t^3P_1^3$$

$$\Big(\frac{4}{7}P_1^4 - \frac{4}{5}P_1^2 + \frac{1}{3}\Big) - \frac{11}{240}\pi\Big\} + \frac{32}{27}P_t^4P_1^3 + \frac{64}{7}P_t^7P_1^3\Big(\frac{2}{5}P_1^2 - \frac{1}{3}\Big) + \frac{32}{5}P_t^5P_1^3$$

$$\Big(\frac{4}{7}P_1^4 - \frac{4}{5}P_1^2 + \frac{1}{3}\Big) - \frac{11}{960}\pi\Big] \tag{D-33}$$

Similarly upon integration of I_2, I_3 and I_4 with the second trial velocities and substitution into Equation D-1, the dissipation integral assumes the same form as Equation D-14 but with different expressions for f_1 to f_9:

$$f_1 = 64\left[\frac{8}{105}P_t^7P_1 + \frac{2}{3}P_t^5P_1^3 + 4P_t^3P_1^3\left(\frac{P_1^2}{5} - \frac{1}{3}\right) + 2P_tP_1^3\left(\frac{P_1^4}{7} - \frac{2}{5}P_1^2 + \frac{1}{3}\right) - \frac{3}{16}\pi P_t^4 + \frac{3}{16}\pi P_t^2 \right] - \frac{15}{4}\pi$$

$$f_2 = 128\left[\frac{32}{315}P_t^7P_1^3 + \frac{P_t^5P_1^3}{15}\left(\frac{67}{5}P_1^2 - \frac{32}{3}\right) + P_t^3P_1^3(P_1^2-1)^2 + P_tP_1^3\left(\frac{P_1^6}{3} - P_1^4 + P_1^2 - \frac{1}{3}\right)\right] - \frac{8}{3}\pi P_t^4 + \frac{\pi}{3}P_t^2 - \frac{7}{20}\pi$$

$$f_3 = 32\left[\frac{107}{945}P_t^9P_1^3 + \frac{4}{15}P_t^7P_1^3\left(\frac{34}{7}P_1^2 - \frac{7}{3}\right) + \frac{2}{5}P_t^5P_1^3\left(\frac{47}{7}P_1^4 - \frac{148}{15}P_1^2 + \frac{37}{9}\right) + 4P_t^3P_1^3\left(\frac{2}{3}P_1^6 - \frac{8}{7}P_1^4 + \frac{6}{5}P_1^2 - \frac{1}{3}\right) + P_tP_1^3\left(\frac{9}{11}P_1^8 - \frac{24}{9}P_1^6 + \frac{22}{7}P_1^4 - \frac{8}{5}P_1^2 + \frac{1}{3}\right)\right] - \frac{25}{12}\pi P_t^4 + \frac{97}{60}\pi P_t^2 - \frac{109}{480}\pi$$

$$f_4 = 32\left[\frac{P_t^{11}P_1}{693} + \frac{P_t^9P_1}{315}\left(\frac{29}{3}P_1^2 - 2\right) + \frac{P_t^7P_1}{35}\left(\frac{9}{5}P_1^4 - \frac{8}{3}P_1^2 + \frac{1}{3}\right) + \frac{P_t^5P_1^3}{5}\left(\frac{P_1^4}{7} - \frac{2}{5}P_1^2 + \frac{1}{3}\right)\right] - \frac{3\pi}{16}P_t^4 + \frac{345}{1280}\pi P_t^2 - \frac{713}{7680}\pi$$

$$f_5 = \frac{256}{105}P_t^7P_1\left(\frac{P_t^2}{3} + P_1^2 - 1\right) - \frac{7}{16}\pi$$

$$f_6 = \frac{256}{35}P_t^7P_1^3\left(\frac{P_t^3}{27} + \frac{P_1^2}{5} - \frac{1}{4}\right) - \frac{\pi}{6}P_t^4 + \frac{\pi}{10}P_t^2 - \frac{\pi}{48}$$

$$f_7 = \frac{28}{15}P_t^5P_1 + 8P_t^3P_1\left(\frac{1}{3}P_1^2 - 1\right) + 4P_tP_1\left(\frac{P_1^4}{5} - \frac{2}{3}P_1^2 + 1\right) - \pi P_t^2 - \frac{\pi}{2}$$

$$f_8 = \frac{28}{45}P_t^5P_1^3 + \frac{8}{3}P_t^3P_1^3\left(\frac{3}{5}P_1^2 - 1\right) + 4P_tP_1^8\left(\frac{P_1^4}{7} - \frac{2}{5}P_1^2 + \frac{1}{3}\right) + \frac{\pi}{6}P_t^2 - \frac{\pi}{16}$$

and

$$f_9 = \begin{cases} 0 & \left(\frac{\partial X}{\partial Y} = \frac{X}{Y} \right) \\ \frac{8}{3} P_t^3 P_1^3 \left(\frac{P_t^3}{15} + \frac{P_1^2}{5} - \frac{1}{3} \right) + \frac{\pi}{12} P_t^2 - \frac{\pi}{96} & \left(\frac{\partial X}{\partial Y} = \frac{X}{Y} \right) \end{cases} \quad \text{(D-34)}$$

Here again C_1 is prescribed from the continuity condition as

$$C_1 = \frac{15}{(P_t - 1)^2 (7P_t^2 + 21P_t + 12)} \quad \text{(D-35)}$$

When $P_t = P_1 = 1.50$ and $P_t = P_1 = 1.25$ are substituted into Equations D-20 and D-21, the optimum values of Φ are calculated and the following equations result,

for the case of $\frac{\partial X}{\partial Y} = 0$:

$$f = \frac{98.3}{Re} \qquad \text{for } P_t = 1.50 \quad \text{(D-36)}$$

and

$$f = \frac{478}{Re} \qquad \text{for } P_t = 1.25 \quad \text{(D-37)}$$

and for the case of $\frac{\partial X}{\partial Y} = \frac{X}{Y}$:

$$f = \frac{111}{Re} \qquad \text{for } P_t = 1.50 \quad \text{(D-38)}$$

and

$$f = \frac{555}{Re} \qquad \text{for } P_t = 1.25 \quad \text{(D-39)}$$

APPENDIX E

STEEPEST-DESCENT METHOD OF BOOTH

The n_p-dimensional space in which the object function I is defined may be considered as being made up of a family of $(n_p - 1)$ dimensional hypersurfaces of constant functional value. The minimization process consists of moving from a given contour in the n_p-dimensional space to the one having the smallest value in the neighborhood region of definition. The steepest-descent method is one way of doing this searching by moving along a path which is perpendicular to the surface of constant value (Figure 65).

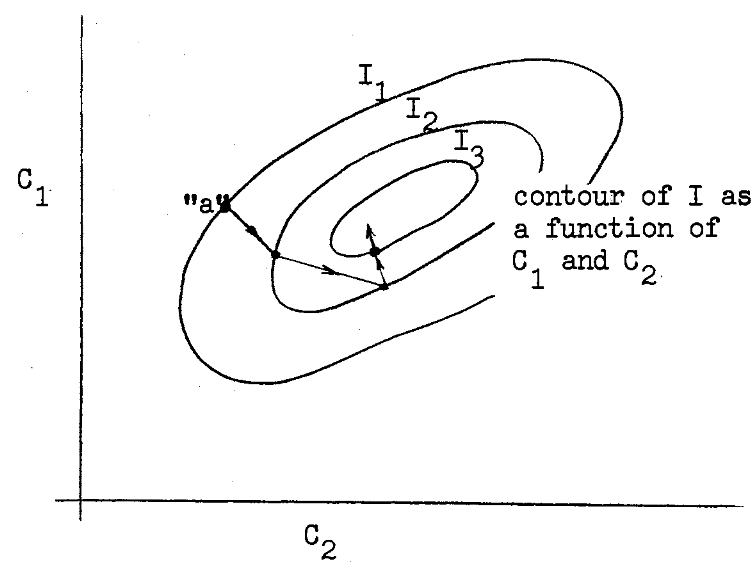

Figure 65. Path Followed by Steepest-descent Method in Two-dimensional Space

Define I as the object function whose minimum is sought. The vector perpendicular to a surface at a given point is given by

$$\vec{\theta} = \text{grad } I = \left(\frac{\partial}{\partial C_1}\vec{i}_1 + \frac{\partial}{\partial C_2}\vec{i}_2 + \ldots\ldots + \frac{\partial}{\partial C_{n_p}}\vec{i}_{n_p}\right)I \qquad \text{(E-1)}$$

where the i_j's are unit vectors along the coordinate axes. Movement along the vector $\vec{\theta}$ can be accomplished by multiplying all of its components by a scale factor B yet to be determined. Thus the component of a vector coincident with $\vec{\theta}$ but having a magnitude B times as large as $\vec{\theta}$ and a direction of maximum decrease of I is

$$dC_i = -B\left(\frac{\partial I}{\partial C_i}\right) \qquad \text{(E-2)}$$

To obtain an estimate of B, the function I is expanded in a Taylor series about a given point "a",

$$I = I_a + \sum_{i=1}^{n_p}\left(\frac{\partial I}{\partial C_i}\right)\bigg|_a dC_i + \text{higher order terms} \qquad \text{(E-3)}$$

Neglecting the higher order terms in Equation E-3 and substituting Equation E-2 for dC_i, one gets

$$I = I_a - B\sum_{i=1}^{n_p}\left(\frac{\partial I}{\partial C_i}\right)^2\bigg|_a \qquad \text{(E-4)}$$

or solving for B,

$$B = \frac{I_a - I}{\sum_{i=1}^{n_p}\left(\frac{\partial I}{\partial C_i}\right)\bigg|_a} \qquad \text{(E-5)}$$

Therefore from Equation E-2 and Equation E-5,

$$\Delta C_i = -\frac{(I_a - I)[\frac{\partial I}{\partial C_i}]_a}{\sum_{i=1}^{n_p}(\frac{\partial I}{\partial C_i})^2\Big|_a} \tag{E-6}$$

Since $0 \leq I_a - I \leq I_a$, Equation E-6 may be rewritten as

$$\Delta C_i = -\xi\left[\frac{I[\frac{\partial I}{\partial C_i}]}{\sum_{i=1}^{n_p}[\frac{\partial I}{\partial C_i}]_a^2}\right] \tag{E-7}$$

where $0 \leq \xi \leq 1$.

Booth suggests an effective procedure for calculating this incremental step ΔC_i for finding the minimum of I, whereby two points in addition to the base point "a" are found and the minimum of the parabola through these points is taken as the minimum of I in that direction. For this method the equation of ΔC_i is

$$\Delta C_i = -\frac{[I(1)-4I(\frac{1}{2})+3I(0)]\ i(0)[\frac{\partial I}{\partial C_i}]_{\xi=0}}{4[I(1)-2I(\frac{1}{2})+I(0)][\sum_{i=1}^{n_p}(\frac{\partial I}{\partial C_i})^2]_{\xi=0}} \tag{E-8}$$

where $I(1)$ is the value of I at the point given by applying the corrections from Equation E-7 with $\xi = 1$, $I(\frac{1}{2})$ the values with half these corrections, and $I(0)$ the value with $\xi = 0$.

APPENDIX F

TUBE SURFACE VORTICITY

The derivation of the equation for estimating the vorticity on tube surface in polar coordinate systems is as follows:
The fundamental governing equations are

$$\frac{\partial \psi}{\partial r}\frac{\partial \zeta}{r\partial \theta} - \frac{\partial \psi}{r\partial \theta}\frac{\partial \zeta}{\partial r} = \frac{2}{Re}\left[\frac{\partial^2 \zeta}{\partial r^2} + \frac{\partial \zeta}{r\partial r} + \frac{\partial^2 \zeta}{r^2\partial \theta^2}\right] \qquad \text{(F-1)}$$

and

$$\zeta = \frac{\partial^2 \psi}{\partial r^2} + \frac{\partial \psi}{r\partial r} + \frac{\partial^2 \psi}{r^2\partial \theta^2} \qquad \text{(F-2)}$$

Write a Maclaurin series expansion of ψ and ζ about the boundary point "B" of Figure 66:

$$\psi_{B+1} = \psi_B + h\left(\frac{\partial \psi}{\partial r}\right)_B + \frac{h^2}{2!}\left(\frac{\partial^2 \psi}{\partial r^2}\right)_B + \frac{h^3}{3!}\left(\frac{\partial^3 \psi}{\partial r^3}\right)_B + \frac{h^4}{4!}\left(\frac{\partial^4 \psi}{\partial r^4}\right)_B + O(h^5) \qquad \text{(F-3)}$$

and

$$\zeta_{B+1} = \;_B + h\left(\frac{\partial \zeta}{\partial r}\right)_B + \frac{h^2}{2!}\left(\frac{\partial^2 \zeta}{\partial r^2}\right)_B + \frac{h^3}{3!}\left(\frac{\partial^3 \zeta}{\partial r^3}\right)_B + \frac{h^4}{4!}\left(\frac{\partial^4 \zeta}{\partial r^4}\right)_B + O(h^5) \qquad \text{(F-4)}$$

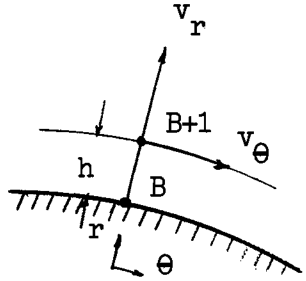

Figure 66. Tube Surface Point

Boundary conditions at "B" are

$$\psi = 0 \tag{F-5}$$

$$v_\theta = \frac{\partial \psi}{\partial r} = 0 \tag{F-6}$$

and

$$v_r = -\frac{\partial \psi}{r \partial \theta} = 0 \tag{F-7}$$

Differentiating Equation F-7 with respect to θ,

$$\frac{1}{r^2}\frac{\partial^2 \psi}{\partial \theta^2} = \frac{\partial v}{\partial (r\theta)}) = 0 \tag{F-8}$$

Thus Equation F-2 becomes with Equations F-6 and F-8,

$$\zeta_B = (\frac{\partial^2 \psi}{\partial r^2})_B \tag{F-9}$$

Differentiating Equation F-2 with respect to r,

$$\frac{\partial \zeta}{\partial r} = \frac{\partial^3 \psi}{\partial r^3} + \frac{1}{r}\frac{\partial^2 \psi}{\partial r^2} - \frac{\partial \psi}{r \partial r} + \frac{\partial^3 \psi}{r^2 \partial r \partial \theta^2} - \frac{2}{r^3}\frac{\partial^2 \psi}{\partial \theta^2} \tag{F-10}$$

But from Equation F-7 and Equation F-8,

$$\frac{\partial}{\partial r}(\frac{\partial v_r}{r \partial \theta}) = \frac{\partial^3 \psi}{r^2 \partial \theta^2 \partial r} - \frac{2}{r^3}\frac{\partial^2 \psi}{\partial \theta^2} = 0$$

Thus;

$$(\frac{\partial^3 \psi}{r^2 \partial r \partial \theta^2})_B = 0 \tag{F-11}$$

Substituting Equations F-6, F-8, F-9 and F-11 into Equation F-10 at "B",

$$\left(\frac{\partial \zeta}{\partial r}\right)_B = \left(\frac{\partial^3 \psi}{\partial r^3}\right)_B + \frac{\zeta_B}{r} \tag{F-12}$$

or

$$\left(\frac{\partial^3 \psi}{\partial r^3}\right)_B = \left(\frac{\partial \zeta}{\partial r}\right)_B - \frac{\zeta_B}{r} \tag{F-13}$$

Differentiating Equation F-10 again with respect to r,

$$\frac{\partial^3 \psi}{\partial r^2} = \frac{\partial^4 \psi}{\partial r^4} + \frac{\partial^3 \psi}{r \partial r^3} - \frac{2 \partial^3 \psi}{r^3 \partial r^2} + \frac{2 \partial \psi}{r^3 \partial r} + \frac{\partial^4 \psi}{r^2 \partial r^2 \partial \theta^2}$$

$$- \frac{2 \partial^3 \psi}{r^3 \partial r \partial \theta^2} + \frac{6 \partial^2 \psi}{r^4 \partial \theta^2} - \frac{2 \partial^3 \psi}{r^2 \partial r \partial \theta^2} \tag{F-14}$$

Substituting Equations F-6, F-8, F-9, F-11 and F-13 into Equation F-14,

$$\left(\frac{\partial^2 \zeta}{\partial r^2}\right)_B = \left(\frac{\partial^4 \psi}{\partial r^4}\right)_B + \frac{1}{r}\left(\frac{\partial \zeta}{\partial r}\right)_B - \frac{3}{r^2} \zeta_B + \frac{1}{r^2}\left(\frac{\partial^4 \psi}{\partial r^2 \partial \theta^2}\right)_B \tag{F-15}$$

Differentiating Equation F-2 with respect to θ twice,

$$\frac{\partial^2 \zeta}{\partial \theta^2} = \frac{\partial^4 \psi}{\partial \theta^2 \partial r^2} + \frac{\partial^3 \psi}{r \partial r \partial \theta^2} + \frac{\partial^4 \psi}{r^2 \partial \theta^4} \tag{F-16}$$

But from Equation F-8,

$$\begin{aligned} \frac{1}{r^3} \frac{\partial^3 \psi}{\partial \theta^3} &= \frac{\partial}{\partial \theta}\left[\frac{\partial v_r}{\partial (r\theta)} \right]_B = 0 \\ \frac{1}{r^4} \frac{\partial^4 \psi}{\partial \theta^4} &= \frac{\partial}{\partial \theta}\left[\frac{\partial^2 v_r}{\partial (r\theta)^2} \right]_B = 0 \end{aligned} \tag{F-17}$$

With Equations F-11 and F-17, Equation F-16 becomes

$$\frac{1}{r^2}\left(\frac{\partial^2\zeta}{\partial\theta^2}\right)_B = \frac{1}{r^2}\left(\frac{\partial^4\psi}{\partial\theta^2\partial r^2}\right)_B + \frac{1}{r^3}\left(\frac{\partial^3\psi}{\partial r\partial\theta^2}\right)_B + \frac{1}{r^2}\left(\frac{\partial^4\psi}{\partial\theta^4}\right)_B$$

thus,

$$\frac{1}{r^2}\left(\frac{\partial^2\psi}{\partial\theta^2}\right)_B = \frac{1}{r^2}\left(\frac{\partial^4\psi}{\partial r^2\partial\theta^2}\right)_B \tag{F-18}$$

Subtracting Equation F-18 from Equation F-15,

$$\left(\frac{\partial^2\zeta}{\partial r^2}\right)_B - \frac{1}{r^2}\left(\frac{\partial^2\zeta}{\partial\theta^2}\right)_B = \left(\frac{\partial^4\psi}{\partial r^4}\right)_B + \frac{1}{r}\left(\frac{\partial^2\zeta}{\partial r}\right)_B \div \frac{3}{r^2}\zeta_B$$

or

$$\left(\frac{\partial^4\psi}{\partial r^4}\right)_B = \left(\frac{\partial^2\zeta}{\partial r^2}\right)_B - \frac{1}{r^2}\left(\frac{\partial^2\zeta}{\partial\theta^2}\right)_B - \frac{1}{r}\left(\frac{\partial\zeta}{\partial r}\right)_B + \frac{3}{r^2}\zeta_B \tag{F-19}$$

Substituting Equations F-5, F-6, F-9, F-13 and F-19 into Equation F-3,

$$\psi_{B+1} = \frac{h^2}{2}\zeta_B + \frac{h^3}{6}\left[\left(\frac{\partial\zeta}{\partial r}\right)_B - \frac{\zeta_B}{r}\right] + \frac{r^4}{24}\left[\left(\frac{\partial^2\zeta}{\partial r^2}\right)_B - \frac{1}{r^2}\left(\frac{\partial^2\zeta}{\partial\theta^2}\right)_B\right.$$

$$\left. - \frac{1}{r^2}\left(\frac{\partial\zeta}{\partial r}\right)_B + \frac{3}{r^2}\zeta_B\right] + 0(h^5) \tag{F-20}$$

Rearranging Equation F-4 for $\left(\frac{\partial\zeta}{\partial r}\right)_B$,

$$\left(\frac{\partial\zeta}{\partial r}\right)_B = \frac{1}{h}(\zeta_{B+1} - \zeta_B) - \frac{h}{2}\left(\frac{\partial^2\zeta}{\partial r^2}\right)_B - \frac{h^2}{6}\left(\frac{\partial^3\zeta}{\partial r^3}\right)_B - \cdots\cdots \tag{F-21}$$

Substituting Equation F-21 into the second term of right hand side of Equation F-20,

$$\psi_{B+1} = \frac{h^2}{2}\zeta_B + \frac{h^3}{6}\left[\left\{\frac{1}{h}(\zeta_{B+1}-\zeta_B) - \frac{h}{2}\left(\frac{\partial^2\zeta}{\partial r^2}\right)_B - \frac{h^2}{6}\left(\frac{\partial^3\zeta}{\partial r^3}\right)_B \cdots\right.\right.$$

$$\cdots \quad - \frac{\zeta_B}{r}\Big] + \frac{h^4}{24}\Big[\left(\frac{\partial^2\zeta}{\partial r^2}\right)_B - \frac{1}{r^2}\left(\frac{\partial^2\zeta}{\partial\theta^2}\right)_B - \frac{1}{r}\left(\frac{\partial\zeta}{\partial r}\right)_B$$

$$+ \frac{3}{r^2}\zeta_B\Big] + O(h^5)$$

Thus,

$$\psi_{B+1} = \frac{h^2}{3}\left(1 - \frac{h}{2r} + \frac{3h^2}{8r^2}\right)\zeta_B + \frac{h^2}{6}\zeta_{B+1} - \frac{h^4}{24}\Big[\left(\frac{\partial^2\zeta}{\partial r^2}\right)_B + \frac{1}{r}\left(\frac{\partial\zeta}{\partial r}\right)_B$$

$$+ \frac{1}{r^2}\left(\frac{\partial^2\zeta}{\partial\theta^2}\right)_B\Big] + O(h^5) \qquad \text{(F-22)}$$

But from Equation F-1 applied at the boundary point B,

$$\frac{2}{Re}\left[\frac{\partial^2\zeta}{\partial r^2} + \frac{\partial\zeta}{r\partial r} + \frac{\partial^2\zeta}{r^2\partial\theta^2}\right]_B = \left[\frac{\partial\psi}{r\partial\theta}\frac{\partial\zeta}{\partial r} - \frac{\partial\psi}{\partial r}\frac{\partial\zeta}{r\partial\theta}\right]_B = 0$$

$$\text{(F-23)}$$

Substituting Equation F-23 into Equation F-22 to eliminate $O(h^4)$ term,

$$\psi_{B+1} = \frac{h^2}{3}\left(1 - \frac{h}{2r} + \frac{3h^2}{8r^2}\right)\zeta_B + \frac{h^2}{6}\zeta_{B+1} + O(h^5) \qquad \text{(F-24)}$$

Solving for ζ_B, one obtains

$$\zeta_B = \left(\frac{1}{1 - \frac{h}{2r} + \frac{3h^2}{8r^2}}\right)\left[\frac{3}{h^2}\psi_{B+1} - \frac{\zeta_{B+1}}{2}\right] + O(h^3)$$

$$\text{(F-25)}$$

APPENDIX G

FORM DRAG AND FRICTION DRAG

<u>Pressure Variation Along the Tube Surface</u> (primed quantities are dimensional)

The θ - component of equation of motion at the surface of a tube is

$$\rho\left(\underbrace{\cancel{\frac{\partial v'_\theta}{\partial t'}}}_{0 \text{ steady state}} + \overset{0}{\cancel{v'_r \frac{\partial v'_\theta}{\partial r'}}} + \overset{0}{\cancel{\frac{v'_\theta}{r'}}} \frac{\partial v'_\theta}{\partial \theta} + \overset{0}{\cancel{\frac{v'_r v'_\theta}{r'}}}\right) = -\frac{\partial P'}{r'\partial \theta'} + \underbrace{\cancel{\rho g_\theta}}_{\text{neglected}}$$

$$+\mu\left[\frac{\partial}{\partial r'}\left(\frac{1}{r'}\frac{\partial}{\partial r'}(r'v'_\theta)\right) + \frac{1}{r'^2}\frac{\partial^2 v'_\theta}{\partial \theta^2} + \frac{2}{r'^2}\frac{\partial v'_r}{\partial \theta}\right]$$

(G-1)

Rearranging Equation G-1,

$$\frac{1}{\mu}\frac{\partial P'}{r'\partial \theta} = \frac{\partial}{\partial r'}\left(\frac{1}{r'}\frac{\partial}{\partial r'}(r'v'_\theta)\right) + \frac{1}{r'^2}\frac{\partial^2 v'_\theta}{\partial \theta^2} + \frac{2}{r'^2}\frac{\partial v'_r}{\partial \theta} \quad \text{(G-2)}$$

Stream function and vorticity are defined by

$$v'_r = -\frac{1}{r'}\frac{\partial \psi'}{\partial \theta} \quad \text{(G-3)}$$

$$v'_\theta = \frac{\partial \psi'}{\partial r'} \quad \text{(G-4)}$$

$$\zeta' = \frac{1}{r'}\left[\frac{\partial}{\partial r'}(r'v'_\theta) - \frac{\partial v'_r}{\partial \theta}\right] \quad \text{(G-5)}$$

From Equations G-5 and G-3,

$$\frac{1}{r'}\frac{\partial}{\partial r'}(r'v'_\theta) = \frac{1}{r'^2}\frac{\partial}{\partial\theta}(r'v'_r) + \zeta'$$

$$= -\frac{1}{r'^2}\frac{\partial^2\psi'}{\partial\theta^2} + \zeta' \tag{G-6}$$

Substituting Equations G-3, G-4 and G-6 into Equation G-2,

$$\frac{1}{\mu}\frac{\partial P'}{r'\partial\theta} = \frac{\partial}{\partial r'}\left[-\frac{1}{r'^2}\frac{\partial^2\psi'}{\partial\theta^2} + \zeta'\right] + \frac{1}{r'^2}\frac{\partial^2 v'_\theta}{\partial\theta^2} + \frac{2}{r'^2}\frac{\partial v'_r}{\partial\theta}$$

$$= \frac{2}{r'^2}\frac{\partial^2\psi'}{\partial\theta^2} - \frac{1}{r'^2}\frac{\partial^3\psi'}{\partial r'\partial\theta^2} + \frac{\partial^3\psi'}{r'^2\partial\theta^2\partial r'} - \frac{2\partial^2\psi'}{r'^3\partial\theta^2}$$

thus,

$$\frac{\partial P'}{r'\partial\theta} = \mu\frac{\partial\zeta'}{\partial r'}\Big]_{r'=R'} \tag{G-7}$$

Normalizing Equation G-7 with respect to $\frac{1}{2}\rho\bar{u}'^2$, and integrating it from $\theta = 0$ to $\theta = \theta$, the dimensionless pressure variation results:

$$P^* - P^*_0 = \Delta P^* = \frac{\Delta P'}{\frac{1}{2}\rho\bar{u}'^2} = \frac{1}{\frac{1}{2}\rho\bar{u}'^2}\int_0^\theta \frac{\partial P'}{r'\partial\theta}\, r'\, d\theta$$

$$= \frac{\mu}{\frac{1}{2}\rho\bar{u}'^2}\int_0^\theta \frac{\partial\zeta'}{\partial r'}\Big]_{r'=R'} r'\, d\theta$$

$$= \frac{4}{\left[\frac{2R'\bar{u}'}{\nu}\right]}\int_0^\theta \left(\frac{\partial\zeta}{\partial r}\right)_{r=R} R\, d\theta$$

Thus,

$$\Delta P^{*} = \frac{4}{Re}\int_{0}^{\theta}\left(\frac{\partial \zeta}{\partial r}\right)_{r=1} d\theta \tag{G-8}$$

The pressure contribution to the total drag coefficient is then,

$$C_p = \int_{0}^{\pi} \Delta P^{*} \cos\theta \, d\theta \tag{G-9}$$

Shear Stress Variation Along the Tube Surface

Shear stress on a tube surface is given by,

$$\tau'_{\theta r} = -\mu\left[r'\frac{\partial}{\partial r'}\left(\frac{v'_{\theta}}{r'}\right) + \frac{1}{r'}\frac{\partial v'_{r}}{\partial \theta}\right] \tag{G-10}$$

Substituting Equations G-3 and G-4 into the right hand side of Equation G-10,

$$\tau'_{\theta r} = -\mu\left[-\frac{\partial^2 \psi'}{\partial r'^2} + \frac{\partial \psi'}{r'\partial r'} + \frac{\partial^2 \psi'}{r'^2 \partial \theta^2}\right] \tag{G-11}$$

But from Equations G-3, G-4 and G-5,

$$\zeta' = \frac{\partial^2 \psi'}{\partial r'^2} + \frac{\partial \psi'}{r'\partial r'} + \frac{\partial^2 \psi'}{r'^2 \partial \theta^2} \tag{G-12}$$

Substituting Equation G-12 into Equation G-11,

$$\tau'_{\theta r} = -\mu\left[\zeta' - 2\frac{\partial^2 \psi'}{\partial r'^2}\right] \tag{G-13}$$

But at the surface of a tube,

$$\zeta'_{r'=R'} = \frac{\partial^2 \psi'}{\partial r'^2} + \frac{\partial \psi'}{r' \partial r'} + \frac{\partial^2 \psi'}{r'^2 \partial \theta^2}$$

$$= \left(\frac{\partial^2 \psi'}{\partial r'^2}\right)_{r'=R'}$$

Thus,

$$\tau'_{\theta r} = \mu \zeta_{r'=R'} \tag{G-14}$$

Normalizing Equation G-14 with respect to $\frac{1}{2}\rho \bar{u}'^2$, and integrating it along the surface of the tube, the dimensionless stress distribution is obtained;

$$\Delta\tau^* = \frac{\Delta\tau'}{\frac{1}{2}\rho\bar{u}'^2} = \frac{\mu}{\frac{1}{2}\rho\bar{u}'^2}\int_0^{\pi} \zeta_{r'=R'} \sin\theta \, d\theta$$

$$= \frac{4}{\left[\frac{2R' \, \bar{u}'}{\nu}\right]}\int_0^{\pi} \zeta_{R=1} \sin\theta \, d\theta$$

Thus,

$$C_f = \frac{4}{Re}\int_0^{\pi} \zeta_{R=1} \sin\theta \, d\theta \tag{G-15}$$

The skin friction contribution to the total drag coefficient is therefore

$$C_D = C_p + C_f \tag{G-16}$$

Vorticity Gradient on Tube Surface

If a parabolic profile of ζ as a function of r is assumed, one may write, referring to Figure 67,

$$\zeta = A_1 r^2 + A_2 r + A_3 \tag{G-17}$$

Therefore,

$$\frac{\partial \zeta}{\partial r} = 2A_1 r + A_2 \tag{G-18}$$

Boundary conditions are,

$$\zeta = \zeta_{i,1} \qquad \text{at } r = R = 1$$

$$\zeta = \zeta_{i,2} \qquad \text{at } r = h+1 \tag{G-19}$$

and

$$\zeta = \zeta_{i,3} \qquad \text{at } r = 2h+1$$

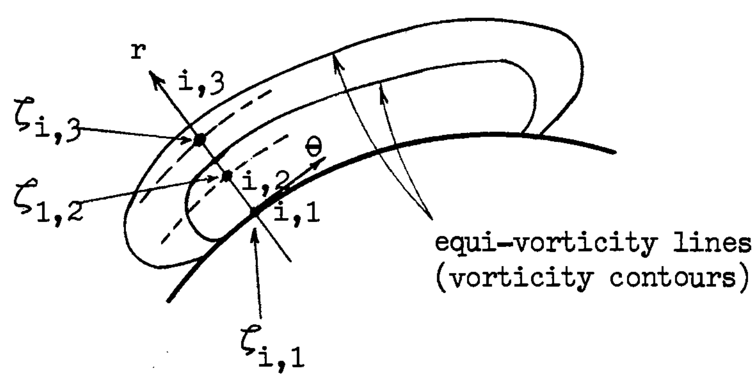

Figure 67. Vorticity Gradient at the Tube Surface

Substituting these boundary conditions into Equation G-17,

$$\zeta_{i,1} = A_1 + A_2 + A_3 \tag{G-20}$$

$$\zeta_{i,2} = A_1(1+h)^2 + A_2(1+h) + A_3 \tag{G-21}$$

and

$$\zeta_{1,3} = A_1(1+h)^2 + A_2(1+h) + A_3 \tag{G-22}$$

Thus, from Equations G-20, G-21 and G-22,

$$\zeta_{i,1} - \zeta_{i,2} = A_1(h^2 + 2h) + A_2 h \tag{G-23}$$

and

$$\zeta_{i,3} - \zeta_{i,2} = A_1(3h^2 + 2h) + A_2 h \tag{G-24}$$

Subtracting Equation G-23 from Equation G-24,

$$\zeta_{i,3} - 2\zeta_{i,2} + \zeta_{i,1} = A_1(3h^2 + 2h - h^2 - 2h)$$

or

$$A_1 = \frac{1}{2h^2}[\zeta_{i,3} - 2\zeta_{i,2} + \zeta_{i,1}] \tag{G-25}$$

Substituting Equation G-25 into Equation G-23, one finds

$$A_2 = \frac{4\zeta_{i,2} - \zeta_{i,3} - 3\zeta_{i,1}}{2h} - \frac{\zeta_{i,3} - 2\zeta_{i,2} + \zeta_{i,1}}{h^2} \tag{G-26}$$

Substituting Equations G-25 and G-26 into Equation G-18, one obtains

$$\left(\frac{\partial\zeta}{\partial r}\right)_{r=R} = \frac{1}{h}[2\zeta_{i,2} - \frac{1}{2}\zeta_{i,3} - \frac{3}{2}\zeta_{i,1}] \tag{G-27}$$

APPENDIX H

WALL EFFECT CORRECTION

BY GRAETZ SOULTION

A solution of the Navier-Stokes equations for steady laminar flow in ducts of rectangular cross section (Figure 68; (a)) found by Graetz (14) may be written in terms of the differential pressure drop, $(\frac{dP}{dx})_{duct}$,

$$Q = \frac{g_c}{\mu}\left(\frac{dP}{dx}\right)_{duct}\left[\frac{Z_1^3 Z_2}{12} - \frac{16}{Z_1}\sum_{m=0}^{\infty} M^{-5}\tanh\left(\frac{MZ_2}{2}\right)\right] \qquad \text{(H-1)}$$

where Q = volumetric flow rate

$$M = (2m + 1)\pi / Z_1 \qquad \text{(H-2)}$$

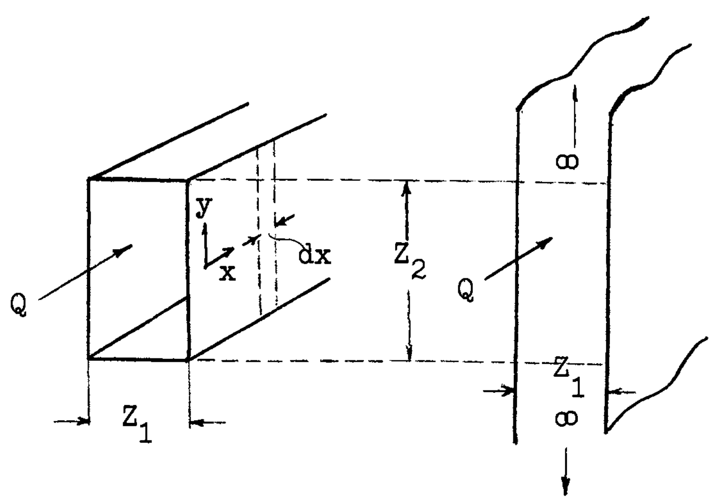

(a) Rectangular Duct (b) Narrow Slit

Figure 68. Narrow Slit and Rectangular Cross Sectional Duct

After substitution of Equation H-2 and rearrangement, Equation H-1 may be expressed as

$$\left(\frac{dP}{dx}\right)_{duct} = \frac{12\mu Q}{g_c Z_1^3 Z_2} \Big/ \left[1 - 0.627a \sum_{m=0}^{\infty} (2m+1)^{-5} \tanh \frac{(2m+1)\pi}{2a}\right] \qquad \text{(H-3)}$$

where $a = Z_1/Z_2$ (H-4)

On the other hand, for the laminar flow in a narrow slit of infinite height (Figure 68; (b)), the differential pressure drop, $\left(\frac{dP}{dx}\right)_{\infty}$, with the same height Z_2 and the flow rate Q as in the duct flow, is given (17) by

$$\left(\frac{dP}{dx}\right)_{\infty} = \frac{12\mu Q}{g_c Z_1^3 Z_2} \qquad \text{(H-5)}$$

From Equations H-3 and H-5, the following expression results;

$$\frac{\left(\frac{dP}{dx}\right)_{\infty}}{\left(\frac{dP}{dx}\right)_{duct}} = f(a) \qquad \text{(H-6)}$$

where

$$f(a) = 1 - 0.627a \sum_{m=0}^{\infty} (2m+1)^{-5} \tanh \frac{(2m+1)\pi}{2a} \qquad \text{(H-7)}$$

In applying Equation H-6 for estimating the correction factor of wall effect in tube bank flow, it is assumed that the pressure gradient in the y-direction is negligible so that Z_1 is taken as the clearance between tubes perpendicular to x-axis (Figure 69).

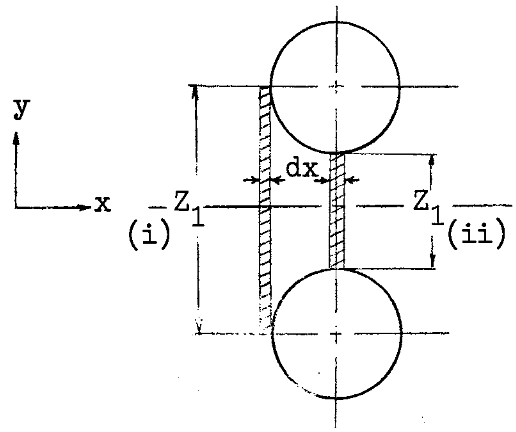

Figure 69. Two Extreme Cases for Wall Effect Correction

The following two extreme cases may be considered for estimating the limits of the correction factors:

(i) Z_1 is taken as the transverse tube pitch, or $Z_1 = P_t D_t$.

(ii) Z_1 is taken as the minimum tube clearance, i.e., $(P_t - 1)D_t$.

In both cases Z_2 is the tube length of 6 inches for the Delaware ideal tube bank. Table V shows the correction factors calculated for the two cases with two pitch ratios used.

TABLE V GRAETZ CORRECTION FACTORS FOR TUBE BANK FLOW

P_t	case	$a = Z_1/Z_2$	f(a)	1/f(a)	% correction
1.50	(i)	0.0938	0.8883	1.1257	12.6
	(ii)	0.0313	0.9591	1.0426	4.3
1.25	(i)	0.0781	0.9048	1.1051	10.5
	(ii)	0.0156	0.9791	1.0213	2.1

APPENDIX I

COMPUTER PROGRAM FOR OBTAINING STREAM FUNCTION AND VORTICITY

The computer program for solving the Navier-Stokes equations for vorticity and stream function for tube bank flow is written in FORTRAN IV for use on the Oklahoma State University Computing Center's IBM 360 Model 50 digital computer. The block diagram of the program is shown in Figure 15. The basic feature of the program is that the computation is broken down into sub-calculations with specific and independent functions. A description of each of the subroutines is presented in the following sections. Approximate computer times and number of iterations required are listed in Table VI along with other system parameters.

Main Program

This is the executive program for the entire calculation. The main program arranges the subroutines in order for iterative computation and is independent of the working equations used. The data input and output subroutines and the major calculational subroutines are called by the main program at the appropriate time during the iterative process.

Subroutine COUNT

COUNT calculates tagged constants and parameters needed to establish tag array and geometrical parameters at various boundaries necessary for

TABLE VI

COMPUTER EXECUTION TIME

FOR CONVERGED SOLUTION

Pitch ratio P_t	Reynolds number Re	Basic mesh size h	Number of total field points in entire system	Number of iterations	Computer time (hrs)
1.50	1	0.10	1318		
	5	0.10	1358		
	10	0.10	1358		
	10	0.05	5241		
	20	0.05	5341	91	0.40
	50	0.05	6543	158	0.75
	100	0.05	6203	173	0.78
1.25	1	0.05	3897	313	0.93
	5	0.05	3897	110	0.31
	10	0.05	3897	123	0.37
	20	0.05	3897	146	0.44
	50	0.05	3897	236	0.63
	100	0.05	5189	275	0.93

iterative computation. Figure 70 shows a typical geometry involved at a boundary in which tagged parameters are calculated.

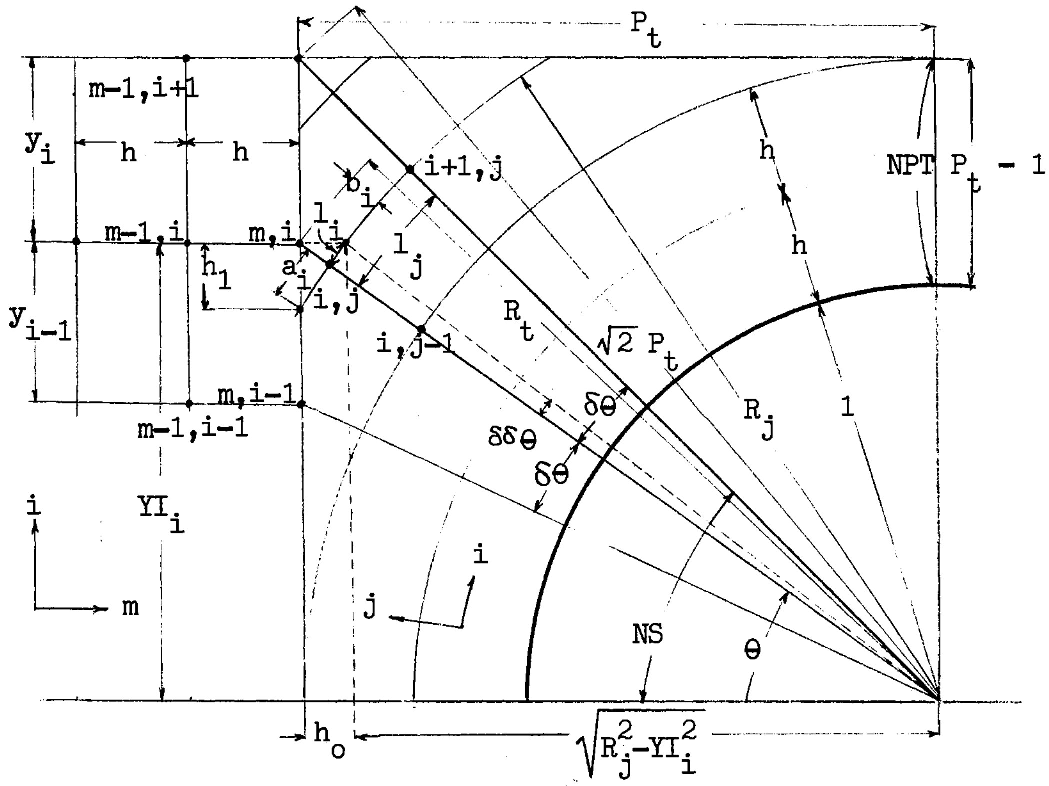

Figure 70. Geometry for Calculating Parameters and Constants

Here, the parameters and constants depicted in Figure 70 are defined as follows:

$$\left.\begin{aligned}
\delta\theta &= 4/NS \\
\theta &= i\,\delta\theta \\
h &= (P_t - 1)/NPT \\
R_t &= P_t/\cos\theta \\
YI_i &= R_t \sin\theta \\
R_j &= h(j-1) \\
a_i &= R_j(\theta - \cos^{-}[P_t/R_j])
\end{aligned}\right\} \quad \text{(I-1)}$$

$$b_i = R_t - R_j$$

$$h_o = P_t - \sqrt{R_j^2 - YI_i^2}$$

$$\delta\delta\theta = \sin^{-}(YI_i/R_j) - \theta$$

$$l_i = R_j\,\delta\delta\theta$$

Subroutine COUNT is called by the main program at the initialization stage of the iterative process.

Subroutine GUESS

GUESS is the subroutine program that generates the initial guess for stream function and vorticity at all the field mesh points. As the initial guess of ζ and ψ, the values of laminar velocity profile in a non-uniform tube bank channel are used. GUESS is called only at the beginning of the calculation of series of Reynolds numbers studied.

Subroutine DATA

DATA reads in the stream function and vorticity at all the field mesh points from punched-out cards as the initial guess. DATA is called at the beginning of the iterative computation.

Subroutine DISK

DISK is used to read the initial guess of stream function and vorticity from the permanent storage disk which was used in the later phase of the study. The basic structure of the subroutine is the same as the subroutine DATA.

Subroutine SQUARE

SQUARE is the subroutine that is responsible for calculation of all the inner field vorticity and stream function of rectangular coordinate inlet and outlet sections. Equations 4-44 and 4-50 are utilized in this subroutine.

Subroutine STMESH

STMESH is the subroutine that performs the matching calculation at the boundary between rectangular inlet section and polar section of the first unit cell of tube bank. Finite difference expressions used in this subroutine program are as follows:

For a representative boundary point (m,i) in rectangular section in Figure 71, the finite differencing method is applied to the governing equations, Equations 4-19 and 4-20, at the points (m,i+1), (m,i-1), (m+1,i) and "O".

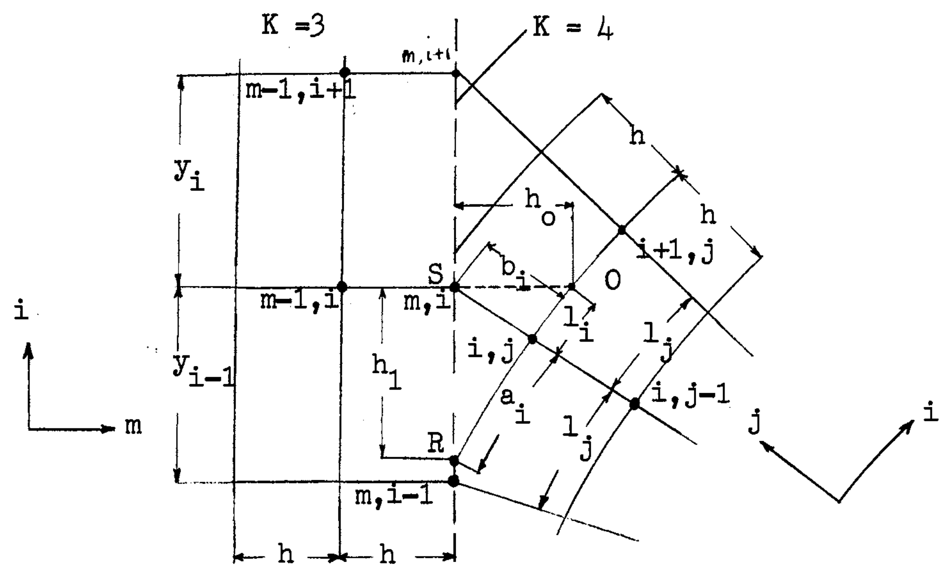

Figure 71. Rectangular-Polar Matching Plane

The following final expressions result;

$$\zeta^{k+1}_{i,m} = \left(\frac{1}{hh_o + y_i y_{i-1}}\right)\Big[\frac{y_i y_{i-1}}{h+h_o}(h\zeta_o + h_o\zeta^{k+1}_{i,m-1}) + \frac{hh_o}{y_i+y_{i-1}}(y_{i-1}\zeta^{k}_{i+1,m}$$

$$+ y_i\zeta^{k+1}_{i-1,m}) + \frac{Re\ h\ h_o y_i y_{i-1}}{4(h+h_o)(y_i+y_{i-1})}\Big\{(\psi_o - \psi^{k+1}_{i,m-1})(\zeta^{k}_{i+1,m}$$

$$-\zeta^{k+1}_{i-1,m}) - (\psi^{k}_{i+1,m} - \psi^{k+1}_{i-1,m})(\zeta_o - \zeta^{k+1}_{i,m-1})\Big\}\Big] \qquad \text{(I-1)}$$

and

$$\psi^{k+1}_{i,m} = \left(\frac{1}{hh_o + y_i y_{i-1}}\right)\Big[\frac{y_i y_{i-1}}{h+h_o}(h\psi_o + h_o\psi^{k+1}_{i,m-1}) + \frac{hh_o}{y_i+y_{i-1}}(y_{i-1}\psi^{k}_{i+1,m}$$

$$+ y_i\psi^{k+1}_{i-1,m}) - \frac{hh_o y_i y_{i-1}}{2}\zeta^{k+1}_{i,m}\Big] \qquad \text{(I-2)}$$

where ζ_o and ψ_o are the vorticity and the stream function at irregular star "O" whose values are interpolated from the two points (i+1,j) and (i,j) by, respectively

$$\zeta_o = \zeta_{i+1,j} l_i/l_j + \zeta_{i,j}(1 - l_i/l_j) \qquad \text{(I-3)}$$

and

$$\psi_o = \psi_{i+1,j} l_i/l_j + \psi_{i,j}(1 - l_i/l_j) \qquad \text{(I-4)}$$

Similarly, for a boundary point (i,j) in polar coordinates of the section K = 4 where the points "R", "S", (i,j-1) and (i+1,j) are used, the working equations become,

$$\zeta^{k+1}_{i,j} = \left(\frac{1}{a_i l_j + b_i h}\right)\Big[\frac{a_i l_j}{h+b_i}(b_i \zeta^{k+1}_{i,j-1} + h\zeta_S) + \frac{a_i l_j b_i h}{2r(b_i+h)}(\zeta_S - \zeta^{k+1}_{i,j-1}) + \frac{b_i h}{a_i + l_j}(a_i \zeta^{k}_{i+1,j} + l_j \zeta_R) + \frac{Re\, a_i l_j b_i h}{4(a_i+l_j)(b_i+h)}\Big\{(\psi_S - \psi^{k+1}_{i,j-1})(\zeta^{k}_{i+1,j} - \zeta_R) - (\psi^{k}_{i+1,j} - \psi_R)(\zeta_S - \zeta^{k+1}_{i,j-1})\Big\}\Big] \tag{I-5}$$

and

$$\psi^{k+1}_{i,j} = \left(\frac{1}{a_i l_j + b_i h}\right)\Big[\frac{a_i l_j}{b_i + h}(b_i \psi^{k+1}_{i,j-1} + h\psi_S) + \frac{a_i l_j b_i h}{2r(b_i+h)}(\psi_S - \psi^{k+1}_{i,j-1}) + \frac{b_i h}{a_i + h}(a_i \psi^{k}_{i+1,j} + l_j \psi_R) - \frac{a_i l_j b_i h}{2}\zeta^{k+1}_{i,j}\Big] \tag{I-6}$$

where the ζ's and ψ's at the irregular stars "S" and "R" are given by

$$\zeta_S = \zeta^{k+1}_{i,m} \tag{I-7}$$

$$\psi_S = \psi^{k+1}_{i,m} \tag{I-8}$$

$$\zeta_R = \zeta^{k+1}_{i-1,m} h_1/y_{i-1} + \zeta^{k+1}_{i,m}(1 - h_1/y_{i-1}) \tag{I-9}$$

$$\psi_R = \psi^{k+1}_{i-1,m} h_1/y_{i-1} + \psi^{k+1}_{i,m}(1 - h_1/y_{i-1}) \tag{I-10}$$

Subroutine TUBE

TUBE is the subroutine that commands calculations in the entire tube section. This subroutine calls the subroutines POLAR, TTMESH, and TSMESH and patches these together with the boundary point equations in the process of computational sweep at every iteration. For an irregular star (i,j) like the one shown in Figure 72, the same expressions as Equations I-5 and I-6 are used but with different boundary values for ψ_R, ζ_R, ψ_S and ζ_S, that is,

$$\psi_S = \psi_R = P_t - 1 \tag{I-11}$$

and

$$\zeta_S = \zeta_R = 0 \tag{I-12}$$

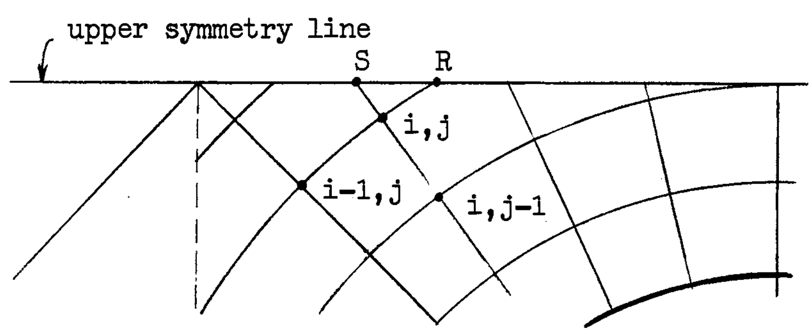

Figure 72. Irregular Stars on the Upper Symmetry Line

Subroutine POLAR

POLAR is responsible for calculation of all the inner field stream functions and vorticities of polar coordinate sections including tube surfaces. Equations 4-36, 4-47 and 4-51 are utilized in this subroutine.

Subroutine TTMESH

TTMESH is the subroutine that carries out the matching calculations at the unit cell-to-cell boundaries in polar coordinate sections (Figure-73).

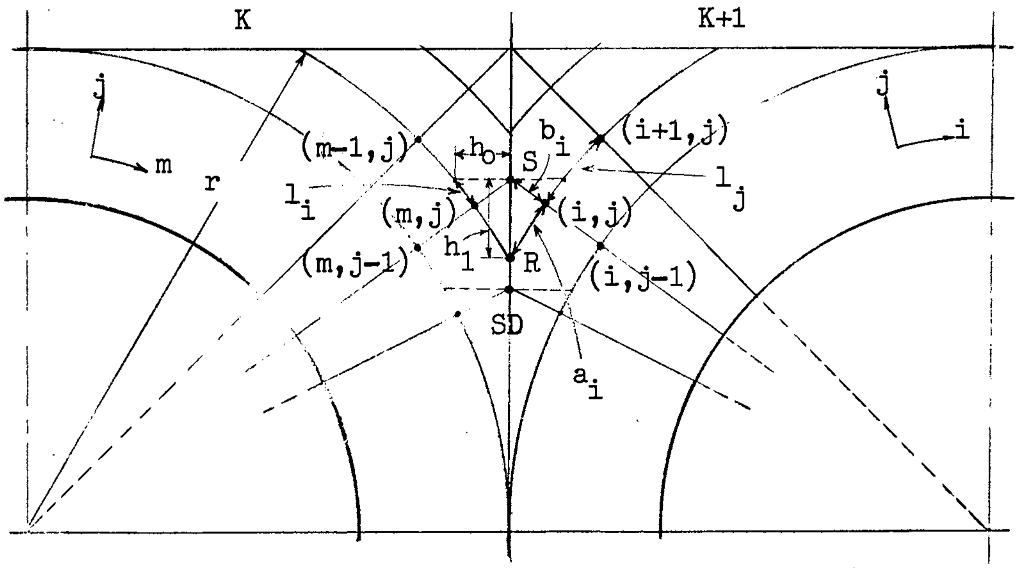

Figure 73. Polar-Polar Matching Plane

Finite difference equations used are given as follows:
For a typical boundary point (m,j) of the section K in Figure 73, the finite differencing method applied to the governing equations, Equations 4-25 and 4-26, at the points (m-1,j), (m,j-1), "R", and "S". The resulting equations are

$$\zeta^{k+1}_{m,j} = \left(\frac{1}{a_m l_j + b_i h}\right)\Big[\frac{a_m l_j}{b_i + h}(b_i \zeta^{k+1}_{m,j-1} + h\zeta_S) + \frac{a_m l_j b_i h}{2r(b_i + h)}(\zeta_S - \zeta^{k+1}_{m,j-1})$$

$$+ \frac{b_i h}{a_m + l_j}(a_m \zeta^{k+1}_{m-1,j} + l_j \zeta_R) + \frac{Re\, a_m l_j b_i h}{4(a_m + l_j)(b_i + h)}\Big\{(\psi_S - \psi^{k+1}_{m,j-1})$$

$$(\zeta_R-\zeta^{k+1}_{m-1,j}) - (\psi_R-\psi^{k+1}_{m-1,j})(\zeta_S-\zeta^{k+1}_{m,j-1})\Big\}\Big] \tag{I-13}$$

and

$$\psi^{k+1}_{m,j} = \left(\frac{1}{a_m l_j + b_i h}\right)\Big[\frac{a_m l_j}{b_i + h}(b_i\psi^{k+1}_{m,j-1} + h\psi_S) + \frac{a_m l_j b_i h}{2r(b_i + h)}(\psi_S - \psi^{k+1}_{m,j-1}) + \frac{b_i h}{a_m + l_j}(a_m\psi^{k+1}_{m-1,j} + l_j\psi_R) - \frac{a_m l_j b_i h}{2}\zeta^{k+1}_{m,j}\Big] \tag{I-14}$$

Similarly, for a boundary point (i,j) of the section K+1, for which the mesh points "R", "S", (i+1,j) and (i,j-1) are employed, the working equations become

$$\zeta^{k+1}_{i,j} = \left(\frac{1}{a_i l_j + b_i h}\right)\Big[\frac{a_i l_j}{b_i + h}(b_i\zeta^{k+1}_{i,j-1} + h\zeta_S) + \frac{a_i l_j b_i h}{2r(b_i+h)}(\zeta_S - \zeta^{k+1}_{i,j-1}) + \frac{b_i h}{a_i + h}(a_i\zeta^{k}_{i+1,j} + l_j\zeta_R) + \frac{Re\,a_i l_j b_i h}{4(a_i+l_j)(b_i+h)}\Big\{(\psi_S-\psi^{k+1}_{i,j-1})(\zeta^{k}_{i+1,j}-\zeta_R) - (\psi^{k}_{i+1,j}-\psi_R)(\zeta_S-\zeta^{k+1}_{i,j-1})\Big\}\Big] \tag{I-15}$$

and

$$\psi^{k+1}_{i,j} = \left(\frac{1}{a_i l_j + b_i h}\right)\Big[\frac{a_i l_j}{b_i + h}(b_i\psi^{k+1}_{i,j-1} + h\psi_S) + \frac{a_i l_j b_i h}{2r(b_i+h)}(\psi_S-\psi^{k+1}_{i,j-1}) + \frac{a_i h}{a_i + h}(a_i\psi^{k}_{i+1,j} + l_j\psi_R) - \frac{a_i l_j b_i h}{2}\zeta^{k+1}_{i,j}\Big] \tag{I-16}$$

Here, the values of ζ and ψ at the irregular stars "R" and "S" in Equations I-13 to I-16 are interpolated as follows;

$$\zeta_S = \frac{1}{2}[(\zeta^{k+1}_{m-1,j}+\zeta^{k}_{i+1,j})l_i/l_j+(\zeta^{k+1}_{m,j}+\zeta^{k}_{i,j})(1-l_i/l_j)] \qquad \text{(I-17)}$$

$$\psi_S = \frac{1}{2}[(\psi^{k+1}_{m-1,j}+\psi^{k}_{i+1,j})l_i/l_j+(\psi^{k+1}_{m,j}+\psi^{k}_{i,j})(1-l_i/l_j)] \qquad \text{(I-18)}$$

$$\zeta_R = \zeta_{SD}h_1/y_{i-1}+ \zeta_S(1 - h_1/y_{i-1}) \qquad \text{(I-19)}$$

and

$$\psi_R = \psi_{SD}h_1/y_{i-1}+ \psi_S(1 - h_1/y_{i-1}) \qquad \text{(I-20)}$$

where

$$\zeta_{SD}= \frac{1}{2}[(\zeta^{k+1}_{m,j-1}+\zeta^{k}_{i,j-1})l_{i-1}/l_{j-1}+(\zeta^{k}_{m+1,j-1}+\zeta^{k}_{i-1,j-1})(1-l_{i-1}/l_{j-1})] \qquad \text{(I-21)}$$

and

$$\psi_{SD}= \frac{1}{2}[(\psi^{k+1}_{m,j-1}+\psi^{k}_{i,j-1})l_{i-1}/l_{j-1}+(\psi^{k}_{m+1,j-1}+\psi^{k}_{i-1,j-1})(1-l_{i-1}/l_{j-1})] \qquad \text{(I-22)}$$

Subroutine TSMESH

TSMESH is the subroutine that performs the matching calculation at the boundary of the polar tube section K=8 and the rectangular section K=9. TSMESH is the mirror image of subroutine STMESH. The finite difference equations used and the geometry involved should be referred to the section of subroutine STMESH.

Subroutine STORE

STORE is the subroutine that stores the intermediate or final results of stream function and vorticity in the permanent strage disk of the computer according to the control parameters in the main program. STORE is called by the main program after each completed calculation.

Subroutine PRINT

PRINT is the subroutine that prints out all or part of the results, or punches out all the results of stream function and vorticity. The print-out format is specified by the internal command.

Input Data Card

The input data cards required for the program are arranged in the following order:

CARD 1

CARD 2 "Format specifications"

The first two cards are for built-in format specifications of the input and output data.

READ: (FM1(I),I=1,18)
READ: (FM2(I),I=1,18)

FORMAT: 18A4

CARD 3 "Control parameters and constants for iterative computation"

This card contains nine constants and parameters required for the operation of the program. Each of them is described below:

NI = number of incremental steps in x-direction to be specified for the inlet section K=1.

NT = number of tube rows. Three tube rows are used in this study.

N2 = number of incremental steps in x-direction to be specified for the outlet section K=12.

NS = number of incremental steps in the θ - direction per an angular distance of $\pi/4$ to be specified at polar tube section.

NPT = number of incremental steps to be specified in r-direction at the minimum clearance of the tube bank flow channel.
= 10 at Re=10 to 100 for P_t=1.50.
= 5 at Re= 1 to 100 for P_t=1.25 and at Re=1, 5 and 10 for P_t=1.50.

ITMAX = number of maximum iterations at a time to be specified.

EPSMAX = limit for $\sum_{i,j} (\zeta^{k+1}_{i,j} - \zeta^{k}_{i,j})$ and $\sum_{i,j} (\psi^{k+1}_{i,j} - \psi^{k}_{i,j})$.

PT = inline square pitch ratio

Re = Reynolds number

READ: NI, NT, N2, NS, NPT, ITMAX, EPSMAX,
PT, RE

FORMAT: 6I5, 3F10.5

CARD 4 and thereafter

In these cards the stream function and the vorticity are punched that are read in as initial guess.

READ: F(K,I,J)
V(K,I,J)

FORMAT: 18A4

```
C
C ... STEADY STATE VISCOUS FLOW ACROSS BANKS OF TUBES AT LOW REYNOLS NUMBERS ...
C
C ... AUTHOR: KOHEI ISHIHARA, SCHOOL OF CHEMICAL ENGINEERING, OKLAHOMA STATE
C                                UNIVERSITY, STILLWATER, OKLAHOMA 74074  MAY,1971 .
C
C ... NUMERICAL SOLUTIONS OF THE NAVIER-STOKES EQUATIONS FOR VORTICITY AND
C     STREAM FUNCTION ....
C     V(I,J)=VORTICITY
C     F(I,J)=STREAM FUNCTION
C ... POLAR AND RECTANGULAR COORDINATE SYSTEMS ARE USED ...
C
      COMMON F(12,50,45),V(12,50,45)
      COMMON RR(20,3),HI(20,3),R(50),HLJ(50),N(50)
      COMMON Y(20),RI(20),SS(20),HOI(20),G(20),YI(20)
      COMMON FMI(18),FM2(18)
      COMMON RE,H,PT,DH
      COMMON NI,NT,NO,NS,NPT,NP,NSS,NIN,NIN1,NI1,NO1,NTK,NS1,NS2,NO2
  300 FORMAT(18A4)
      READ(5,300) (FM1(I),I=1,18)
      READ(5,300) (FM2(I),I=1,18)
      READ (5,100) NI,NT,N2,NS,NPT,ITMAX,EPSMAX,PT,RE
      WRITE(6,200) NI,NT,N2,NS,NPT,ITMAX,EPSMAX,PT,RE
  100 FORMAT(6I5,4F10.5)
  200 FORMAT(/,5X'NI=',I2,1X'NT=',I2,1X'N2=',I2,1X'NS=',I2,1X'NPT=',I2,1
     1X'ITMAX=',I3,1X'EPSMAX=',F8.4,1X'PT=',F8.4,1X'RE=',F8.4,/)
      H=(PT-1.)/NPT
      DH=1.-H/2.+3.*H*H/8.
      IF(PT.EQ.1.5) GO TO 1
      DPT=0.5/(PT-1.)
      GO TO 2
    1 CONTINUE
      DPT=1.
    2 CONTINUE
      NIN=4*NPT*DPT-2
      NS2=2*NS-1
      NS1=NS+1
      NTK=NT*2+3
      NP=10
      NI1=NI+1
      NIN1=NIN+1
      NSS=NS-1
      NO=NS2+2
      NO1=NO+1
      NO2=N2+1
      WRITE(6,201) H,DH,NTK,NIN,NS1,NS2,NP,NSS,NIN1,NI1,NO1,NO2
  201 FORMAT(/,5X'H=',F8.4,1X,'DH=',F8.4,1X'NTK=',I2,1X'NIN=',I2,1X'NS1=
     1',I2,1X'NS2=',I2,1X'NP=',I2,1X'NSS=',I2,1X'NIN1=',I2,1X'NI1=',I2,
     21X'NO1=',I2,1X'NO2=',I2,/)
      CALL COUNT
C ... ESTABLISH INITIAL GUESS FOR VORTICITY FIELD AND STREAM FUNCTION ....
      REWIND 3
      CALL DISK(3)
C ... PRINT OUT INITIAL GUESS ...
      WRITE(6,208)
  208 FORMAT(/,'INITIAL GUESS OF STREAM FUNCTION AND VORTICITY',/)
      CALL PRINT(6)
C ... CALCULATE SUCCESSIVE APPROXIMATION FOR STREAM FUNCTION AND VORTICITY ...
      ITER=0
      NN=100
   20 CONTINUE
      K=1
      EPSV=0.
      EPSF=0.
      ITER=ITER+1
C ... INLET SECTION(SPECIFIED) ...
      DO 22 J=1,NS
      F(K,NI+2,J)=F(K+1,3,J)
      V(K,NI+2,J)=V(K+1,3,J)
   22 CONTINUE
      CALL SQUARE(2,K,NI1,EPSV,EPSF)
      K=K+1
C ... INLET SECTION(BUILT-IN) ...
      DO 23 J=1,NS
      F(K,1,J)=F(K-1,NI1,J)
      V(K,1,J)=V(K-1,NI1,J)
   23 CONTINUE
      CALL SQUARE(1,K,NIN,EPSV,EPSF)
      CALL STMESH(K,NIN1,EPSV,EPSF)
      K=K+1
C ... MAIN SECTION ...
      CALL TUBE(K,EPSV,EPSF)
      K=K+1
C ... OUTLET SECTION(BUILT-IN) ...
      DO 25 J=1,NS
      F(K,NIN+2,J)=(F(K+1,1,J)+F(K+1,2,J))/2.
      V(K,NIN+2,J)=(V(K+1,1,J)+V(K+1,2,J))/2.
   25 CONTINUE
      CALL SQUARE(1,K,NIN1,EPSV,EPSF)
      K=K+1
      DO 27 J=1,NS
      F(K,1,J)=F(K-1,NIN1,J)
      V(K,1,J)=V(K-1,NIN1,J)
   27 CONTINUE
      DO 28 J=1,NS
      F(K,NO1,J)=F(K+1,2,J)
      V(K,NO1,J)=V(K+1,2,J)
   28 CONTINUE
      CALL SQUARE(2,K,NO,EPSV,EPSF)
C ... OUTLET SECTION(SPECIFIED) ...
      K=K+1
      DO 29 J=1,NS
      F(K,1,J)=F(K-1,NO,J)
      V(K,1,J)=V(K-1,NO,J)
   29 CONTINUE
      DO 19 J=1,NS
      F(K,NO1,J)= (F(K+1,1,J)+F(K+1,2,J))/2.
      V(K,NO1,J)= (V(K+1,1,J)+V(K+1,2,J))/2.
   19 CONTINUE
      CALL SQUARE(2,K,NO,EPSV,EPSF)
      K=K+1
      DO 18 J=1,NS
      F(K,1,J)=F(K-1,NO,J)
      V(K,1,J)=V(K-1,NO,J)
   18 CONTINUE
      CALL SQUARE(3,K,N2,EPSV,EPSF)
```

```
      NEND=NO2
      DO 40 J=1,NS
      F(K,NEND,J)=F(K,NEND-4,J)-2.*F(K,NEND-3,J)+2.*F(K,NEND-1,J)
      V(K,NEND,J)=V(K,NEND-4,J)-2.*V(K,NEND-3,J)+2.*V(K,NEND-1,J)
   40 CONTINUE
C ... PRINT OUT SUCCESSIVE RESULTS ...
      WRITE(6,207) ITER
  207 FORMAT(/,2X'ITER=',I3,/)
      IF(ITER.EQ.NN) GO TO 30
      GO TO 31
   30 CONTINUE
      NN=NN+50
      REWIND 3
      CALL STORE(3)
      CALL PRINT(6)
C ... STOP ITERATION IF COMPUTED VALUES SHOW LITTLE FURTHER CHANGE OR
C                     NUMBER OF ITERATIONS IS TOO LARGE ....
   31 CONTINUE
      WRITE(6,204)EPSF,EPSV
  204 FORMAT(/,10X,' EPSF =',F10.5,2X' EPSV =',F10.5,/)
      IF(EPSF.LE.EPSMAX) GO TO 32
      GO TO 33
   32 IF(EPSV.LE.EPSMAX) GO TO 34
   33 IF(ITER-ITMAX) 20,35,35
C ... PRINT VALUES OF THE ITERATION COUNTER "ITER" AND THE FINAL
C                     STREAM FUNCTION AND VORTICITY ...
   34 WRITE(6,202) ITER
  202 FORMAT(5X,'CONVERGENCE CONDITION HAS BEEN REACHED AFTER',I3,2X'ITE
     1RATIONS',/,5X'STREAM FUNCTION AND VORTICITY FIELD IS GIVEN BY')
      CALL PRINT(7)
      REWIND 3
      CALL STORE(3)
      CALL PRINT(6)
      GO TO 36
C ... COMMENT IN CASE "ITER" EXCEEDS ITMAX ...
   35 WRITE(6,206)
  206 FORMAT(5X,'NO CONVERGENCE.  CURRENT VALUES OF F AND V ARE GIVEN AB
     1OVE',/)
      REWIND 3
      CALL STORE(3)
      CALL PRINT(6)
   36 CALL EXIT
      END
```

```
      SUBROUTINE COUNT
C
C ... THIS SUBROUTINE CALCULATES TAGGED PARAMETERS AND CONSTANTS NECESSARY FOR
C     SUBSEQUENT NUMERICAL COMPUTATION ....
C
      COMMON F(12,50,45),V(12,50,45)
      COMMON RR(20,3),HI(20,3),R(50),HLJ(50),N(50)
      COMMON Y(20),RI(20),SS(20),HOI(20),G(20),YI(20)
      COMMON FM1(18),FM2(18)
      COMMON RE,H,PT,DH
      COMMON NI,NT,NO,NS,NPT,NP,NSS,NIN,NIN1,NI1,NO1,NTK,NS1,NS2,NO2
      DIMENSION AS(20),DS(3),YR(20,3)
      PI=3.1415926536
      DAS=PI/(4.*(NS-1))
      A=2.
      NPM=( SQRT(A)*PT-1.)/H+1
      DO 2 J=1,NPM
      R(J)=H*(J-1)+1.
      HLJ(J)=R(J)*DAS
    2 CONTINUE
      DO 1 I=1,NS
      AS(I)=DAS*(I-1)
      RT =PT/ COS(AS(I))
      RI(I)=RT
      YI(I)=RT* SIN(AS(I))
      IF(I.EQ.1) GO TO 3
      Y(I-1)=YI(I)-YI(I-1)
    3 CONTINUE
      N(I)=(RT-1.)/H+1
      NPB=N(I)
      RAD= SQRT(R(NPB)*R(NPB)-YI(I)*YI(I))
      SS(I)=RT-R(NPB)
      HOI(I)=PT-RAD
      DDS= ARSIN(YI(I)/R(NPB))-AS(I)
      G(I)=DDS/DAS
      IF(I.EQ.1) GO TO 5
      KN=N(I)-N(I-1)
      IF(KN.EQ.0) GO TO 6
      JK=0
      GO TO 7
    6 KN=1
      JK=1
    7 CONTINUE
      DO 4 K=1,KN
      J=N(I-1)+K-JK
      DS(K)=AS(I)- ARCOS(PT/R(J))
      IF(DS(K).LT.DAS) GO TO 10
      DS(K)=DAS
   10 CONTINUE
      RR(I,K)=R(J)*DS(K)
      AR=R(J)*R(J)-PT*PT
      IF(AR.LE.0.) GO TO 8
      YR(I,K)= SQRT(AR)
      HI(I,K)=(YI(I)-YR(I,K))/Y(I-1)
      GO TO 9
    8 YR(I,K)=YI(I-1)
      HI(I,K)=1.0
    9 CONTINUE
    4 CONTINUE
    5 CONTINUE
    1 CONTINUE
      RETURN
      END
```

```
      SUBROUTINE GUESS
C
C ... THIS SUBROUTINE GENERATES THE INITIAL GUESS OF THE SOLUTION ...
C
      COMMON F(12,50,45),V(12,50,45)
      COMMON RR(20,3),HI(20,3),R(50),HLJ(50),N(50)
      COMMON Y(20),RI(20),SS(20),HOI(20),G(20),YI(20)
      COMMON FM1(18),FM2(18)
      COMMON RE,H,PT,DH
      COMMON NI,NT,NO,NS,NPT,NP,NSS,NIN,NIN1,NI1,NO1,NTK,NS1,NS2,NO2
      PTSQ=(PT-1.)*(PT-1.)
C ... INLET SECTION ...
      K=1
      DO 1 I=1,NI1
      F(K,I,1)=0.
      V(K,I,1)=0.
      DO 1 J=2,NS
      F(K,I,J)=(PT-1.)*YI(J)/PT
      V(K,I,J)=0.
    1 CONTINUE
      K=K+1
C ... INLET SECTION(BUILT-IN) ...
      DO 3 I=1,NIN1
      F(K,1,1)=0.
      V(K,I,1)=0.
      DO 3 J=2,NS
      F(K,I,J)=(PT-1.)*YI(J)/PT
      V(K,I,J)=0.
    3 CONTINUE
      K=K+1
C ... MAIN SECTION ...
C ... FIRST HALF OF A TUBE ....
    9 CONTINUE
      DO 4 I=1,NS
      NPB=N(I)
      RII=RI(I)-1.
      DO 4 J=1,NPB
      RJ=R(J)-1.
      F(K,I,J)=(PT-1.)*(I-1)*RJ*RJ/(RII*RII*(NS -1))
      V(K,I,J)= 1.5  *(I-1)*(RI(I)-R(J))/(RII         *(NS2-1))/PTSQ
    4 CONTINUE
      DO 5 I=NS1,NS2
      M=NS2-I+1
      NPB=N(M)
      RIM=RI(M)-1.
      DO 5 J=1,NPB
      RJ=R(J)-1.
      F(K,I,J)=(PT-1.)*RJ*RJ/(RIM*RIM)
      V(K,I,J)= 1.5  *(I-1)*(RI(M)-R(J))/(RIM         *(NS2-1))/PTSQ
    5 CONTINUE
      K=K+1
C ... SECOND HALF ...
      DO 6 I=1,NSS
      NPB=N(I)
      RII=RI(I)-1.
      DO 6 J=1,NPB
      RJ=R(J)-1.
      F(K,I,J)=(PT-1.)*RJ*RJ/(RII*RII)
      V(K,I,J)= 1.5  *(NS2-I)*(RI(I)-R(J))/(RII         *(NS2-1))/PTSQ
    6 CONTINUE
      DO 7 I=NS ,NS2
      M=NS2-I+1
      NPB=N(M)
      RIM=RI(M)-1.
      DO 7 J=1,NPB
      RJ=R(J)-1.
      F(K,I,J)=(PT-1.)*(M-1)*RJ*RJ/(RIM*RIM*(NS -1))
      V(K,I,J)= 1.5  *(M-1)*(RI(M)-R(J))/(RIM         *(NS2-1))/PTSQ
    7 CONTINUE
      K=K+1
      IF(K.EQ.NTK) GO TO 8
      GO TO 9
    8 CONTINUE
C ... OUTLET SECTION(BUILT-IN) ...
      DO 10 I=1,NIN1
      F(K,I,1)=0.
      V(K,I,1)=0.
      DO 10 J=2,NS
      F(K,I,J)=(PT-1.)*YI(J)/PT
      V(K,I,J)=0.
   10 CONTINUE
C ... OUTLET SECTION(SPECIFIED) ....
      KOUT=1
      NOUT=NO1
   70 CONTINUE
      K=K+1
      DO 12 I=1,NOUT
      F(K,I,1)=0.
      V(K,I,1)=0.
      DO 12 J=2,NS
      F(K,I,J)=(PT-1.)*YI(J)/PT
      V(K,I,J)=0.
   12 CONTINUE
      KOUT=KOUT+1
      GO TO (70,70,72,71),KOUT
   72 CONTINUE
      NOUT=NO2
      GO TO 70
   71 CONTINUE
      RETURN
      END
```

```
      SUBROUTINE DATA
C
C ... THIS SUBROUTINE READS THE DATA FROM THE PUNCHED-OUT DATA CARDS ...
C
      COMMON F(12,50,45),V(12,50,45)
      COMMON RR(20,3),HI(20,3),R(50),HLJ(50),N(50)
      COMMON Y(20),RI(20),SS(20),HOI(20),G(20),YI(20)
      COMMON FM1(18),FM2(18)
      COMMON RE,H,PT,DH
      COMMON NI,NT,NO,NS,NPT,NP,NSS,NIN,NIN1,NI1,NO1,NTK,NS1,NS2,NO2
      DIMENSION JN1(4),JN2(4)
  101 FORMAT(10F8.5)
      NC=N(NS)/NP
      JN1(1)=1
      JN2(1)=NP
      IF(NC.EQ.1) GO TO 18
      DO 9 L=2,NC
      JN1(L)=JN2(L-1)+1
      JN2(L)=JN2(L-1)+NP
    9 CONTINUE
   18 CONTINUE
      KW=1
   19 CONTINUE
      K=1
C ... INLET SECTION(SPECIFIED) ...
      NC=NS/NP
      DO 24 I=1,NI1
      GO TO (25,26),KW
   25 IF(NS.GT.NP) GO TO 60
      READ(5,FM2) (F(K,I,J),J=1,NS)
      GO TO 24
   60 DO 50 L=1,NC
      JN=JN1(L)
      JNP=JN2(L)
      READ (5,FM2) (F(K,I,J),J=JN,JNP)
   50 CONTINUE
      IF(NS.LE.JNP) GO TO 24
      JN=JNP+1
      READ (5,FM2) (F(K,I,J),J=JN,NS)
      GO TO 24
   26 IF(NS.GT.NP) GO TO 61
      READ(5,FM2) (V(K,I,J),J=1,NS)
      GO TO 24
   61 DO 51 L=1,NC
      JN=JN1(L)
      JNP=JN2(L)
      READ (5,FM2) (V(K,I,J),J=JN,JNP)
   51 CONTINUE
      IF(NS.LE.JNP) GO TO 24
      JN=JNP+1
      READ (5,FM2) (V(K,I,J),J=JN,NS)
   24 CONTINUE
      K=K+1
C ... INLET SECTION(BUILT-IN) ...
      DO 27 I=1,NIN1
      GO TO (28,29),KW
   28 IF(NS.GT.NP) GO TO 62
      READ(5,FM2) (F(K,I,J),J=1,NS)
      GO TO 27
   62 DO 53 L=1,NC
      JN=JN1(L)
      JNP=JN2(L)
      READ (5,FM2) (F(K,I,J),J=JN,JNP)
   53 CONTINUE
      IF(NS.LE.JNP) GO TO 27
      JN=JNP+1
      READ (5,FM2) (F(K,I,J),J=JN,NS)
      GO TO 27
   29 IF(NS.GT.NP) GO TO 63
      READ(5,FM2) (V(K,I,J),J=1,NS)
      GO TO 27
   63 DO 54 L=1,NC
      JN=JN1(L)
      JNP=JN2(L)
      READ (5,FM2) (V(K,I,J),J=JN,JNP)
   54 CONTINUE
      IF(NS.LE.JNP) GO TO 27
      JN=JNP+1
      READ (5,FM2) (V(K,I,J),J=JN,NS)
   27 CONTINUE
      K=K+1
   30 CONTINUE
C ... MAIN SECTION ...
C ... FIRST QUATER ...
      DO 31 I=1,NS
      NPB=N(I)
      NC=NPB/NP
      GO TO (32,33),KW
   32 IF(NPB.GT.NP) GO TO 1
      READ (5,FM2) (F(K,I,J),J=1,NPB)
      GO TO 31
    1 DO 2 L=1,NC
      JN=JN1(L)
      JNP=JN2(L)
      READ (5,FM2) (F(K,I,J),J=JN,JNP)
    2 CONTINUE
      IF(NPB.LE.JNP) GO TO 31
      JN=JNP+1
      READ (5,FM2) (F(K,I,J),J=JN,NPB)
      GO TO 31
   33 IF(NPB.GT.NP) GO TO 3
      READ (5,FM2) (V(K,I,J),J=1,NPB)
      GO TO 31
    3 DO 4 L=1,NC
      JN=JN1(L)
      JNP=JN2(L)
      READ (5,FM2) (V(K,I,J),J=JN,JNP)
    4 CONTINUE
      IF(NPB.LE.JNP) GO TO 31
      JN=JNP+1
      READ (5,FM2) (V(K,I,J),J=JN,NPB)
   31 CONTINUE
C ... SECOND QUATER ...
      DO 34 I=NS1,NS2
      NPB=N(NS2-I+1)
      NC=NPB/NP
```

```
      GO TO (35,36),KW
   35 IF(NPB.GT.NP) GO TO 5
      READ (5,FM2) (F(K,I,J),J=1,NPB)
      GO TO 34
    5 DO 6 L=1,NC
      JN=JN1(L)
      JNP=JN2(L)
      READ (5,FM2) (F(K,I,J),J=JN,JNP)
    6 CONTINUE
      IF(NPB.LE.JNP) GO TO 34
      JN=JNP+1
      READ (5,FM2) (F(K,I,J),J=JN,NPB)
      GO TO 34
   36 IF(NPB.GT.NP) GO TO 7
      READ (5,FM2) (V(K,I,J),J=1,NPB)
      GO TO 34
    7 DO 8 L=1,NC
      JN=JN1(L)
      JNP=JN2(L)
      READ (5,FM2) (V(K,I,J),J=JN,JNP)
    8 CONTINUE
      IF(NPB.LE.JNP) GO TO 34
      JN=JNP+1
      READ (5,FM2) (V(K,I,J),J=JN,NPB)
   34 CONTINUE
      K=K+1
      IF(K.EQ.NTK) GO TO 37
      GO TO 30
   37 CONTINUE
C ... OUTLET SECTION(BUILT-IN) ...
      NC=NS/NP
      DO 38 I=1,NIN1
      GO TO (39,40),KW
   39 IF(NS.GT.NP) GO TO 64
      READ(5,FM2) (F(K,I,J),J=1,NS)
      GO TO 38
   64 DO 55 L=1,NC
      JN=JN1(L)
      JNP=JN2(L)
      READ (5,FM2) (F(K,I,J),J=JN,JNP)
   55 CONTINUE
      IF(NS.LE.JNP) GO TO 38
      JN=JNP+1
      READ (5,FM2) (F(K,I,J),J=JN,NS)
      GO TO 38
   40 IF(NS.GT.NP) GO TO 65
      READ(5,FM2) (V(K,I,J),J=1,NS)
      GO TO 38
   65 DO 56 L=1,NC
      JN=JN1(L)
      JNP=JN2(L)
      READ (5,FM2) (V(K,I,J),J=JN,JNP)
   56 CONTINUE
      IF(NS.LE.JNP) GO TO 38
      JN=JNP+1
      READ (5,FM2) (V(K,I,J),J=JN,NS)
   38 CONTINUE
C ... OUTLET SECTION(SPECIFIED) ...
      KOUT=1
      NOUT=NO1
   70 CONTINUE
      K=K+1
      DO 42 I=1,NOUT
      GO TO (43,44),KW
   43 IF(NS.GT.NP) GO TO 66
      READ(5,FM2) (F(K,I,J),J=1,NS)
      GO TO 42
   66 DO 57 L=1,NC
      JN=JN1(L)
      JNP=JN2(L)
      READ (5,FM2) (F(K,I,J),J=JN,JNP)
   57 CONTINUE
      IF(NS.LE.JNP) GO TO 42
      JN=JNP+1
      READ (5,FM2) (F(K,I,J),J=JN,NS)
      GO TO 42
   44 IF(NS.GT.NP) GO TO 67
      READ(5,FM2) (V(K,I,J),J=1,NS)
      GO TO 42
   67 DO 58 L=1,NC
      JN=JN1(L)
      JNP=JN2(L)
      READ (5,FM2) (V(K,I,J),J=JN,JNP)
   58 CONTINUE
      IF(NS.LE.JNP) GO TO 42
      JN=JNP+1
      READ (5,FM2) (V(K,I,J),J=JN,NS)
   42 CONTINUE
      KOUT=KOUT+1
      GO TO (70,70,72,71),KOUT
   72 CONTINUE
      NOUT=NO2
      GO TO 70
   71 CONTINUE
      IF(KW.EQ.2) GO TO 45
      KW=KW+1
      GO TO 19
   45 CONTINUE
      RETURN
      END
```

```
      SUBROUTINE DISK(M)
C
C ... THIS SUBROUTINE READS THE DATA FROM THE PERMANENT STORAGE DISK ...
C
      COMMON F(12,50,45),V(12,50,45)
      COMMON RR(20,3),HI(20,3),R(50),HLJ(50),N(50)
      COMMON Y(20),RI(20),SS(20),HOI(20),G(20),YI(20)
      COMMON FM1(18),FM2(18)
      COMMON RE,H,PT,DH
      COMMON NI,NT,NO,NS,NPT,NP,NSS,NIN,NIN1,NI1,NO1,NTK,NS1,NS2,NO2
      KW=1
   19 CONTINUE
      K=1
C ... INLET SECTION(SPECIFIED) ...
      DO 24 I=1,NI1
      GO TO (25,26),KW
   25 READ (M)      (F(K,I,J),J=1,NS)
      GO TO 24
   26 READ (M)      (V(K,I,J),J=1,NS)
   24 CONTINUE
      K=K+1
C ... INLET SECTION(BUILT-IN) ...
      DO 27 I=1,NIN1
      GO TO (28,29),KW
   28 READ (M)      (F(K,I,J),J=1,NS)
      GO TO 27
   29 READ (M)      (V(K,I,J),J=1,NS)
   27 CONTINUE
      K=K+1
   30 CONTINUE
C ... MAIN SECTION ...
C ... FIRST QUATER ...
      DO 31 I=1,NS
      NPB=N(I)
      GO TO (32,33),KW
   32 READ (M)      (F(K,I,J),J=1,NPB)
      GO TO 31
   33 READ (M)      (V(K,1,J),J=1,NPB)
   31 CONTINUE
C ... SECOND QUATER ...
      DO 34 I=NS1,NS2
      NPB=N(NS2-I+1)
      GO TO (35,36),KW
   35 READ (M)      (F(K,1,J),J=1,NPB)
      GO TO 34
   36 READ (M)      (V(K,I,J),J=1,NPB)
   34 CONTINUE
      K=K+1
      IF(K.EQ.NTK) GO TO 37
      GO TO 30
   37 CONTINUE
C ... OUTLET SECTION(BUILT-IN) ...
      DO 38 I=1,NIN1
      GO TO (39,40),KW
   39 READ (M)      (F(K,I,J),J=1,NS)
      GO TO 38
   40 READ (M)      (V(K,I,J),J=1,NS)
   38 CONTINUE
C ... OUTLET SECTION(SPECIFIED) ...
      KOUT=1
      NOUT=NO1
   70 CONTINUE
      K=K+1
      DO 42 1=1,NOUT
      GO TO (43,44),KW
   43 READ (M)      (F(K,I,J),J=1,NS)
      GO TO 42
   44 READ (M)      (V(K,I,J),J=1,NS)
   42 CONTINUE
      KOUT=KOUT+1
      GO TO (70,70,72,71),KOUT
   72 CONTINUE
      NOUT=NO2
      GO TO 70
   71 CONTINUE
      IF(KW.EQ.2) GO TO 45
      KW=KW+1
      GO TO 19
   45 CONTINUE
      RETURN
      END
```

```
      SUBROUTINE SQUARE(M,K,NC,EPSV,EPSF)
C
C ... THIS SUBROUTINE EXECUTES RECTANGULAR FIELD CALCULATION ...
C
      COMMON F(12,50,45),V(12,50,45)
      COMMON RR(20,3),HI(20,3),R(50),HLJ(50),N(50)
      CCMMON Y(20),RI(20),SS(20),HOI(20),G(20),YI(20)
      COMMON FM1(18),FM2(18)
      COMMON RE,H,PT,DH
      COMMON NI,NT,NO,NS,NPT,NP,NSS,NIN,NIN1,NI1,NO1,NTK,NS1,NS2,NO2
      GO TO (2,3,4),M
    2 E=H
      GO TO 5
    3 E=H+H
      GO TO 5
    4 E=H+H+H+H
    5 EE=E*E
      PI=3.1415926536
      W=2./(1.+PI*SQRT(FLOAT(NC*NC+NSS*NSS))/(NC*NSS))
      DO 1 I=2,NC
      DO 1 J=2,NSS
      HOLOV=V(K,I,J)
      HOLDF=F(K,1,J)
      VIJ=(Y(J)*Y(J-1)*(V(K,I+1,J)+V(K,I-1,J))/2.+EE*(Y(J-1)*V(K,I,J+1)
     1+Y(J)*V(K,I,J-1))/(Y(J)+Y(J-1))+RE*E*Y(J)*Y(J-1)/(8.*(Y(J)+Y(J-1)
     2))*((F(K,I+1,J)-F(K,I-1,J))*(V(K,i,J+1)-V(K,I,J-1))-(V(K,I+1,J)-
     3V(K,I-1,J))*(F(K,I,J+1)-F(K,1,J-1))))/(EE+Y(J)*Y(J-1))
      FIJ=(Y(J)*Y(J-1)*(F(K,I+1,J)+F(K,I-1,J))/2.+EE*(Y(J-1)*F(K,I,J+1)
     1+Y(J)*F(K,I,J-1))/(Y(J)+Y(J-1))-EE*Y(J)*Y(J-1)*V(K,I,J)/2.)*W/
     2(EE+Y(J)*Y(J-1))+(1.-W)*F(K,1,J)
      DV=VIJ-HOLOV
      DF=F1J-HOLDF
      F(K,1,J)=F1J
      V(K,I,J)=VIJ
      EPSV=EPSV+ABS(DV)
      EPSF=EPSF+ABS(DF)
    1 CONTINUE
      RETURN
      END
```

```
      SUBROUTINE STMESH(K,M,EPSV,EPSF)
C
C ... THIS SUBROUTINE PERFORMS THE MATCHING CALCULATION ON RECTANGULAR-POLAR
C     BOUNDARY ...
C
      COMMON F(12,50,45),V(12,50,45)
      COMMON RR(20,3),HI(20,3),R(50),HLJ(50),N(50)
      COMMON Y(20),RI(20),SS(20),HOI(20),G(20),YI(20)
      COMMON FM1(18),FM2(18)
      COMMON RE,H,PT,DH
      COMMON NI,NT,NO,NS,NPT,NP,NSS,NIN,NIN1,NI1,NO1,NTK,NS1,NS2,NO2
      K1=K+1
      DO 1 J=2,NSS
      I=N(J)
      HOLDF=F(K,M,J)
      HOLDV=V(K,M,J)
      G1=G(J)
      G2=1.-G1
      VO=G1*V(K1,J+1,I)+G2*V(K1,J,I)
      FO=G1*F(K1,J+1,I)+G2*F(K1,J,I)
      YP=Y(J)*Y(J-1)
      YA=Y(J)+Y(J-1)
      HO=HOI(J)
      HP=H*HO
      HA=H+HO
      VMJ=(YP*(H*VO+HO*V(K,M-1,J))/HA+HP*(Y(J-1)*V(K,M,J+1)+
     1Y(J)*V(K,M,J-1))/YA+RE*HP*YP/(4.*HA*YA)*((FO-F(K,M-1,J))*
     2(V(K,M,J+1)-V(K,M,J-1))-(F(K,M,J+1)-F(K,M,J-1))*(VO-V(K,M-1,J))))
     3/(HP+YP)
      FMJ=(YP*(H*FO+HO*F(K,M-1,J))/HA+HP*(Y(J-1)*F(K,M,J+1)+
     1Y(J)*F(K,M,J-1))/YA-HP*YP*VMJ/2.)/(HP+YP)
      DV=VMJ-HOLDV
      DF=FMJ-HOLDF
      V(K,M,J)=VMJ
      F(K,M,J)=FMJ
      EPSV=EPSV+ABS(DV)
      EPSF=EPSF+ABS(DF)
    1 CONTINUE
      DO 2 I=2,NS
      B=SS(I)
      JK=N(I)-N(I-1)
      IF(JK.EQ.D) GO TO 7
      GO TO 8
    7 JK=1
    8 CONTINUE
      DO 2 L=1,JK
      KS=JK+1-L
      H1=HI(I,KS)
      H2=1.-H1
      J=N(I)-L+1
      HOLDF=F(K1,I,J)
      HOLDV=V(K1,I,J)
      A=RR(I,KS)
      HL=HLJ(J)
      IF(L.EQ.1) GO TO 3
      FS=F(K1,I,J+1)
      VS=V(K1,I,J+1)
      B=H
```

```
      GO TO 4
    3 FS=F(K,M,I)
      VS=V(K,M,I)
    4 IF(N(I).EQ.N(I-1)) GO TO 9
      VR=H1*V(K,M,I-1)+H2*V(K,M,I)
      FR=H1*F(K,M,I-1)+H2*F(K,M,I)
      GO TO 10
    9 VR=V(K1,I-1,J)
      FR=F(K1,I-1,J)
   10 CONTINUE
      IF(I.EQ.NS) GO TO 5
      VR1=V(K1,I+1,J)
      FR1=F(K1,I+1,J)
      GO TO 6
    5 VR1=0.
      FR1=PT-1.
      HL=A
    6 CONTINUE
      BK=B*H
      BPK=B+H
      AL=A*HL
      APL=A+HL
      AK=AL+BK
      VIJ=(AL*(B*V(K1,I,J-1)+H*VS)/BPK+AL*BK*(VS-V(K1,I,J-1))/(2.*R(J)*
     1BPK)+BK*(A*VR1+HL*VR)/APL-RE*AL*BK*((FS-F(K1,I,J-1))*(VR1-VR)-
     2(FR1-FR)*(VS-V(K1,I,J-1)))/((APL+BPK)*4.))/AK
      FIJ=(AL*(B*F(K1,I,J-1)+H*FS)/BPK+AL*BK*(FS-F(K1,I,J-1))/(2.*R(J)*
     1BPK)+BK*(A*FR1+HL*FR)/APL-AL*BK*VIJ/2.)/AK
      DV=VIJ-HOLDV
      DF=FIJ-HOLDF
      V(K1,I,J)=VIJ
      F(K1,I,J)=FIJ
      EPSV=EPSV+ABS(DV)
      EPSF=EPSF+ABS(DF)
    2 CONTINUE
      RETURN
      END
```

```
      SUBROUTINE TUBE(K,EPSV,EPSF)
C
C ... THIS SUBROUTINE COMMANDS THE TUBE SECTION CALCULATIONS ...
C
      COMMON F(12,50,45),V(12,50,45)
      COMMON RR(20,3),HI(20,3),R(50),HLJ(50),N(50)
      COMMON Y(20),RI(20),SS(20),HOI(20),G(20),YI(20)
      COMMON FM1(18),FM2(18)
      COMMON RE,H,PT,DH
      COMMON NI,NT,NO,NS,NPT,NP,NSS,NIN,NIN1,NI1,NO1,NTK,NS1,NS2,NO2
      NJ1=N(1)
      NTC=1
      NS3=NS2-1
   15 CONTINUE
C ... FIRST QUATER ...
      DO 1 I=2,NS
      IF(N(I).EQ.N(I-1)) GO TO 20
      NJ=N(I-1)
      GO TO 21
   20 NJ=N(I)-1
   21 CONTINUE
      JK=N(I)-NJ
      CALL POLAR(K,I,NJ,JK,EPSV,EPSF)
    1 CONTINUE
C ... SECOND QUATER ...
      DO 9 I=NS1,NS2
      M=NS2-I+1
      IF(I.EQ.NS2) GO TO 13
      IF(N(M).EQ.N(M-1)) GO TO 22
      FR=PT-1.
      VR=0.
      NJ=N(M-1)
      GO TO 23
   13 NJ=NJ1-1
      DO 16 J=1,NJ1
      F(K,I+1,J)=F(K+1,2,J)
      V(K,I+1,J)=V(K+1,2,J)
   16 CONTINUE
      JK=1
      CALL POLAR(K,I,NJ,JK,EPSV,EPSF)
      GO TO 9
   22 NJ=N(M)-1
      FR=F(K,I+1,N(M))
      VR=V(K,I+1,N(M))
   23 CONTINUE
      JK=N(M)-NJ
      DO 2 L=1,JK
      KS=JK+1-L
      B=SS(M)
      J=NJ+KS
      HOLDF=F(K,I,J)
      HOLDV=V(K,I,J)
      HL=HLJ(J)
      A=RR(M,KS)
      IF(L.EQ.1)  GO TO 3
      FS=F(K,I,J+1)
      VS=V(K,I,J+1)
      B=H
```

```
      GO TO 4
    3 FS=PT-1.
      VS=0.
    4 CONTINUE
      AL=A*HL
      BK=B*H
      APL=A+HL
      BPK=B+H
      AK=AL+BK
      VIJ=(AL*(B*V(K,I,J-1)+H*VS)/BPK+AL*BK*(VS-V(K,I,J-1))/(2.*R(J)*
     1BPK)+BK*(A*V(K,I-1,J)+HL*VR)/APL-RE*AL*BK/(4.*APL*BPK)*((FS-
     2F(K,I,J-1))*(VR-V(K,I-1,J))-(VS-V(K,I,J-1))*(FR-F(K,I-1,J))))/AK
      FIJ=(AL*(B*F(K,I,J-1)+H*FS)/BPK+AL*BK*(FS-F(K,I,J-1))/(2.*R(J)*
     1BPK)+BK*(A*F(K,I-1,J)+HL*FR)/APL-AL*BK*VIJ/2.)/AK
      DV=VIJ-HOLDV
      DF=FIJ-HOLDF
      V(K,I,J)=VIJ
      F(K,I,J)=FIJ
      EPSV=EPSV+ABS(DV)
      EPSF=EPSF+ABS(DF)
    2 CONTINUE
      CALL POLAR(K,I,NJ,JK,EPSV,EPSF)
    9 CONTINUE
      K=K+1
C ... THIRD QUATER ...
      DO 6 J=1,NJ1
      F(K,1,J)=F(K-1,NS2,J)
      V(K,1,J)=V(K-1,NS2,J)
    6 CONTINUE
      DO 17 I=2,NSS
      IF(N(I).EQ.N(I-1)) GO TO 24
      FR=PT-1.
      VR=0.
      NJ=N(I-1)
      GO TO 25
   24 NJ=N(I)-1
      FR=F(K,I-1,N(I))
      VR=V(K,I-1,N(I))
   25 CONTINUE
      JK=N(I)-NJ
      DO 5 L=1,JK
      KS=JK+1-L
      B=SS(I)
      J=NJ+KS
      HOLDV=V(K,I,J)
      HOLDF=F(K,I,J)
      HL=HLJ(J)
      A=RR(I,KS)
      IF(L.EQ.1) GO TO 7
      FS=F(K,I,J+1)
      VS=V(K,I,J+1)
      B=H
      GO TO 8
    7 FS=PT-1.
      VS=0.
    8 CONTINUE
      AL=A*HL
      BK=B*H
      APL=A+HL
      BPK=B+H
      AK=AL+BK
      VIJ=(AL*(B*V(K,I,J-1)+H*VS)/BPK+AL*BK*(VS-V(K,I,J-1))/(2.*R(J)*
     1BPK)+BK*(A*V(K,I+1,J)+HL*VR)/APL-RE*AL*BK/(4.*APL*BPK)*((FS-
     2F(K,I,J-1))*(V(K,I+1,J)-VR)-(F(K,I+1,J)-FR)*(VS-V(K,I,J-1))))/AK
      FIJ=(AL*(B*F(K,I,J-1)+H*FS)/BPK+AL*BK*(FS-F(K,I,J-1))/(2.*R(J)*
     1BPK)+BK*(A*F(K,I+1,J)+HL*FR)/APL-AL*BK*VIJ/2.)/AK
      DV=VIJ-HOLDV
      DF=FIJ-HOLDF
      V(K,I,J)=VIJ
      F(K,I,J)=FIJ
      EPSV=EPSV+ABS(DV)
      EPSF=EPSF+ABS(DF)
    5 CONTINUE
      CALL POLAR(K,I,NJ,JK,EPSV,EPSF)
   17 CONTINUE
C ... LAST QUATER ...
      DO 10 I=NS,NS3
      M=NS2-I+1
      IF(N(M).EQ.N(M-1)) GO TO 26
      NJ=N(M-1)
      GO TO 27
   26 NJ=N(M)-1
   27 CONTINUE
      JK=N(M)-NJ
      IF(NTC.EQ.NT) GO TO 11
      CALL TTMESH(K,I,NJ,JK,EPSV,EPSF)
      GO TO 14
   11 CALL TSMESH(K,I,NJ,JK,EPSV,EPSF)
   14 CALL POLAR(K,I,NJ,JK,EPSV,EPSF)
   10 CONTINUE
      IF(NTC.EQ.NT) GO TO 12
      K=K+1
      NTC=NTC+1
      GO TO 15
   12 RETURN
      END
```

```
      SUBROUTINE POLAR(K,I,NJ,JK,EPSV,EPSF)
C
C ... THIS SUBROUTINE EXECUTES INNER FIELD CALCULATION OF POLAR SECTION ...
C
      COMMON F(12,50,45),V(12,50,45)
      COMMON RR(20,3),HI(20,3),R(50),HLJ(50),N(50)
      COMMON Y(20),RI(20),SS(20),HOI(20),G(20),YI(20)
      COMMON FM1(18),FM2(18)
      COMMON RE,H,PT,DH
      COMMON NI,NT,NO,NS,NPT,NP,NSS,NIN,NIN1,NI1,NO1,NTK,NS1,NS2,NO2
      NPB=NJ+JK
      NJ1=NPB -1
      JK=NPB -NJ
      JK1=JK+1
      PI=3.1415926536
      W=2./(1.+PI*SQRT(FLOAT(I*I+NJ1*NJ1))/(I*NJ1))
      DO 1 M=JK1,NJ1
      J=NPB +1-M
      V(K,I,1)=(3.*F(K,I,2)/(H*H)-.5*V(K,I,2))/DH
      HL=HLJ(J)
      PKL=H*HL
      AKL=H*H+HL*HL
      HOLDV=V(K,I,J)
      HOLDF=F(K,I,J)
      VIJ=PKL*(PKL*((V(K,I,J+1)+V(K,I,J-1))/(H*H)+(V(K,I,J+1)-V(K,I,J-I)
     1)/(2.*R(J)*H)+(V(K,I+1,J)+V(K,I-1,J))/(HL*HL))-RE/8.*((F(K,I,J+1)-
     2F(K,I,J-1))*(V(K,I+1,J)-V(K,I-1,J))- (F(K,I+1,J)-F(K,I-1,J))*
     3(V(K,I,J+1)-V(K,I,J-1))))/(2.*AKL)
      FIJ=PKL*PKL/(2.*AKL)*((F(K,I,J+1)+F(K,I,J-1))/(H*H)+(F(K,I,J+1)-
     1F(K,I,J-1))/(2.*R(J)*H)+(F(K,I+1,J)+F(K,I-1,J))/(HL*HL)-VIJ)*W+
     2(1.-W)*F(K,I,J)
      DV=VIJ-HOLDV
      DF=FIJ-HOLDF
      V(K,I,J)=VIJ
      F(K,I,J)=FIJ
      EPSV=EPSV+ABS(DV)
      EPSF=EPSF+ABS(DF)
    1 CONTINUE
      RETURN
      END
```

```
      SUBROUTINE TTMESH(K,M,NJ,JK,EPSV,EPSF)
C
C ... THIS SUBROUTINE PERFORMS THE MATCHING CALCULATION ON POLAR-POLAR BOUNDARY
C
      COMMON F(12,50,45),V(12,50,45)
      COMMON RR(20,3),HI(20,3),R(50),HLJ(50),N(50)
      COMMON Y(20),RI(20),SS(20),HOI(20),G(20),YI(20)
      COMMON FM1(18),FM2(18)
      COMMON RE,H,PT,DH
      COMMON NI,NT,NO,NS,NPT,NP,NSS,NIN,NIN1,NI1,NO1,NTK,NS1,NS2,NO2
      KW=1
      K1=K+1
      I=NS*2-M
      JU=N(I)
      JD=N(I-1)
      G1=G(I)
      G2=1.-G1
      G3=G(I-1)
      G4=1.-G3
   20 CONTINUE
      DO 1 L=1,JK
      KS=JK+1-L
      B=SS(I)
      J=NJ+KS
      H1=HI(I,KS)
      H2=1.-H1
      A=RR(I,KS)
      HL=HLJ(J)
      IF(M.EQ.NS) GO TO 11
      FS=(G1*(F(K1,I+1,JU)+F(K,M-1,JU))+G2*(F(K1,1,JU)+F(K,M,JU)))/2.
      VS=(G1*(V(K1,I+1,JU)+V(K,M-1,JU))+G2*(V(K1,I,JU)+V(K,M,JU)))/2.
      GO TO 12
   11 FS=PT-1.
      VS=0.
   12 CONTINUE
      FSD=(G3*(F(K1,I,JD)+F(K,M,JD))+G4*(F(K1,I-1,JD)+F(K,M+1,JD)))/2.
      VSD=(G3*(V(K1,I,JD)+V(K,M,JD))+G4*(V(K1,I-1,JD)+V(K,M+1,JD)))/2.
      GO TO (2,3),KW
    2 HOLDV=V(K,M,J)
      HOLDF=F(K,M,J)
      GO TO 4
    3 HOLDV=V(K1,I,J)
      HOLDF=F(K1,1,J)
    4 CONTINUE
      GO TO (5,6),KW
    5 IF(M.EQ.NS) GO TO 30
      FRM=F(K,M-1,J)
      VRM=V(K,M-1,J)
      GO TO 7
   30 FRM=PT-1.
      VRM=0.
      HL=A
      GO TO 7
    6 IF(M.EQ.NS) GO TO 32
      FRI=F(K1,I+I,J)
      VRI=V(K1,I+1,J)
      GO TO 7
   32 FRI=PT-1.
```

```
      VRI=0.
      HL=A
    7 CONTINUE
      FR=H1*FSD+H2*FS
      VR=H1*VSD+H2*VS
      IF(L.EQ.1)  GO TO 8
      GO TO (24,25),KW
   24 FS=F(K,M,J+1)
      VS=V(K,M,J+1)
      B=H
      GO TO 8
   25 FS=F(K1,I,J+1)
      VS=V(K1,I,J+1)
      B=H
    8 CONTINUE
      IF(N(I).EQ.N(I-1)) GO TO 14
      GO TO 23
   14 GO TO (21,22),KW
   21 VR=V(K,M+1,J)
      FR=F(K,M+1,J)
      A=HL
      GO TO 23
   22 VR=V(K1,I-1,J)
      FR=F(K1,I-1,J)
      A=HL
   23 CONTINUE
      AL=A*HL
      APL=A+HL
      BK=B*H
      BPK=B+H
      AK=AL+BK
      GO TO (9,10),KW
    9 CONTINUE
      VMJ=(AL*(B*V(K,M,J-1)+H*VS)/BPK+AL*BK/(2.*R(J)*BPK)*(VS-V(K,M,J-1)
     1)+BK*(A*VRM+HL*VR)/APL-RE*AL*BK/(4.*APL*BPK)*((FS-F(K,M,J-1))*(VR-
     2VRM)-(FR-FRM)*(VS-V(K,M,J-1)))))/AK
      FMJ=(AL*(B*F(K,M,J-1)+H*FS)/BPK+AL*BK/(2.*R(J)*BPK)*(FS-F(K,M,J-1)
     1)+BK*(A*FRM+HL*FR)/APL-AL*BK*VMJ/2.)/AK
      DV=VMJ-HCLDV
      DF=FMJ-HOLDF
      V(K,M,J)=VMJ
      F(K,M,J)=FMJ
      GO TO 18
   10 CONTINUE
      VIJ=(AL*(B*V(K1,I,J-1)+H*VS)/BPK+AL*BK/(2.*R(J)*BPK)*
     1(VS-V(K1,I,J-1))+BK*(A*VRI+HL*VR)/APL-RE*AL*BK/(4.*APL*BPK)*((FS-
     1F(K1,I,J-1))*(VRI-VR)-(VS-V(K1,I,J-1))*(FRI-FR)))/AK
      FIJ=(AL*(B*F(K1,I,J-1)+H*FS)/BPK+AL*BK/(2.*R(J)*BPK)*
     1(FS-F(K1,I,J-1))+BK*(A*FRI+HL*FR)/APL-AL*BK*VIJ/2.)/AK
      DV=VIJ-HOLDV
      DF=FIJ-HOLDF
      F(K1,I,J)=FIJ
      V(K1,I,J)=VIJ
   18 EPSV=EPSV+ABS(DV)
      EPSF=EPSF+ABS(DF)
    1 CONTINUE
      GO TO (19,40),KW
   19 KW=KW+1
      GO TO 20
   40 CONTINUE
      RETURN
      END
```

```
      SUBROUTINE TSMESH(K,M,NJ,JK,EPSV,EPSF)
C
C ... THIS SUBROUTINE PERFORMS THE MATCHING CALCULATION  ON POLAR-RECTANGULAR
C     MATCHING PLANE ....
C
      COMMON F(12,50,45),V(12,50,45)
      COMMON RR(20,3),HI(20,3),R(50),HLJ(50),N(50)
      COMMON Y(20),RI(20),SS(20),HOI(20),G(20),YI(20)
      COMMON FM1(18),FM2(18)
      COMMON RE,H,PT,DH
      COMMON NI,NT,NO,NS,NPT,NP,NSS,NIN,NIN1,NI1,NO1,NTK,NS1,NS2,NO2
      I=NS*2-M
      K1=K+1
      DO 1 L=1,JK
      KS=JK+1-L
      B=SS(I)
      J=NJ+KS
      HL=HLJ(J)
      A=RR(I,KS)
      H1=HI(I,KS)
      H2=1.-H1
      HOLDV=V(K,M,J)
      HOLDF=F(K,M,J)
      IF(L.EQ.1)  GO TO 2
      FS=F(K,M,J+1)
      VS=V(K,M,J+1)
      B=H
      GO TO 5
    2 CONTINUE
      FS=F(K1,1,I)
      VS=V(K1,1,I)
    5 CONTINUE
      BK=B*H
      BPK=B+H
      IF(N(I).EQ.N(I-1)) GO TO 7
      VR=H1*V(K1,1,I-1)+H2*V(K1,1,I)
      FR=H1*F(K1,1,1-1)+H2*F(K1,1,I)
      GO TO 8
    7 VR=V(K,M+1,J)
      FR=F(K,M+1,J)
    8 CONTINUE
      IF(M.EQ.NS) GO TO 3
      VR1=V(K,M-1,J)
      FR1=F(K,M-1,J)
      GO TO 4
    3 CONTINUE
      FR1=PT-1.
      VR1=0.
      HL=A
    4 CONTINUE
      AL=A*HL
      APL=A+HL
      AK=AL+BK
      VMJ=(AL*(B*V(K,M,J-1)+H*VS)/BPK+AL*BK*(VS-V(K,M,J-1))/(2.*R(J)*
     1BPK)+BK*(A*VR1+HL*VR)/APL-RE*AL*BK*((FS-F(K,M,J-1))*(VR-VR1)-
     2(FR-FR1)*(VS-V(K,M,J-1)))/((APL+BPK)*4.))/AK
      FMJ=(AL*(B*F(K,M,J-1)+H*FS)/BPK+AL*BK*(FS-F(K,M,J-1))/(2.*R(J)*
     1BPK)+BK*(A*FR1+HL*FR)/APL-AL*BK*VMJ/2.)/AK
      DV=VMJ-HOLDV
      DF=FMJ-HOLDF
      F(K,M,J)=FMJ
      V(K,M,J)=VMJ
      EPSV=EPSV+ABS(DV)
      EPSF=EPSF+ABS(DF)
    1 CONTINUE
      J=NJ+JK
      IF(I.EQ.NS) GO TO 6
      G1=G(I)
      G2=1.-G1
      HO=HOI(I)
      HOLDV=V(K1,1,I)
      HOLDF=F(K1,1,I)
      VO=GI*V(K,M-1,J)+G2*V(K,M,J)
      FO=G1*F(K,M-1,J)+G2*F(K,M,J)
      YP=Y(I)*Y(I-1)
      YA=Y(I)+Y(I-1)
      HP=H*HO
      HA=H+HO
      VIJ=(YP*(H*VO+HO*V(K1,2,I))/HA+HP*(Y(I-1)*V(K1,1,I+1)+
     1Y(I)*V(K1,1,I-1))/YA+RE*HP*YP/(4.*HA*YA)*((F(K1,2,I)-FO)*
     2(V(K1,1,I+1)-V(K1,1,I-1))-(F(K1,1,I+1)-F(K1,1,I-1))*(V(KI,2,I)-VO)
     3))/(HP+YP)
      FIJ=(YP*(H*FO+HO*F(K1,2,I))/HA+HP*(Y(I-1)*F(K1,1,I+1)+
     1Y(I)*F(K1,1,I-1))/YA-HP*YP*VIJ/2.)/(HP+YP)
      DV=VIJ-HOLDV
      DF=FIJ-HOLDF
      F(K1,1,I)=FIJ
      V(K1,1,I)=VIJ
      EPSV=EPSV+ABS(OV)
      EPSF=EPSF+ABS(DF)
    6 CONTINUE
      RETURN
      END
```

```
      SUBROUTINE STORE(M)
C
C ... THIS SUBROUTINE STORES INTERMEDIATE OR FINAL RESULTS OF SOLUTION IN THE
C     PERMANENT STORAGE DISK ...
C
      COMMON F(12,50,45),V(12,50,45)
      COMMON RR(20,3),HI(20,3),R(50),HLJ(50),N(50)
      COMMON Y(20),RI(20),SS(20),HOI(20),G(20),YI(20)
      COMMON FM1(18),FM2(18)
      COMMON RE,H,PT,DH
      COMMON NI,NT,NO,NS,NPT,NP,NSS,NIN,NIN1,NI1,NO1,NTK,NS1,NS2,NO2
      KW=1
   19 CONTINUE
      K=1
C ... INLET SECTION(SPECIFIED) ...
      DO 24 I=1,NI1
      GO TO (25,26),KW
   25 WRITE(M)      (F(K,I,J),J=1,NS)
      GO TO 24
   26 WRITE(M)      (V(K,I,J),J=1,NS)
   24 CONTINUE
      K=K+1
C ... INLET SECTION(BUILT-IN) ...
      DO 27 I=1,NIN1
      GO TO (28,29),KW
   28 WRITE(M)      (F(K,I,J),J=1,NS)
      GO TO 27
   29 WRITE(M)      (V(K,I,J),J=1,NS)
   27 CONTINUE
      K=K+1
   30 CONTINUE
C ... MAIN SECTION ...
C ... FIRST QUATER ...
      DO 31 I=1,NS
      NPB=N(I)
      GO TO (32,33),KW
   32 WRITE(M)      (F(K,I,J),J=1,NPB)
      GO TO 31
   33 WRITE(M)      (V(K,I,J),J=1,NPB)
   31 CONTINUE
C ... SECOND QUATER ...
      DO 34 I=NS1,NS2
      NPB=N(NS2-I+1)
      GO TO (35,36),KW
   35 WRITE(M)      (F(K,I,J),J=1,NPB)
      GO TO 34
   36 WRITE(M)      (V(K,I,J),J=1,NPB)
   34 CONTINUE
      K=K+1
      IF(K.EQ.NTK) GO TO 37
      GO TO 30
   37 CONTINUE
C ... OUTLET SECTION(BUILT-IN) ...
      DO 38 I=1,NIN1
      GO TO (39,40),KW
   39 WRITE(M)      (F(K,I,J),J=1,NS)
      GO TO 38
   40 WRITE(M)      (V(K,I,J),J=1,NS)
   38 CONTINUE
C ... OUTLET SECTION(SPECIFIED) ...
      KOUT=1
      NOUT=NO1
   46 CONTINUE
      K=K+1
      DO 42 I=1,NOUT
      GO TO (43,44),KW
   43 WRITE(M)      (F(K,I,J),J=1,NS)
      GO TO 42
   44 WRITE(M)      (V(K,I,J),J=1,NS)
   42 CONTINUE
      KOUT=KOUT+1
      GO TO (46,46,48,47),KOUT
   48 CONTINUE
      NOUT=NO2
      GO TO 46
   47 CONTINUE
      IF(KW.EQ.2) GO TO 45
      KW=KW+1
      GO TO 19
   45 CONTINUE
      RETURN
      END
```

```
      SUBROUTINE PRINT(M)
C
C ... THIS SUBROUTINE PRINTS OR PUNCHES OUT INTERMEDIATE OR FINAL SOLUTION ...
C
      COMMON F(12,50,45),V(12,50,45)
      COMMON RR(20,3),HI(20,3),R(50),HLJ(50),N(50)
      COMMON Y(20),RI(20),SS(20),HOI(20),G(20),YI(20)
      COMMON FM1(18),FM2(18)
      COMMON RE,H,PT,DH
      COMMON NI,NT,NO,NS,NPT,NP,NSS,NIN,NIN1,NI1,NO1,NTK,NS1,NS2,NO2
      DIMENSION FMT(18)
      IF(M.EQ.6) GO TO 1
      JS=1
      NSM=NS1
      DO 2 I=1,18
      FMT(I)=FM2(I)
    2 CONTINUE
      GO TO 4
    1 CONTINUE
      JS=(N(NS)+3)/NP
      IF(JS.EQ.1) GO TO 50
      GO TO 52
   50 NSM=NS1
      GO TO 51
   52 CONTINUE
      NSM=NS1+1
   51 CONTINUE
      DO 3 I=1,18
      FMT(I)=FM1(I)
    3 CONTINUE
    4 CONTINUE
      KW=1
   19 CONTINUE
      K=1
      IF(M.EQ.6) GO TO 23
      GO TO 22
   23 CONTINUE
      GO TO (20,21),KW
   20 WRITE(M,203)
      GO TO 22
   21 WRITE(M,205)
  203 FORMAT(/,5X'STREAM FUNCTION',/)
  205 FORMAT(/,5X'VORTICITY FIELD',/)
   22 CONTINUE
C ... INLET SECTION(SPECIFIED) ...
      DO 24 I=1,NI1,JS
      GO TO (25,26),KW
   25 WRITE(M,FMT) (F(K,I,J),J=1,NS,JS)
      GO TO 24
   26 WRITE(M,FMT) (V(K,I,J),J=1,NS,JS)
   24 CONTINUE
      K=K+1
C ... INLET SECTION(BUILT-IN) ...
      DO 27 I=1,NIN1,JS
      GO TO (28,29),KW
   28 WRITE(M,FMT) (F(K,I,J),J=1,NS,JS)
      GO TO 27
   29 WRITE(M,FMT) (V(K,I,J),J=1,NS,JS)
   27 CONTINUE
      K=K+1
   30 CONTINUE
C ... MAIN SECTION ...
C ... FIRST QUATER ...
      DO 31 I=1,NS,JS
      NPB=N(I)
      GO TO (32,33),KW
   32 WRITE(M,FMT) (F(K,I,J),J=1,NPB,JS)
      GO TO 31
   33 WRITE(M,FMT) (V(K,I,J),J=1,NPB,JS)
   31 CONTINUE
C ... SECOND QUATER ...
      DO 34 I=NSM,NS2,JS
      NPB=N(NS2-I+1)
      GO TO (35,36),KW
   35 WRITE(M,FMT) (F(K,I,J),J=1,NPB,JS)
      GO TO 34
   36 WRITE(M,FMT) (V(K,I,J),J=1,NPB,JS)
   34 CONTINUE
      K=K+1
      IF(K.EQ.NTK) GO TO 37
      GO TO 30
   37 CONTINUE
C ... OUTLET SECTION(BUILT-IN) ...
      DO 38 I=1,NIN1,JS
      GO TO (39,40),KW
   39 WRITE(M,FMT) (F(K,I,J),J=1,NS,JS)
      GO TO 38
   40 WRITE(M,FMT) (V(K,I,J),J=1,NS,JS)
   38 CONTINUE
C ... OUTLET SECTION(SPECIFIED) ...
      KOUT=1
      NOUT=NO1
   46 CONTINUE
      K=K+1
      DO 42 I=1,NOUT,JS
      GO TO (43,44),KW
   43 WRITE(M,FMT) (F(K,I,J),J=1,NS,JS)
      GO TO 42
   44 WRITE(M,FMT) (V(K,I,J),J=1,NS,JS)
   42 CONTINUE
      KOUT=KOUT+1
      GO TO (46,46,48,47),KOUT
   48 CONTINUE
      NOUT=NO2
      GO TO 46
   47 CONTINUE
      IF(KW.EQ.2) GO TO 45
      KW=KW+1
      GO TO 19
   45 CONTINUE
      RETURN
      END
```

APPENDIX J

COMPUTER PROGRAM FOR PLOTTING STREAM FUNCTION AND VORTICITY CONTOURS

This computer program developed for plotting contours of stream function and vorticity obtained from numerical solution of the Navier-Stokes equations is written in FORTRAN IV for use on the Oklahoma State University Computing Center's IBM 360 Model 65 computer which has a terminal connection to the CALCOMP 565 digital plotter.

Figure 74 is the block diagram showing the operation of the program. Approximate plotting time required for one complete figure was about four plot-units or one hour (one plot-unit is 15 minutes). A brief description of the subroutine functions is given in the following sections.

Main Program

The main program arranges the subroutines to perform the plotting of contours of stream function and vorticity starting at built-in rectangular inlet section to rectangular outlet sections through series of three polar tube sections. The equi-vorticity lines are plotted first on the upper-half of the symmetry line in the channel and then the contours of stream function are traced on the lower-half of the section.

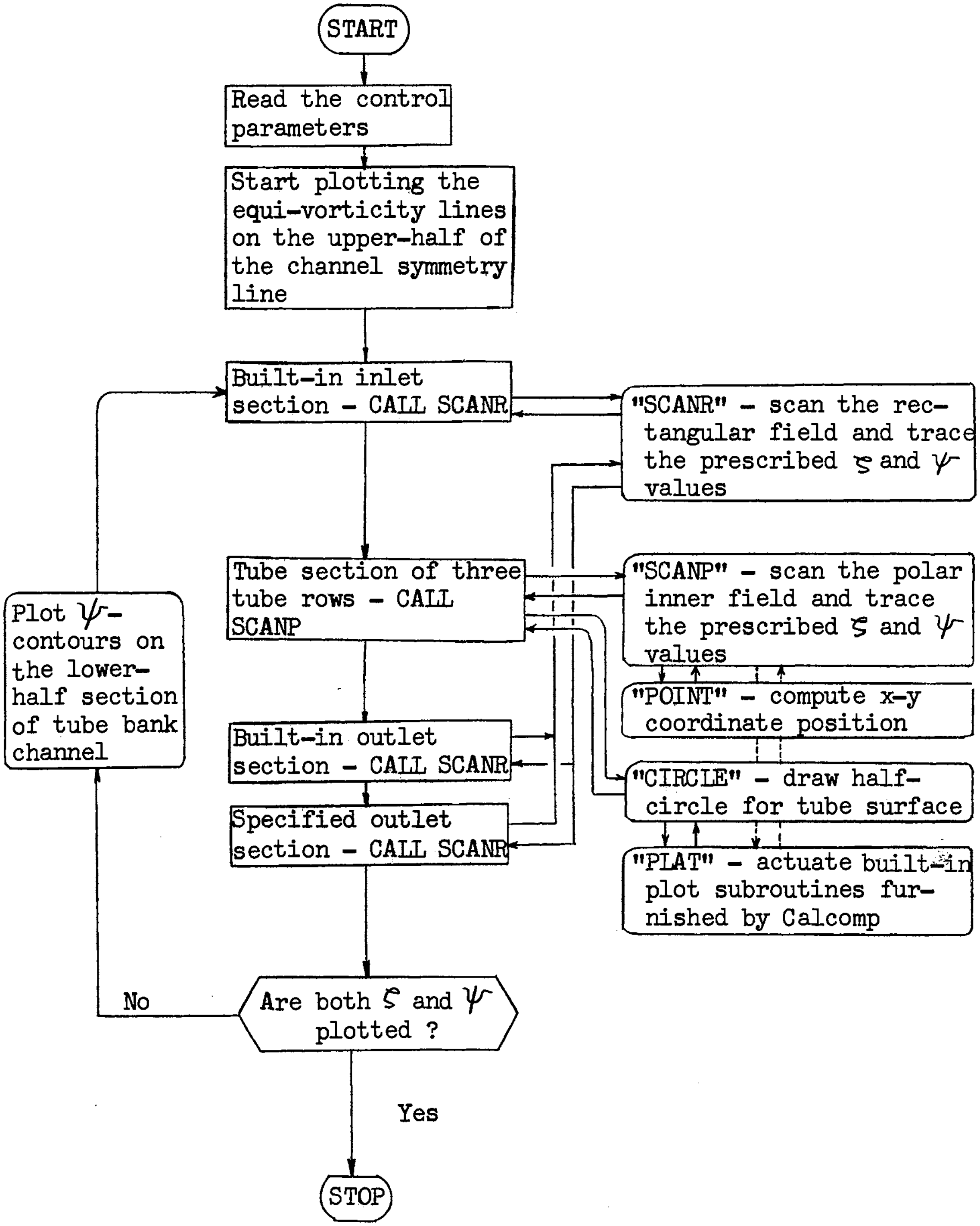

Figure 74. Computer Block Diagram of Plotting Program

Subroutine SCANR

SCANR is the subroutine that scans the rectangular mesh field to locate the point of prescribed values of ζ and ψ to be traced out successively.

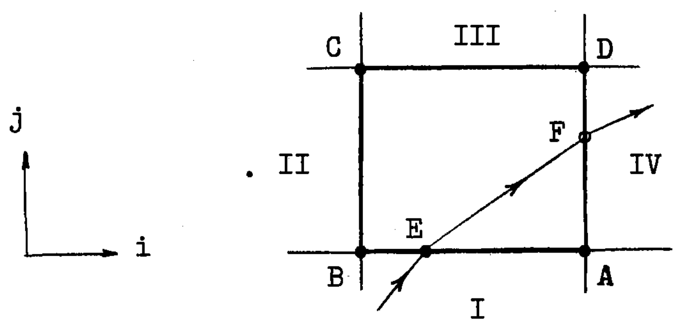

Figure 75. Search Procedure in a Rectangular Mesh Cell

Basic search procedure for points to be traced is that the values at the four mesh points A, B, C and D at the corner of border I, II, III and IV of every rectangular mesh cell (Figure 75) in the field are examined in this sequence and compared with the prescribed value of the vorticity (or stream function) to be traced: if a prescribed value falls between the values of a pair of mesh points at the edges of a border, say I, the point, say E, is located by linear interpolation on the border line I and the plotter pen is placed down; the three other border lines are similarly searched and if another point, say F, is found, say on the border IV, the pen is moved to the new location. Thus any prescribed value can be systematically traced out in the field except the boundary regions where irregular stars exist.

Subroutine SCANP

SCANP is the subroutine that scans the polar field to locate the points of prescribed values of ζ and ψ to be traced successively. The basic function of this subroutine is the same as SCANR except the working equations used for interpolating the point on the border line which is not linear.

Subroutine POINT

POINT is responsible for computing x-y coordinate location for every point in polar section to be traced by the plotter pen. POINT is called by the subroutine SCANP at every time when a point to be located is found.

Subroutine CIRCLE

CIRCLE draws the half-circle for locating tube surfaces for three tube rows. CIRCLE is called by the main program at appropriate time.

Subroutine PLAT

PLAT activates the built-in plotting subroutines supplied by Calcomp and determines the status of pen position, up or down, so that the plotter pen traces properly the desired paths.

Input Data Cards

The input data cards required for the program operation are arranged in the following order:

CARD 1 "Control parameters"

This card contains five constants, i.e., NS, NPT, NCOUNT, PT and RE, which are required for the operation of the program. All the constants except NCOUNT are described in the last section of Appendix I. NCOUNT is the number of prescribed contour values of vorticity or stream function to be plotted.

CARD 2 or CARD 3 if necessary

This card(s) contains the contour values of vorticity to be plotted. The values are read by the following format:

```
READ:   (F(M),M=1,NCOUNT)
FORMAT:  10F8.5
```

CARD 3 (4) to the last card for vorticity

In these cards the vorticity values are punched that are read in by every two i-incremental steps at a time:

```
READ:   (Q(1,J),J=1,NJ)
READ:   (Q(2,J),J=1,NJ)
FORMAT:  10F8.5
```

CARD 1 (and 2 if necessary) of the data set for plotting stream function

This card comes right after the last card of vorticity data and is similar to the CARD 2 for vorticity.

This card contains the values of stream function to be plotted. The values are read by

```
READ:   (F(M),M=1,NCOUNT)
FORMAT:   10F8.5
```

CARD 2 (or 3) and thereafter

In these rest of the cards the converged solution of stream function has been punched. The values are read by every two i-increments at a time:

```
READ:   (Q(1,J),J=1,NJ)
READ:   (Q(1,J),J=1,NJ)
FORMAT:   10F8.5
```

```
C
C ... COUNTOURS OF STREAM FUNCTION AND VORTICITY FOR FLOW ACROSS TUBE BANK ...
C
C ... AUTHOR: KOHEI ISHIHARA, SCHOOL OF CHEMICAL ENGINEERING, OKLAHOMA STATE
C                              UNIVERSITY, STILLWATER, OKLAHOMA 74074  MAY,1971 .
C
      COMMON F(19),Q(2,23),AS(37),YI(19),N(19)
      COMMON RE,PT,H,DAS,P,PS,XO,S
      COMMON KW,NQ,NCOUNT,NS,NSS,NS1,NS2,NIN1,NO1
C
      CALL PLOTS
      READ(5,100) NS,NPT,NCOUNT,PT,RE
  100 FORMAT(3I5,2F10.5)
      H=(PT-1.)/NPT
      NIN=4*NPT-2
      NS1=NS+1
      NS2=2*NS-1
      NIN1=NIN+1
      NSS=NS-1
      NO=NIN1
      NO1=NO+1
      P=3.1415926536
      DAS=P/(4.*NSS)
      PS=0.0
      S=2.
      DO 20 I=1,NS
      AS(I)=DAS*(I-1)
      N(I)=(PT/COS(AS(I))-1.)/H+1.
      YI(I)=PT*TAN(AS(I))*S
   20 CONTINUE
      DO 21 I=NS1,NS2
      AS(I)=DAS*(I-1)
   21 CONTINUE
      XMIN=0.0
      YMIN=-PT*S
      XMAX=(2.*H*(NIN+NO)+6.*PT)*S
      YMAX=PT*S
C .... SET THE ORIGIN ....
      CALL PLOTC(XMIN,-11.0,-3)
C .... RESET THE ORIGIN .....
      CALL PLOTC(XMIN,5.5,-3)
C .... FRAMING AND SCALING ....
      CALL PLOTC(XMIN,YMIN,3)
      CALL PLOTC(XMAX,YMIN,2)
      CALL PLOTC(XMAX,YMAX,3)
      CALL PLOTC(XMIN,YMAX,2)
      CALL PLOTC(XMIN,0.0,3)
      XE=(H*NIN+PT-1.)*S
      CALL PLOTC(XE,0.0,2)
C .... TITLING ....
      X=S*(H*NIN+PT)-1.2
      T=4.
      CALL SYMBOL(X+0.1,1.0,.056*T,'VORTICITY',0.0,9)
      CALL SYMBOL(X+0.5,0.70,.056*T,'(X100)',0.0,6)
      CALL SYMBOL(X-0.4,-0.60,.056*T,'STREAM FUNCTION',0.0,15)
      CALL SYMBOL(X+0.4,-0.90,.056*T,'(X1000)',0.0,7)
      DO 2  I=1,3
      CALL SYMBOL(X-0.5,0.40,.056*T,'RE=     ;PT=',0.0,11)
      CALL NUMBER(X+0.4,0.40,.056*T,RE,0.0,-1)
      CALL NUMBER(X+2.1,0.4,.056*T,PT,0.0,2)
      FPN=I
      CALL SYMBOL(X-0.2,-0.15,0.07*T,'TUBE NO.',0.0,8)
      CALL NUMBER(X+2.5,-0.15,0.07*T,FPN,0.0,-1)
      X=X+2.*PT*S
    2 CONTINUE
      KW=1
C .... INLET(BUILT-IN) ....
   13 CONTINUE
   99 FORMAT(10F8.5)
      READ(5,99) (F(M),M=1,NCOUNT)
  202 FORMAT(6X5HF(M)=,15F7.4)
      WRITE(6,202) (F(M),M=1,NCOUNT)
C .... INLET SECTION(BUILT-IN) ....
      XO=0.0
      READ(5,99) (Q(1,J),J=1,NS)
      E=H*S
      DO 1 I=2,NIN1
      READ(5,99) (Q(2,J),J=1,NS)
      DO 24 J=1,NS
      IF(Q(2,J).EQ.0.0) GO TO 24
      GO TO 26
   24 CONTINUE
      GO TO 25
   26 CONTINUE
      CALL SCANR(E,NSS,I-1)
   25 CONTINUE
      DO 1 J=1,NS
      Q(1,J)=Q(2,J)
    1 CONTINUE
      XO=S*PT+E*NIN
      CALL CIRCLE
      NQ=1
    5 CONTINUE
C  .... FIRST QUATER ....
      NJ=N(1)
      READ(5,99) (Q(1,J),J=1,NJ)
      DO 3 I=2,NS
      NJ=N(I)
      READ(5,99) (Q(2,J),J=1,NJ)
      IF(NQ.GT.2) GO TO 28
      DO 27 J=1,NJ
      IF(Q(2,J).EQ.0.0) GO TO 27
      GO TO 28
   27 CONTINUE
      GO TO 29
   28 CONTINUE
      NJ1=N(I-1)-1
      CALL SCANP(E,NJ1,I-1)
   29 CONTINUE
      DO 3 J=1,NJ
      Q(1,J)=Q(2,J)
    3 CONTINUE
C .... SECOND QUATER ......
      NQ=NQ+1
      DO 4 I=NS1,NS2
      M=NS2+1-I
```

```
      NJ=N(M)
      READ(5,99) (Q(2,J),J=1,NJ)
      NJ1=NJ-1
      CALL SCANP(E,NJ1,I-1)
      DO 4 J=1,NJ
      Q(1,J)=Q(2,J)
    4 CONTINUE
C .... THIRD QUATER ....
C .... FORTH QUATER ....
      NQ=NQ+1
      IF(NQ-5) 6,8,9
    6 PS=P/2.
      GO TO 5
    8 CONTINUE
      IF(KW.EQ.2) GO TO 14
      XI=XO+S
      CALL PLOTC(XI,0.0,3)
      XE=XI+2.*(PT-1.)*S
      CALL PLOTC(XE,0.0,2)
   14 CONTINUE
      XO=XO+2.*PT*S
      PS=0.0
      CALL CIRCLE
      GO TO 5
    9 IF(NQ-9) 6,8,11
   11 IF(NQ-13) 6,12,12
   12 CONTINUE
      PS=0.0
      IF(KW.EQ.2) GO TO 22
      XI=XO+S
      CALL PLOTC(XI,0.0,3)
      XE=E*NIN+XO+PT*S
      CALL PLOTC(XE,0.0,2)
   22 CONTINUE
      XO=XO+PT*S
C .... OUTLET(BUILT-IN) ....
      READ(5,99) (Q(1,J),J=1,NS)
      DO 10 I=2,NIN1
      READ(5,99) (Q(2,J),J=1,NS)
      CALL SCANR(E,NSS,I-1)
      DO 10 J=1,NS
      Q(1,J)=Q(2,J)
   10 CONTINUE
C .... OUTLET SECTION(SPECIFIED) .....
      XO=XO+E*NIN
      CALL PLOTC(XO,0.0,3)
      E=2.*H*S
      IF(KW.EQ.2) GO TO 23
      XE=XO+E*NO
      CALL PLOTC(XE,0.0,2)
   23 CONTINUE
      READ(5,99) (Q(1,J),J=1,NS)
      DO 15 I=2,NO1
      READ(5,99) (Q(2,J),J=1,NS)
      CALL SCANR(E,NSS,I-1)
      DO 15 J=1,NS
      Q(1,J)=Q(2,J)
   15 CONTINUE
      IF(KW-2) 17,18,18
   17 KW=KW+1
      P=-P
      DAS=-DAS
      DO 30 I=1,NS2
      AS(I)=-AS(I)
   30 CONTINUE
      DO 31 I=1,NS
      YI(I)=-YI(I)
   31 CONTINUE
      GO TO 13
   18 CONTINUE
      STOP
      END
```

```
      SUBROUTINE PLAT(X,Y,M)
C
C ... THIS SUBROUTINE ACTUATES THE LIBRARY PLOTTING SUBROUTINES FURNISHED BY
C     CALCOMP AND DETERMINES THE STATUS OF PEN POSITION ...
C
      COMMON F(19),Q(2,23),AS(37),YI(19),N(19)
      COMMON RE,PT,H,DAS,P,PS,XO,S
      COMMON KW,NQ,NCOUNT,NS,NSS,NS1,NS2,NIN1,NO1
C
      GO TO(1,2),M
    1 CALL PLOTC(X,Y,3)
      CALL PLOTC(X,Y,2)
      M=2
      RETURN
    2 CALL PLOTC(X,Y,2)
      RETURN
      END
```

```
      SUBROUTINE CIRCLE
C
C ... THIS SUBROUTINE DRAWS THE HALF-CIRCLE FOR LOCATING THE TUBE SURFACE ...
C
      COMMON F(19),Q(2,23),AS(37),YI(19),N(19)
      COMMON RE,PT,H,DAS,P,PS,XO,S
      COMMON KW,NQ,NCOUNT,NS,NSS,NS1,NS2,NIN1,NO1
C
      NP=4*NSS+1
      M=1
      DO 1 I=1,NP
      SXY=PS+DAS*(I-1)
      CALL POINT(S  ,SXY,X,Y)
      CALL PLAT(X,Y,M)
    1 CONTINUE
      CALL PLOTC(X,Y,3)
      RETURN
      END
```

```
      SUBROUTINE SCANR(E,NJ,I)
C
C ... THIS SUBROUTINE LOCATES THE POINTS FOR PRESCRIBED VALUES OF VORTICITY OR
C     STREAM FUNCTION AND TRACES IT OUT THROUGH RECTANGULAR FLOW SECTIONS ...
C
      COMMON F(19),Q(2,23),AS(37),YI(19),N(19)
      COMMON RE,PT,H,DAS,P,PS,XU,S
      COMMON KW,NQ,NCOUNT,NS,NSS,NS1,NS2,NIN1,ND1
C
      EA1=E*(I-1)
      DO 1 L=1,NCOUNT
      KS=1
      IF(F(L)) 50,51,50
   50 NJ1=1
      NJ2=NJ
      GO TO 52
   51 CONTINUE
      IF(KW.EQ.1) GO TO 24
      GO TO 25
   24 CONTINUE
      XE=H*NIN1*S
      XEO=6.*PT*S+XE
      IF(XO.LT.XE.OR.XO.GT.XEO) GO TO 1
   25 CONTINUE
      NJ1=2
      NJ2=NJ-1
   52 CONTINUE
      DO 2 J=NJ1,NJ2
      M=1
      DIJ=F(L)-Q(1,J)
      DI1=F(L)-Q(2,J)
      QFI=DIJ*DI1
      DJ1=F(L)-Q(1,J+1)
      QFJ=DIJ*DJ1
      YJ=YI(J)
      YJ1=YI(J+1)
      IF(KS) 16,17,16
   17 CALL PLAT(XCC,YSC,M)
      GO TO 5
C .... BORDER I ....
   16 IF(QFI) 3,4,5
    3 DX=DIJ/(Q(2,J)-Q(1,J))
      Y=YJ
      X=XO+EA1+E*DX
      CALL PLAT(X,Y,M)
      GO TO 5
    4 Y=YJ
      IF(DIJ) 40,6,40
   40 X=XO+EA1+E
      CALL PLAT(X,Y,M)
      GO TO 5
    6 X=XO+EA1
      CALL PLAT(X,Y,M)
C .... BORDER II ....
    5 IF(QFJ) 7,8,9
    7 DY=DIJ/(Q(1,J+1)-Q(1,J))
      X=XO+EA1
      Y=YJ+DY*(YJ1-YJ)
      CALL PLAT(X,Y,M)
      GO TO 9
    8 X=XO+EA1
      IF(DJ1) 19,15,19
   15 Y=YJ1
      CALL PLAT(X,Y,M)
      GO TO 9
   19 Y=YJ
      CALL PLAT(X,Y,M)
    9 KS=1
C .... BORDER III ....
      DIJ=F(L)-Q(2,J+1)
      QFI=DIJ*DJ1
      IF(QFI) 10,11,12
   10 DX=DJ1/(Q(2,J+1)-Q(1,J+1))
      Y=YJ1
      X=XO+EA1+DX*E
      XCC=X
      CALL PLAT(X,Y,M)
      YSC=Y
      KS=0
      GO TO 12
   11 Y=YJ1
      IF(DJ1) 18,20,18
   20 X=XO+EA1
      CALL PLAT(X,Y,M)
      GO TO 12
   18 X=XO+EA1+E
      CALL PLAT(X,Y,M)
C .... BORDER VI .....
   12 QFJ=DIJ*DI1
      IF(QFJ) 13,21,2
   13 DY=DI1/(Q(2,J+1)-Q(2,J))
      X=XO+EA1+E
      Y=YJ+DY*(YJ1-YJ)
      CALL PLAT(X,Y,M)
      GO TO 2
   21 X=XO+EA1+E
      IF(DIJ) 22,23,22
   23 Y=YJ1
      CALL PLAT(X,Y,M)
      IF(DI1) 2,22,2
   22 Y=YJ
      CALL PLAT(X,Y,M)
    2 CONTINUE
    1 CONTINUE
      CALL PLOTC(X,Y,3)
      RETURN
      END
```

```
      SUBROUTINE SCANP(E,NJ,I)
C
C ... THIS SUBROUTINE LOCATES THE POINTS FOR PRESCRIBED VALUES OF VORTICITY OR
C     STREAM FUNCTION AND TRACES IT OUT THROUGH POLAR TUBE SECTIONS ...
C
      COMMON F(19),Q(2,23),AS(37),YI(19),N(19)
      COMMON RE,PT,H,DAS,P,PS,XO,S
      COMMON KW,NQ,NCOUNT,NS,NSS,NS1,NS2,NIN1,NO1
C
      DO 1 L=1,NCOUNT
      KS=1
      IF(F(L)) 50,51,50
   50 NJ1=1
      GO TO 52
   51 CONTINUE
      IF(NQ.LE.2) GO TO 1
      IF(PS) 54,55,54
   54 IF(NS2-1-I) 53,1,53
   55 IF(I-1) 53,1,53
   53 NJ1=2
   52 CONTINUE
      DO 2 J=NJ1,NJ
      M=1
      DIJ=F(L)-Q(1,J)
      DI1=F(L)-Q(2,J)
      QFI=DIJ*DI1
      DJ1=F(L)-Q(1,J+1)
      QFJ=DIJ*DJ1
      RJ=E*(J-1)+S
      IF(KS) 16,17,16
   17 X=XCC
      Y=YSC
      GO TO 5
C .... BORDER I ....
   16 IF(QFI) 3,4,29
    3 DX=DIJ/(Q(2,J)-Q(1,J))
      CALL POINT(RJ,PS+AS(I)+DAS*DX,X,Y)
      GO TO 5
    4 IF(DI1) 6,19,6
   19 CALL POINT(RJ,PS+AS(I+1),X,Y)
      GO TO 5
    6 CALL POINT(RJ,PS+AS(I),X,Y)
    5 CALL PLAT(X,Y,M)
C .... BORDER II ....
   29 IF(QFJ) 7,8,30
    7 DY=DIJ/(Q(1,J+1)-Q(1,J))
      CALL POINT(RJ+E*DY,PS+AS(I),X,Y)
      GO TO 9
    8 IF(DIJ) 15,20,15
   20 CALL POINT(RJ,PS+AS(I),X,Y)
      GO TO 9
   15 CALL POINT(RJ+E,PS+AS(I),X,Y)
    9 CALL PLAT(X,Y,M)
   30 KS=1
C .... BORDER III ....
      DIJ=F(L)-Q(2,J+1)
      QFI=DIJ*DJ1
      IF(QFI) 10,11,31
   10 DX=DJ1/(Q(2,J+1)-Q(1,J+1))
      CALL POINT(RJ+E,PS+AS(I)+DAS*DX,X,Y)
      KS=0
      XCC=X
      YSC=Y
      GO TO 12
   11 IF(DJ1) 18,21,18
   21 CALL POINT(RJ+E,PS+AS(I),X-Y)
      GO TO 12
   18 CALL POINT(RJ+E,PS+AS(I+1),X,Y)
   12 CALL PLAT(X,Y,M)
C .... BORDER VI .....
   31 QFJ=DIJ*DI1
      IF(QFJ) 13,22,2
   13 DY=DI1/(Q(2,J+1)-Q(2,J))
      CALL POINT(RJ+E*DY,PS+AS(I+1),X,Y)
      GO TO 14
   22 IF(DIJ) 23,24,23
   24 CALL POINT(RJ+E,PS+AS(I+1),X,Y)
      IF(DI1) 14,25,14
   25 CALL PLAT(X,Y,M)
   23 CALL POINT(RJ,PS+AS(I+1),X,Y)
   14 CALL PLAT(X,Y,M)
    2 CONTINUE
    1 CONTINUE
      CALL PLOTC(X,Y,3)
      RETURN
      END
```

```
      SUBROUTINE POINT(RXY,SXY,X,Y)
C
C ... THIS SUBROUTINE COMPUTES THE X-Y COORDINATES IN TUBE BANK FLOW CHANNEL ...
C
      COMMON F(19),Q(2,23),AS(37),YI(19),N(19)
      COMMON RE,PT,H,DAS,P,PS,XO,S
      COMMON KW,NQ,NCOUNT,NS,NSS,NS1,NS2,NIN1,NO1
C
      X=XO-RXY*COS(SXY)
      Y=RXY*SIN(SXY)
      RETURN
      END
```

APPENDIX K

COMPUTER PROGRAM FOR CALCULATING FORM DRAG AND FRICTION DRAG

This computer program ia also written in FORTRAN IV for use on the Oklahoma State University Computing Center's IBM 360 computer. The block diagram of the program is shown in Figure 76.

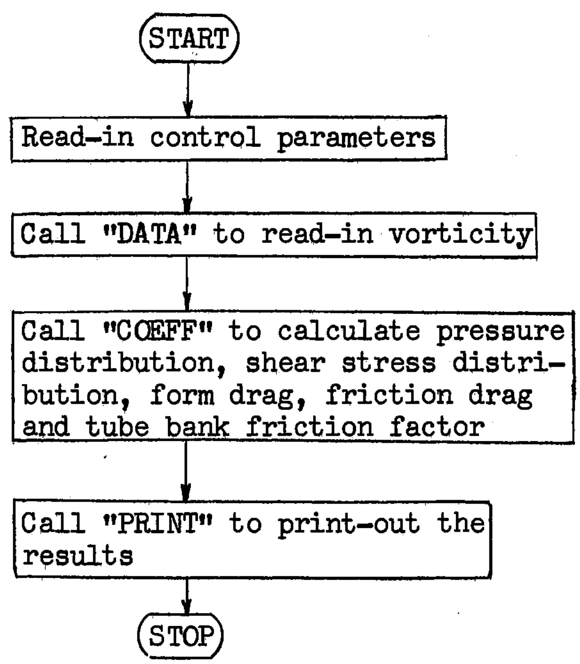

Figure 76. Computer Block Diagram for Calculating Form Drag and Friction Drag

A description of each of the subroutine functions and input data cards required are as follows.

Main Program

This is the executive program for the entire calculation. The main program arranges the subroutines in proper order for calculating form drag and friction drag. The main program calls the data input subroutine at the early stage of the calculation, then the subroutine of drag calculation and finaly the output subroutine.

Subroutine COUNT

This subroutine is explained in Appendix I.

Subroutine DATA and DISK

These subroutines are also described in Appendix I. The only difference in these subroutines from the previous ones is that only the vorticity is read in for the calculation.

Subroutine COEFF

COEFF is the subroutine that calculates the pressure and shear stress distributions around the tube, form drag coefficient, friction drag coefficient and tube bank friction factor from the converged solution of the vorticity at particular Reynolds number.

Input Data Cards

The input data cards required for the program are arranged in the following order:

$\boxed{\text{CARD 1}}$

$\boxed{\text{CARD 2}}$ "Format specifications"

These first two cards are exactly the same cards as $\boxed{\text{CARD 1}}$ and $\boxed{\text{CARD 2}}$ in Appendix I for format specifications.

READ: (FM1(I),I=1,18)
READ: (FM2(I),I=1,18)

FORMAT: 18A4

$\boxed{\text{CARD 3}}$ "Control variables and parameters"

This is also exactly the same one as $\boxed{\text{CARD 3}}$ of Appendix I.

READ: NI,NT,N2,NS,NPT,ITMAX,EPSMAX,PT,RE

FORMAT: 6I5, 3F10.5

Nomenclature of the constants above should be referred to Appendix I.

$\boxed{\text{CARD 4 and thereafter}}$ "Vorticity values"

These cards contain the vorticity values that have been punched upon the convergence of the solution at the particular Reynolds number.

READ: V(K,I,J)

FORMAT: 18A4

```
C
C.... IDEAL TUBE BANK FRICTION FACTOR OF VISCOUS FLOW AT LOW REYNOLDS NUMBERS ..
C
C ... AUTHOR: KOHEI ISHIHARA, SCHOOL OF CHEMICAL ENGINEERING, OKLAHOMA STATE
C                               UNIVERSITY, STILLWATER, OKLAHOMA 74074  MAY,1971 .
C
      COMMON P(3,80),PC(3,80),DP(3,80),A(3,80),B(3,80),DCF(3,80),C(3,80)
      COMMON DCP(3,80), V(7,40,50)  ,N(40),FM1(18),FM2(18),FMT(18)
      COMMON RE,H,PT,PL,NI,NT,NO,NS,NPT,DAS
      COMMON NS1,NS2,NSS,NP,NP1,NIN,NI1,NIN1,NO1,NTK,NO2
C
  300 FORMAT(18A4)
      READ(5,300) (FM1(I),I=1,18)
      READ(5,300) (FM2(I),I=1,18)
      READ (5,100) NI,NT,N2,NS,NPT,ITMAX,EPSMAX,PT,RE
      WRITE(6,200) NI,NT,N2,NS,NPT,ITMAX,EPSMAX,PT,RE
  100 FORMAT(6I5,4F10.5)
  200 FORMAT(/,5X'NI=',I2,1X'NT=',I2,1X'N2=',I2,1X'NS=',I2,1X'NPT=',I2,1
     1X'ITMAX=',I3,1X'EPSMAX=',F8.4,1X'PT=',F8.4,1X'RE=',F8.4,/)
      H=(PT-1.)/NPT
      NIN=4.*NPT-2
      NS2=2*NS-1
      NS1=NS+1
      NTK=NT*2+1
      NP=10
      NP1=11
      NI1=NI+1
      NIN1=NIN+1
      NO=NS2
      NO1=NO+1
      NO2=N2+1
      PI=3.1415926536
      DAS=PI/(4.*(NS-1))
      WRITE(6,201) H,DAS ,NTK,NIN,NS1,NS2
  201 FORMAT(/,5X'H=',F8.4,1X,'DAS= ',F8.4,1X'NTK=',I2,1X'NIN=',I2,1X
     1'NS1=',I2,1X'NS2=',I2,/)
  101 FORMAT(5X,I5,3X,I5,3(3X,F8.4),3X,F8.3,3(3X,F8.4))
      WRITE(6,203)
  203 FORMAT(1H1,10X'INTEGRATION OF PRESSURE AND FRICTION LOSS ROUND THE
     1 TUBE SURFACE',/)
      DO 1 I=1,NS
      RT=PT/ COS(DAS*(I-1))
      N(I)=(RT-1.)/H+1
    1 CONTINUE
      CALL DATA
      K=1
    2 CONTINUE
  202 FORMAT(/,5X'CF=',F8.4,2X'CP=',F8.4,2X'CD=',F8.4,2X,'F =',F8.4,2X,
     1'FOR TUBE NO.=',I2)
      CALL COEFF(K,IN,NE,CF,CP,CD)
      F=CD/(4.*PT)
      WRITE(6,202) CF,CP,CD,F,K
      WRITE(6,103)
  103 FORMAT(/,9X'I',7X'M',3X'VORTICITY',3X'V. GRAD.',6X'DP',9X'P',9X'PC
     1',9X'DCF',8X'DCP',/)
      DO 50 I=1,IN
      M=I
      WRITE(6,101) I,M,A(K,I),B(K,I),DP(K,I),P(K,I),PC(K,I),DCF(K,I),
     1DCP(K,I)
   50 CONTINUE
      IN1=IN+1
      DO 60 I=IN1,NE
      M=I-IN+1
      WRITE(6,101) I,M,A(K,I),B(K,I),DP(K,I),P(K,I),PC(K,I),DCF(K,I),
     1DCP(K,I)
   60 CONTINUE
      IF(K.EQ.NT) GO TO 3
      K=K+1
      PC(K,1)=PC(K-1,NE)
      P(K,1)=P(K-1,NE)
      GO TO 2
    3 CONTINUE
      CALL EXIT
      END
```

```
      SUBROUTINE DATA
C
C ... THIS SUBROUTINE READS THE VORTICITY DATA FROM THE PUNCHED-OUT DATA CARDS .
C
      COMMON P(3,80),PC(3,80),DP(3,80),A(3,80),B(3,80),DCF(3,80),C(3,80)
      COMMON DCP(3,80), V(7,40,50)   ,N(40),FM1(18),FM2(18),FMT(18)
      COMMON RE,H,PT,PL,NI,NT,NO,NS,NPT,DAS
      COMMON NS1,NS2,NSS,NP,NP1,NIN,NI1,NIN1,NO1,NTK,NO2
      DIMENSION JN1(4),JN2(4)
C
      NC=N(NS)/NP
      JN1(1)=1
      JN2(1)=NP
      IF(NC.EQ.1) GO TO 18
      DO 9 L=2,NC
      JN1(L)=JN2(L-1)+1
      JN2(L)=JN2(L-1)+NP
    9 CONTINUE
   18 CONTINUE
      K=1
   30 CONTINUE
      DO 31 I=1,NS
      NPB=N(I)
      NC=NPB/NP
   33 IF(NPB.GT.NP) GO TO 3
      READ (5,FM2) (V(K,I,J),J=1,NPB)
      GO TO 31
    3 DO 4 L=1,NC
      JN=JN1(L)
      JNP=JN2(L)
      READ (5,FM2) (V(K,I,J),J=JN,JNP)
    4 CONTINUE
      IF(NPB.LE.JNP) GO TO 31
      JN=JNP+1
      READ (5,FM2) (V(K,I,J),J=JN,NPB)
   31 CONTINUE
C ... SECOND QUATER ...
      DO 34 I=NS1,NS2
      NPB=N(NS2-I+1)
      NC=NPB/NP
   36 IF(NPB.GT.NP) GO TO 7
      READ (5,FM2) (V(K,I,J),J=1,NPB)
      GO TO 34
    7 DO 8 L=1,NC
      JN=JN1(L)
      JNP=JN2(L)
      READ (5,FM2) (V(K,I,J),J=JN,JNP)
    8 CONTINUE
      IF(NPB.LE.JNP) GO TO 34
      JN=JNP+1
      READ (5,FM2) (V(K,I,J),J=JN,NPB)
   34 CONTINUE
      K=K+1
      IF(K.EQ.NTK) GO TO 37
      GO TO 30
   37 CONTINUE
      RETURN
      END
```

```
      SUBROUTINE COEFF(KT,IN,NE,CF,CP,CD)
C
C ... THIS SUBROUTINE CALCULATES VORTICITY GRADIENT, PRESSURE VARIATION,
C     SHEAR STRESS VARIATION, FORM DRAG, AND FRICTION DRAG ...
C
C ... CD= TOTAL DRAG COEFFICIENT ALONG THE SURFACE OF A CYLINDER ...
C ... CP= PRESSURE COEFFICIENT ...
C ... CF= SHEAR STRESS COEFFICIENT ...
C ... P= PRESSURE DROP ALONG THE SURFACE OF THE CYLINDER ...
C
      COMMON P(3,80),PC(3,80),DP(3,80),A(3,80),B(3,80),DCF(3,80),C(3,80)
      COMMON DCP(3,80), V(7,40,50)   ,N(40),FM1(18),FM2(18),FMT(18)
      COMMON RE,H,PT,PL,NI,NT,NO,NS,NPT,DAS
      COMMON NS1,NS2,NSS,NP,NP1,NIN,NI1,NIN1,NO1,NTK,NO2
C
      CONST=4.*DAS/RE
      IN=(NS-1)*2+1
      NE=(NS-1)*4+1
      K=(KT-1)*2+1
      CP=0.0
      CF=0.0
      P(KT,1)=0.
      DP(KT,1)=0.
      DCF(KT,1)=0.
      B(KT,1)=0.
      C(KT,1)=1.
      DO 1 I=2,IN
      A(KT,I)=V(K,I,1)
      B(KT,I)=(2.*V(K,I,2)-.5*V(K,I,3)-1.5*V(K,I,1))/H
      DP(KT,I)= CONST*B(KT,I)
      C(KT,I)=COS(DAS*(I-1))
      P(KT,I)=P(KT,I-1)+DP(KT,I)
      DCF(KT,I)=    SIN(DAS*(I-1))*V(K,I,1)*CONST
      CF=CF+DCF(KT,I)
    1 CONTINUE
      IN1=IN+1
      DO 2 I=IN1,NE
      M=I-IN+1
      A(KT,I)=V(K+1,M,1)
      B(KT,I)=(2.*V(K+1,M,2)-.5*V(K+1,M,3)-1.5*V(K+1,M,1))/H
      DP(KT,I)= CONST*B(KT,I)
      C(KT,I)=COS(DAS*(I-1))
      P(KT,I)=P(KT,I-1)+DP(KT,I)
      DCF(KT,I)=    SIN(DAS*(I-1))*V(K+1,M,1)*CONST
      CF=CF+DCF(KT,I)
    2 CONTINUE
      DO 3 I=1,NE
      PC(KT,I)= P(KT,I)*C(KT,I)
      DCP(KT,I)= DAS*PC(KT,I)
      CP=CP+DCP(KT,I)
    3 CONTINUE
      CD=CF+CP
      RETURN
      END
```

VITA

Kohei Ishihara

Candidate for the Degree of

Doctor of Philosophy

Thesis: INCOMPRESSIBLE VISCOUS FLOW ACROSS BANKS OF TUBES AT LOW REYNOLDS NUMBERS

Major Field: Chemical Engineering

Biographical:

Personal Data: Born in Kyoto City, Kyoto, Japan, April 9, 1941, to Ujio and Sue Ishihara.

Education: Graduated from Takashima High School at Imazu, Shiga, Japan in March, 1961; received a Bachelor of Science degree in chemical engineering from Kyoto University, Kyoto, Japan, March, 1965; received a Master of Science degree in chemical engineering from Oklahoma State University, Stillwater, Oklahoma, May, 1967: completed requirements for the degree of Doctor of Philosophy in chemical engineering at Oklahoma State University, May, 1971.

Professional Experience: Summer employment in Sekaicho Rubber Company, Osaka, Japan, during the month of August, 1964; employed as research and teaching assistant of the School of Chemical Engineering, Oklahoma State University during the school years of 1965 - 1970; summer employment in the Research Department of Chicago Bridge and Iron Company, Plainfield, Illinois, June to September in 1968 and in 1969.